

**NIST Technical Note
NIST TN 2375**

Per- and Polyfluoroalkyl Substances in Stressed Structural Firefighter Gloves and Hoods, and Wildland Firefighter Coats, Shirts, and Pants

Andre L. Thompson
Andrew C. Maizel
Audrey F. Tombaugh
Halen D. Solomon
Bruce Benner
Alix E. Rodowa
Michelle Donnelly
Rick D. Davis

This publication is available free of charge from:

<https://doi.org/10.6028/NIST.TN.2375>

NIST Technical Note
NIST TN 2375

Per- and Polyfluoroalkyl Substances in Stressed Structural Firefighter Gloves and Hoods, and Wildland Firefighter Coats, Shirts, and Pants

Rick D. Davis
Michelle Donnelly
Andrew C. Maizel*
Halen D. Solomon*
Andre L. Thompson
Audrey F. Tombaugh
*Fire Research Division
Engineering Laboratory*

Bruce Benner
Alix E. Rodowa
*Chemical Sciences Division
Material Measurement Laboratory*

**Former NIST employee; all work for this publication was done while at NIST*

This publication is available free of charge from:
<https://doi.org/10.6028/NIST.TN.2375>

May 2026



U.S. Department of Commerce
Howard Lutnick, Secretary

National Institute of Standards and Technology
Craig Burkhardt, Acting Under Secretary of Commerce for Standards and Technology and Acting NIST Director

NIST TN 2375
May 2026

This work was carried out by the National Institute of Standards and Technology (NIST), an agency of the US government, and, by statute, is not subject to copyright in USA. Certain commercial entities, equipment, or materials may be identified in this document in order to describe an experimental procedure or concept adequately. Such identification is not intended to imply recommendation or endorsement by the National Institute of Standards and Technology, nor is it intended to imply that the entities, materials, or equipment are necessarily the best available for the purpose. The policy of NIST is to use metric units of measurement in all its publications, and to provide statements of uncertainty for all original measurements. In this document, however, data from organizations outside NIST are shown, which may include measurements in non-metric units or measurements without uncertainty statements.

NIST Technical Series Policies

[Copyright, Fair Use, and Licensing Statements](#)

[NIST Technical Series Publication Identifier Syntax](#)

Publication History

Approved by the NIST Editorial Review Board on 2026-05-05

How to Cite this NIST Technical Series Publication

Thompson, AL (2026) Per- and Polyfluoroalkyl Substances in Stressed Structural Firefighter Gloves and Hoods, and Wildland Firefighter Coats, Shirts, and Pants. (National Institute of Standards and Technology, Gaithersburg, MD), NIST Technical Note (TN) NIST TN 2375. <https://doi.org/10.6028/NIST.TN.2375>

NIST Author ORCID iDs

Andre Thompson: 0000-0001-5717-6902

Andrew Maizel: 0000-0002-2981-5241

Audrey F. Tombaugh: 0009-0008-4656-2742

Halen Solomon: 0000-0002-8664-9577

Bruce Benner: 0000-0002-7589-5625

Alix E. Rodowa: 0000-0002-3990-2111

Michelle Donnelly: 0000-0003-1800-5515

Rick Davis: 0000-0003-2264-0490

Contact Information

rick.davis@nist.gov

Abstract

Structural and Wildland firefighter gear textiles have been found to contain per- and polyfluoroalkyl substances (PFAS), representing a potential source of exposure for firefighters. In this study, structural firefighter turnout gear refers to only the multilayered protective gloves and single-layer hoods of their entire turnout ensemble (the jacket and pants were reported previously). Wildland firefighter gear refers only to the single-layer coat, shirt, and pants. Previous studies have found higher concentrations of PFAS in older or used gear, though the source of PFAS relative to these increased concentrations remains unclear. To assess whether stressors experienced during use contribute to increased PFAS levels, this National Institute of Standards and Technology Technical Note reports measured concentrations of 56 PFAS in 22 textiles from structural firefighter gloves and hoods, wildland shirts, coats, and pants following exposure to abrasion, thermal stressing, or weathering (i.e., ultraviolet radiation with elevated humidity). Compared with corresponding unstressed textiles, glove layers showed higher individual and total summed (total) PFAS concentrations after thermal stressing, and hood textiles showed higher total PFAS after abrasion and thermal stressing. Wildland textiles exhibited lower total PFAS after abrasion and weathering. Median total PFAS concentrations in glove layers increased from $180 \mu\text{g}/\text{kg} \pm 17 \mu\text{g}/\text{kg}$ in new textiles to $1330 \mu\text{g}/\text{kg} \pm 270 \mu\text{g}/\text{kg}$ following thermal stressing. In hood textiles, median total PFAS concentrations increased from $1.07 \mu\text{g}/\text{kg} \pm 0.14 \mu\text{g}/\text{kg}$ to $4.00 \mu\text{g}/\text{kg} \pm 0.79 \mu\text{g}/\text{kg}$ after abrasion and from $1.07 \mu\text{g}/\text{kg} \pm 0.14 \mu\text{g}/\text{kg}$ to $86 \mu\text{g}/\text{kg} \pm 15 \mu\text{g}/\text{kg}$ following thermal stressing. Median total PFAS concentrations in wildland textiles decreased from $5520 \mu\text{g}/\text{kg} \pm 930 \mu\text{g}/\text{kg}$ to $942 \mu\text{g}/\text{kg} \pm 125 \mu\text{g}/\text{kg}$ after abrasion and from $5520 \mu\text{g}/\text{kg} \pm 930 \mu\text{g}/\text{kg}$ to $1450 \mu\text{g}/\text{kg} \pm 90 \mu\text{g}/\text{kg}$ following weathering. These shifts largely reflected changes in the most abundant PFAS in unstressed textiles: methyl perfluorobutane sulfonamidoethanol (MeFBSE), 6:2 fluorotelomer alcohol (6:2 FTOH), and 6:2 fluorotelomer sulfonic acid (6:2 FTS) in glove textile layers; perfluorobutanoic acid (PFBA) and 6:2 FTS in hood textiles; and 6:2 FTOH and 6:2 fluorotelomer methacrylate (6:2 FTMAC) in wildland firefighter gear textiles. While stressing altered PFAS concentrations, the targeted methods employed here cannot distinguish whether changes in PFAS concentrations post stressing arose from chemical transformation of untargeted PFAS or from enhanced extractability due to textile degradation and fluoropolymer breakdown.

Keywords

Abrasion; firefighter; gloves; hoods; per- and polyfluoroalkyl substances; PFAS; stressing; turnout gear; weathering; wildland firefighter

Table of Contents

Executive Summary	1
1. Introduction	2
2. Materials and Methods	3
2.1. Chemicals and Consumables.....	3
2.2. Structural Firefighter Gloves	3
2.3. Structural Firefighter Hoods	4
2.4. Wildland Firefighter Coats, Shirts, and Pants.....	5
2.5. PFAS Analytical Standards	6
2.6. PFAS Analysis	6
2.7. Abrasion	9
2.8. Thermal Stressing.....	9
2.9. Weathering.....	10
3. Results	11
3.1. Abrasion	11
3.1.1. Changes in Textile Mass with Abrasion	11
3.1.2. PFAS in Abraded Firefighter Hoods and Wildland Textiles.....	12
3.1.3. PFAS Changes After Abrasion	14
3.2. Thermal Stressing.....	16
3.2.1. Change in Textile Mass After Thermal Stressing	16
3.2.2. PFAS Changes in Thermally Stressed Gloves and Hoods Textiles.....	17
3.2.3. PFAS Changes After Thermal Stressing.....	19
3.3. Weathering.....	23
3.3.1. PFAS in Weathered Wildland Coats, Shirts, and Pants.....	23
3.3.2. PFAS Changes in Weathered Wildland Coats, Shirts, and Pants	25
4. Discussion	27
5. Summary	39
6. Future Work	39
7. References	74
Appendix A. Experimental Details	79
A.1. PFAS Analytical Standards and NIST Reference Materials.....	79
A.2. PFAS Analysis.....	85
A.3. Quality Control Results.....	85
A.3.1. Reporting Limits.....	85
A.3.2. NIST Reference Materials 8446 and 8447	85

A.3.3.	Method Reproducibility Materials (OS-FRM)	86
A.3.4.	PFAS Concentrations in Stressed Firefighter Gloves, Hoods, and Wildland Coats, Shirts, and Pants	87
Appendix B.	List of Abbreviations and Acronyms	97

List of Tables

Table 1. Class names and abbreviations as well as individual compound names, abbreviations, analytical method used for quantification (i.e., NV for nonvolatile, SV for semivolatile, or V for volatile) as well as Chemical Abstract Service Registry Numbers (CAS RN) of all PFAS analyzed in this publication.	7
Table 2. Average and standard deviation of the quadruplicate measurements of fractional mass change in textile samples after abrasion. Positive values indicate increased mass following abrasion while negative values indicate decreased mass following abrasion.	11
Table 3. Average and standard deviation of measured fractional mass change in textile samples following thermal stressing. Negative values indicate decreasing mass. All thermal stressing results were done in triplicate.	16
Table 4. Median changes in total PFAS concentrations by stressing and textile type. ⊕ ⊕ > + 150 %, ⊕ + 25 % to + 150 %, 🌀 - 25 % to + 25 %, ⊖ < - 25 %. NS – not studied.	28
Table 5. Measured PFAS concentrations (μg-PFAS / kg-textile; ± standard deviation of triplicate measurements) and reporting limits for GL-A-MB after thermal stressing.	40
Table 6. Measured PFAS concentrations (μg-PFAS / kg-textile; ± standard deviation of triplicate measurements) and reporting limits for GL-A-TL after thermal stressing.	41
Table 7. Measured PFAS concentrations (μg-PFAS / kg-textile; ± standard deviation of triplicate measurements) and reporting limits for GL-B-IL after thermal stressing.	42
Table 8. Measured PFAS concentrations (μg-PFAS / kg-textile; ± standard deviation of triplicate measurements) and reporting limits for GL-B-TL after thermal stressing.	43
Table 9. Measured PFAS concentrations (μg-PFAS / kg-textile; ± standard deviation of triplicate measurements) and reporting limits for GL-C-IL after thermal stressing.	44
Table 10. Measured PFAS concentrations (μg-PFAS / kg-textile; ± standard deviation of triplicate measurements) and reporting limits for GL-C-MB after thermal stressing.	45
Table 11. Measured PFAS concentrations (μg-PFAS / kg-textile; ± standard deviation of triplicate measurements) and reporting limits for GL-C-TL after thermal stressing.	46
Table 12. Measured PFAS concentrations (μg-PFAS / kg-textile; ± standard deviation of triplicate measurements) and reporting limits for GL-D-IL after thermal stressing.	47
Table 13. Measured PFAS concentrations (μg-PFAS / kg-textile; ± standard deviation of triplicate measurements) and reporting limits for GL-D-MB after thermal stressing.	48
Table 14. Measured PFAS concentrations (μg-PFAS / kg-textile; ± standard deviation of triplicate measurements) and reporting limits for GL-D-TL after thermal stressing.	49
Table 15. Measured PFAS concentrations (μg-PFAS / kg-textile; ± standard deviation of triplicate measurements) and reporting limits for abraded HD-A.	50
Table 16. Measured PFAS concentrations (μg-PFAS / kg-textile; ± standard deviation of triplicate measurements) and reporting limits for HD-A after thermal stressing.	51
Table 17. Measured PFAS concentrations (μg-PFAS / kg-textile; ± standard deviation of triplicate measurements) and reporting limits for abraded HD-B.	52
Table 18. Measured PFAS concentrations (μg-PFAS / kg-textile; ± standard deviation of triplicate measurements) and reporting limits for HD-B after thermal stressing.	53
Table 19. Measured PFAS concentrations (μg-PFAS / kg-textile; ± standard deviation of triplicate measurements) and reporting limits for abraded HD-C.	54
Table 20. Measured PFAS concentrations (μg-PFAS / kg-textile; ± standard deviation of triplicate measurements) and reporting limits for HD-C after thermal stressing.	55
Table 21. Measured PFAS concentrations (μg-PFAS / kg-textile; ± standard deviation of triplicate measurements) and reporting limits for abraded HD-D.	56

Table 22. Measured PFAS concentrations ($\mu\text{g-PFAS / kg-textile}$; \pm standard deviation of triplicate measurements) and reporting limits for HD-D after thermal stressing.	57
Table 23. Measured PFAS concentrations ($\mu\text{g-PFAS / kg-textile}$; \pm standard deviation of triplicate measurements) and reporting limits for abraded HD-E.	58
Table 24. Measured PFAS concentrations ($\mu\text{g-PFAS / kg-textile}$; \pm standard deviation of triplicate measurements) and reporting limits for HD-E after thermal stressing.	59
Table 25. Measured PFAS concentrations ($\mu\text{g-PFAS / kg-textile}$; \pm standard deviation of triplicate measurements) and reporting limits for abraded HD-F.	60
Table 26. Measured PFAS concentrations ($\mu\text{g-PFAS / kg-textile}$; \pm standard deviation of triplicate measurements) and reporting limits for HD-F after thermal stressing.	61
Table 27. Measured PFAS concentrations ($\mu\text{g-PFAS / kg-textile}$; \pm standard deviation of triplicate measurements) and reporting limits for abraded HD-G.	62
Table 28. Measured PFAS concentrations ($\mu\text{g-PFAS / kg-textile}$; \pm standard deviation of triplicate measurements) and reporting limits for HD-G after thermal stressing.	63
Table 29. Measured PFAS concentrations ($\mu\text{g-PFAS / kg-textile}$; \pm standard deviation of triplicate measurements) and reporting limits for abraded HD-H.	64
Table 30. Measured PFAS concentrations ($\mu\text{g-PFAS / kg-textile}$; \pm standard deviation of triplicate measurements) and reporting limits for HD-H after thermal stressing.	65
Table 31. Measured PFAS concentrations ($\mu\text{g-PFAS / kg-textile}$; \pm standard deviation of triplicate measurements) and reporting limits for abraded WL-C.	66
Table 32. Measured PFAS concentrations ($\mu\text{g-PFAS / kg-textile}$; \pm standard deviation of triplicate measurements) and reporting limits for WL-C following controlled weathering.	67
Table 33. Measured PFAS concentrations ($\mu\text{g-PFAS / kg-textile}$; \pm standard deviation of triplicate measurements) and reporting limits for abraded WL-E.	68
Table 34. Measured PFAS concentrations ($\mu\text{g-PFAS / kg-textile}$; \pm standard deviation of triplicate measurements) and reporting limits for WL-E following exposure to controlled weathering.	69
Table 35. Measured PFAS concentrations ($\mu\text{g-PFAS / kg-textile}$; \pm standard deviation of triplicate measurements) and reporting limits for abraded WL-F.	70
Table 36. Measured PFAS concentrations ($\mu\text{g-PFAS / kg-textile}$; \pm standard deviation of triplicate measurements) and reporting limits for WL-F following exposure to controlled weathering.	71
Table 37. Measured PFAS concentrations ($\mu\text{g-PFAS / kg-textile}$; \pm standard deviation of triplicate measurements) and reporting limits for abraded WL-H.	72
Table 38. Measured PFAS concentrations ($\mu\text{g-PFAS / kg-textile}$; \pm standard deviation of triplicate measurements) and reporting limits for WL-H following exposure to controlled weathering.	73
Table 39. Nonvolatile PFAS analytical standards obtained from Wellington Laboratories, with full analyte names, CAS RN, and abbreviations (bold), and analyte concentrations with expanded maximum combined percent relative uncertainty. PFHxS, PFOS, MeFOSAA, and EtFOSAA in PFAC30PAR were present as a mixture of structural isomers.	80
Table 40. Nonvolatile isotopically labeled PFAS internal and injection standards obtained from Wellington Laboratories, with full analyte names, and analyte concentrations with expanded maximum combined percent relative uncertainty where provided.	81
Table 41. Semivolatile PFAS analytical standards purchased from Wellington Laboratories including full analyte names, CAS RN, abbreviations (bold), and analyte concentrations with expanded maximum combined percent relative uncertainty where provided.	82
Table 42. Semivolatile isotopically labeled PFAS internal standards obtained from Wellington Laboratories, with full analyte names, and analyte concentrations with expanded maximum combined percent relative uncertainty where provided.	82

Table 43. Volatile target PFAS analytical standards, supplier, full analyte names, CAS RN, abbreviations (bold), and analyte concentrations with expanded maximum combined percent relative uncertainty where provided..... 83

Table 44. Volatile internal standard PFAS purchased from Wellington Laboratories, including full analyte names, and analyte concentrations with expanded maximum combined percent relative uncertainty where provided..... 84

Table 45. Reference mass fractions for NIST Reference Material 8446 including mean value and expanded uncertainty with 95 % confidence. 84

Table 46. Reference mass fractions NIST Reference Material 8447 including mean value and expanded uncertainty with 95 % confidence. 84

List of Figures

Figure 1. Average PFAS concentrations (μg PFAS/kg textile; ppb mass ratio) from triplicate analysis of structural firefighter hoods (HD-A to HD-H) and wildland firefighter coats (WL-C), pants (WL-E, -F), and shirts (WL-H) following abrasion. Values not meeting QC standards are shown in white.	13
Figure 2. Total PFAS concentrations determined from triplicate analysis of firefighter hood textiles (left) and wildland textiles (right) following abrasion. Error bars indicate the combined standard uncertainty of total concentrations.	14
Figure 3. Total PFAS concentrations from triplicate analysis of abraded firefighter gear textiles (y-axis) versus unstressed textiles (x-axis). Error bars represent combined standard uncertainty. Panel labels denote textile type (HD = firefighter hood textiles; WL = wildland firefighter gear textiles), and individual textiles are identified by marker labels. The dashed line indicates a 1:1 ratio, where concentrations are equal in unstressed and abraded textiles.	15
Figure 4. Average PFAS concentrations (μg PFAS/kg textile or ppb mass ratio) determined from triplicate analysis of structural firefighter glove layers (GL-A to GL-D) and hood textiles (HD-A to HD-H) after thermal stressing. Values not meeting QC standards are shown in white.	18
Figure 5. Total PFAS concentrations determined from triplicate analysis of structural firefighter glove layers (left) and firefighter hood textiles (right) after thermal stressing. Error bars indicate the combined standard uncertainty of total concentrations.	19
Figure 6. Total PFAS concentrations determined from triplicate analysis of firefighter glove layers following thermal stressing (y-axis) compared with corresponding unstressed textiles (x-axis). Error bars represent combined standard uncertainty. Textile type is indicated in panel label (GL = firefighter glove textiles), and individual textiles are indicated with marker labels. The dashed line denotes a 1:1 concentration ratio (i.e., equal concentrations measured in unstressed and textiles after thermal stressing). All glove layers are shown in the upper panel, with a zoomed inset displayed below.	21
Figure 7. Total PFAS concentrations determined from triplicate analysis of firefighter hood textiles following thermal stressing (y-axis) compared with corresponding unstressed textiles (x-axis). Error bars represent combined standard uncertainty. Textile type is indicated in panel label (HD = firefighter hood textiles), and individual textiles are indicated with marker labels. The dashed line denotes a 1:1 concentration ratio (i.e., equal concentrations measured in unstressed and textiles after thermal stressing). All hood textiles are shown in the upper panel, with a zoomed inset displayed below.	22
Figure 8. Average PFAS concentrations (μg PFAS/kg textile or ppb mass ratio) determined from triplicate analysis of wildland firefighter coats (WL-C), pants (WL-E, WL-F) and shirts (WL-H) following weathering.	24
Figure 9. Total PFAS concentrations in wildland firefighter coats (WL-C), pants (WL-E, WL-F), and shirts (WL-H) following weathering. Error bars indicate the combined standard uncertainty of total concentrations. Bar color indicates PFAS class.	25
Figure 10. Total PFAS concentrations determined from triplicate analysis of wildland firefighter coats (WL-C), pants (WL-E, WL-F), and shirts (WL-H) following weathering (y-axis) compared with corresponding unstressed textiles (x-axis). Error bars represent combined standard uncertainty. Textile type is indicated in panel label (WL = wildland firefighter gear textiles), and individual textiles are indicated with marker labels. The dashed line denotes a 1:1 concentration ratio (i.e., equal concentrations measured in unstressed and textiles after weathering).	26
Figure 11. Average total volatile PFAS concentrations determined from triplicate analysis of wildland firefighter coats (WL-C), pants (WL-E, WL-F), and shirts (WL-H) following abrasion (y-axis) compared with corresponding unstressed textiles (x-axis). Error bars represent combined standard uncertainty. Textile type is indicated in panel label (WL = wildland firefighter gear textiles), and individual textiles are	

indicated with marker labels. The dashed line denotes a 1:1 concentration ratio (i.e., equal concentrations measured in unstressed and textiles after abrasion). 29

Figure 12. Average total nonvolatile PFAS concentrations determined from triplicate analysis of hood textiles (left) and wildland textiles (right) following abrasion (y-axis) compared with corresponding unstressed textiles (x-axis). Error bars represent combined standard uncertainty. Textile type is indicated in panel label (HD = firefighter hood textiles; WL = wildland firefighter gear textiles), and individual textiles are indicated with marker labels. The dashed line denoted a 1:1 concentration ratio (i.e., equal concentrations measured in unstressed and textiles after abrasion). 29

Figure 13. Average total volatile PFAS concentrations determined from triplicate analysis of firefighter glove textiles following thermal stressing (y-axis) compared with corresponding unstressed glove textiles (x-axis). Error bars represent combined standard uncertainty. Textile type is indicated in panel label (GL = firefighter glove textiles), and individual textiles are indicated with marker labels. The dashed line denotes a 1:1 concentration ratio (i.e., equal concentrations measured in unstressed and textiles after thermal stressing). All glove layers are shown in the upper panel, with a zoomed inset displayed below. 31

Figure 14. Average total nonvolatile PFAS concentrations determined from triplicate analysis of firefighter gloves textiles (left) and hood textiles (right) following thermal stressing (y-axis) compared with corresponding unstressed textiles (x-axis). Error bars represent combined standard uncertainty. Textile type is indicated in panel label (GL = firefighter glove textiles; HD = firefighter hood textiles), and individual textiles are indicated with marker labels. The dashed line denoted a 1:1 concentration ratio (i.e., equal concentrations measured in unstressed and textiles after thermal stressing). All glove layers and hood textiles are shown in the upper panel, with a zoomed inset displayed below. 32

Figure 15. Average total volatile PFAS concentrations determined from triplicate analysis of wildland firefighter coats (WL-C), pants (WL-E, WL-F), and shirts (WL-H) following weathering (y-axis) compared with corresponding unstressed textiles (x-axis). Error bars represent combined standard uncertainty. Textile type is indicated in panel label (WL = wildland firefighter gear textiles), and individual textiles are indicated with marker labels. The dashed line denotes a 1:1 concentration ratio (i.e., equal concentrations measured in unstressed and textiles after weathering)..... 33

Figure 16. Average total nonvolatile PFAS concentrations determined from triplicate analysis of wildland firefighter coats (WL-C), pants (WL-E, WL-F), and shirts (WL-H) following weathering (y-axis) compared with corresponding unstressed textiles (x-axis). Error bars represent combined standard uncertainty. Textile type is indicated in panel label (WL = wildland firefighter gear textiles), and individual textiles are indicated with marker labels. The dashed line denotes a 1:1 concentration ratio (i.e., equal concentrations measured in unstressed and textiles after weathering)..... 34

Figure 17. Total PFAS concentrations in logarithmic scale (y-axis) in firefighter glove layers (IL, MB, TL) and hood textiles (HD) following different stress conditions (unstressed = stock, circle; abrasion = AS, square; thermal stressing = TS, diamond). Textiles are ordered left to right by increasing total PFAS concentration, and labels indicate textile identity. Glove layers are shown with different grayscale shades, while all hood samples are shown in white..... 38

Figure 18. Total PFAS concentrations in logarithmic scale (y-axis) in wildland firefighter coats (WL-C), pants (WL-E, WL-F), and shirts (WL-H) following different stress conditions (unstressed = stock, circle; abrasion = AS, square; weathering = UV, diamond). Textiles are ordered left to right by increasing total PFAS concentration, and labels indicate textile identity. Wildland firefighter textiles are shown with different grayscale shades. 38

Figure 19. Histograms of reporting limits for individual measurements of nonvolatile (NV; binwidth = 0.125 µg/kg), semivolatile (SV; binwidth = 0.1 µg/kg), and volatile PFAS (V; binwidth = 25 µg/kg). 85

Figure 20. Recoveries of reference PFAS in NIST reference materials 8446 and 8447 across 16 nonvolatile PFAS analytical sequences. 100 % recovery is indicated by a solid line while 70 % and 130 % recoveries are indicated by dashed lines. 86

Figure 21. Recovery of PFAS in OS-FRM that had a previously measured concentration over 0.5 µg/kg across 9 nonvolatile, 11 semivolatile, and 23 volatile PFAS batches. 100 % recovery is indicated by a solid line while 70 % and 130 % recoveries are indicated by dashed lines..... 87

Figure 22. Average PFAS concentrations determined from triplicate analysis of GL-A-MB (left) and GL-A-TL (right) either prior to stressing (new) or following thermal stressing (Heat). Concentrations indicated by shade. Measurements not reported due to unmet QC standards are in white. PFAS concentrations displayed in this figure are also presented in **Table 5** and **Table 6**. 88

Figure 23 Average PFAS concentrations determined from triplicate analysis of GL-B-IL (left) and GL-B-TL (right) either prior to stressing (new) or following thermal stressing (Heat). Concentrations indicated by shade. Measurements not reported due to unmet QC standards are in white. PFAS concentrations displayed in this figure are also presented in **Table 7** and **Table 8**. 89

Figure 24. Average PFAS concentrations determined from triplicate analysis of GL-C-IL (left), GL-C-MB (center), and GL-C-TL (right) either prior to stressing (new) or following thermal stressing (Heat). Concentrations indicated by shade. Measurements not reported due to unmet QC standards are in white. PFAS concentrations displayed in this figure are also presented in **Tables 9 to 11**.. 90

Figure 25. Average PFAS concentrations determined from triplicate analysis of GL-D-IL (left), GL-D-MB (center), and GL-D-TL (right) either prior to stressing (new) or following thermal stressing (Heat). Concentrations indicated by shade. Measurements not reported due to unmet QC standards are in white. PFAS concentrations displayed in this figure are also presented in **Tables 12 to 14**. 91

Figure 26. Average PFAS concentrations determined from triplicate analysis of HD-A (left), HD-B (center), and HD-C (right) either prior to stressing (new), following abrasion (Abr.), or following thermal stressing (Heat). Concentrations indicated by shade. Measurements not reported due to unmet QC standards are in white. PFAS concentrations displayed in this figure are also presented in **Tables 15 to 20**. 92

Figure 27. Average PFAS concentrations determined from triplicate analysis of HD-D (left), HD-E (center), and HD-F (right) either prior to stressing (new), or following abrasion (Abr.), or following thermal stressing (Heat). Concentrations indicated by shade. Measurements not reported due to unmet QC standards are in white. PFAS concentrations displayed in this figure are also presented in **Tables 21 to 26**. 93

Figure 28. Average PFAS concentrations determined from triplicate analysis of HD-G (left) and HD-H (right) either prior to stressing (new), or following abrasion (Abr.), or following thermal stressing (Heat). Concentrations indicated by shade. Measurements not reported due to unmet QC standards are in white. PFAS concentrations displayed in this figure are also presented in **Tables 27 to 30**. 94

Figure 29. Average PFAS concentrations determined from triplicate analysis of WL-C (left) and WL-E (right) either prior to stressing (new) or following abrasion (Abr) or exposure to UV stressing (weath.). Concentrations indicated by shade. Measurements not reported due to unmet QC standards are in white. PFAS concentrations displayed in this figure are also presented in **Tables 31 to 34**. 95

Figure 30. Average PFAS concentrations determined from triplicate analysis of WL-F (left) and WL-H (right) either prior to stressing (new) or following abrasion (Abr) or exposure to UV stressing (weath.). Concentrations indicated by shade. Measurements not reported due to unmet QC standards are in white. PFAS concentrations displayed in this figure are also presented in **Tables 35 to 38**. 96

Preface

This National Institute of Standards and Technology (NIST) Technical Note (TN) is the fourth publication issued in response to Section 338 of the William M. (Mac) Thornberry National Defense Authorization Act for Fiscal Year 2021, also known as the “Guaranteeing Equipment Safety for Firefighters Act of 2020.” The Act directs NIST to “complete a study of the contents and composition of unused personal protective equipment worn by firefighters.”

Two reports, NIST TN 2248 “Per- and Polyfluoroalkyl Substances in New Firefighter Turnout Gear Textiles” and NIST TN 2313 “Per- and Polyfluoroalkyl Substances in Textiles Present in Firefighter Gloves, Hoods, and Wildland Gear” described the types, amounts, and prevalence of PFAS measured in unused structural firefighter gear, including jackets, pants, gloves, hoods, and wildland firefighter coats, shirts, and pants. The Act further directs NIST to examine “the conditions and extent to which PFAS are released into the environment over time from the degradation of personal protective equipment from normal use by firefighters.” NIST TN 2260 “Per- and Polyfluoroalkyl Substances in Firefighter Turnout Gear Textiles Exposed to Abrasion, Elevated Temperature, Laundering, or Weathering” and the present report address this directive by quantifying PFAS occurrence and concentrations in the same firefighter textiles in NIST TN 2248 and NIST TN 2313 subjected to stressing procedures specified in U.S. firefighter gear performance standards.

This Technical Note (TN 2375) is the first to report the PFAS profile in firefighter gloves, hoods, and wildland firefighter coats, shirts, and pants following controlled stressing. More specifically, it documents the changes in 56 nonvolatile, semivolatile, and volatile PFAS after abrasion, thermal stressing, or weathering.

This work represents a collaboration between researchers in the Fire Research Division of the NIST Engineering Laboratory and the Chemical Sciences Division of the NIST Material Measurement Laboratory.

Acknowledgments

We thank United States Senator Jeanne Shaheen and her staff for their support of PFAS-firefighter gear research at NIST.

Author Contributions

Andre Thompson: Conceptualization, Formal Analysis, Investigation, Methodology, Resources, Supervision, Writing; **Andrew Maizel:** Conceptualization, Formal Analysis, Investigation, Methodology, Supervision, Validation, Writing – Review & Editing; **Audrey F. Tombaugh:** Methodology, Investigation, Validation; Writing – Review & Editing; **Halen Solomon:** Methodology, Investigation, Validation; Writing – Review & Editing; **Bruce Benner:** Methodology; Investigation; **Alix Rodowa:** Methodology, Validation, Writing – Review & Editing; **Michelle Donnelly:** Resources, Writing – Review & Editing; **Rick Davis:** Conceptualization, Funding Acquisition; Project Administration; Resources; Supervision.

Executive Summary

This NIST Technical Note evaluates whether exposure to physical stressors, similar to those encountered during firefighting, alters the occurrence and concentrations of per- and polyfluoroalkyl substances (PFAS) in firefighter gear textiles. A total of 10 structural firefighter glove layers, 8 hoods, and 4 wildland firefighter coats, shirts, and pants were exposed to abrasion, thermal stressing, or weathering from ultraviolet radiation and elevated humidity. A total of 56 individual PFAS were quantified using targeted methods that combined solvent extraction with gas and liquid chromatography–mass spectrometry.

This NIST Technical Note reports PFAS detected in a subset of the unused firefighter gear examined in NIST TN 2313 after stressing and uses the same PFAS target list while reporting the concentration of one additional compound. Across all stressed textiles, 26 PFAS were detected above reporting limits. Four compounds, 6:2 fluorotelomer methacrylate (6:2 FTMAC), 6:2 fluorotelomer alcohol (6:2 FTOH), 6:2 fluorotelomer sulfonic acid (6:2 FTS), and methyl perfluorobutane sulfonamidoethanol (MeFBSE), were present above 100 µg/kg in at least one textile. MeFBSE was included in this study, but not in the previous studies reported in the three earlier NIST technical notes.

Changes in total PFAS concentrations varied by gear type and applied stressor:

Glove layers: increased from 180 µg/kg ± 17 µg/kg (unstressed) to 1330 µg/kg ± 270 µg/kg after thermal stressing (643 % increase).

Hoods: increased from 1.07 µg/kg ± 0.14 µg/kg (unstressed) to 4.00 µg/kg ± 0.79 µg/kg after abrasion (274 % increase) and increased from 1.07 µg/kg ± 0.14 µg/kg (unstressed) to 86 µg/kg ± 15 µg/kg after thermal stressing (7930 % increase).

Wildland Firefighter Coats, Shirts, and Pants: decreased from 5520 µg/kg ± 930 µg/kg (unstressed) to 942 µg/kg ± 125 µg/kg after abrasion (83 % decrease) and decreased from 5520 µg/kg ± 930 µg/kg (unstressed) to 1450 µg/kg ± 90 µg/kg following weathering (74 % decrease).

These shifts largely reflected changes in concentrations of PFAS already dominant in unstressed gear (6:2 FTOH, 6:2 FTS, PFBA, and 6:2 FTMAC), rather than the appearance of new PFAS types in our target analyte list. Multiple processes may explain these changes, including: (1) altered extractability due to textile or polymer degradation; (2) degradation of fluorinated polymers into nonpolymeric PFAS; (3) transformation to a different PFAS; (4) volatilization or washout of PFAS; and (5) loss of PFAS with degraded textile fragments. Since the targeted methods applied here cannot distinguish among these mechanisms the PFAS source is unknown. This is the first report to characterize PFAS changes in structural firefighter gloves, hoods, and wildland firefighter coats, shirts, and pants after controlled stressing. The findings indicate that certain stressors, especially thermal stressing and abrasion, increase measurable PFAS concentrations in these textiles. Future work could include: (1) expanding the PFAS analyte list, (2) assessing cumulative effects of repeated or a combination of stressing techniques, (3) characterizing PFAS from a fire scene exposure, and (4) characterizing PFAS transport across firefighter textile layers.

1. Introduction

Per- and polyfluoroalkyl substances (PFAS) are synthetic chemicals that are widely used in consumer products [1], including durable water repellent (DWR) treatments that provide chemical and water resistance to firefighter turnout gear textiles [2]. These DWR chemistries are typically based on side-chain fluorinated polymers [3]. However, the specific sources of PFAS present in firefighter gear remain uncertain and may include applied finishes, polymeric materials, or other components of textile construction. Increasing evidence shows that PFAS are environmentally persistent, bioaccumulative [4,5], and potentially harmful to human health and ecosystems [6-11].

During service, firefighter gear is exposed to sunlight, abrasion, precipitation, temperature fluctuations, and airborne contaminants [12]. Combined with repeated laundering [13], these stressors can contribute to altering the PFAS profile. Laboratory and field studies have shown that UV radiation degrades polyaramid fibers and DWR coatings in turnout gear outer shells [14,15]. PFAS concentrations in DWR-treated textiles have been observed to shift following exposure to heat, abrasion, weathering, and laundering [16-18]. Weathering can generate detectable PFAS not initially present and elevate certain PFAS concentrations by up to two orders of magnitude in both outdoor [16] and laboratory [18] weathering conditions. Abrasion and washing have been shown to reduce total fluorine in weathered textiles [16], while repeated washing decreased some perfluoroalkyl acid (PFAA) concentrations but increased certain n:2 (where n = 4 - 10) fluorotelomer alcohols (FTOHs) [19]. The mechanisms driving these changes remain under investigation, though they may involve physical fiber degradation (increasing extractable PFAS) and chemical breakdown of fluorinated polymers (releasing nonpolymeric PFAS detectable by ion chromatography or mass spectrometry).

Structural firefighter gear typically includes pants, coats, hoods, helmets, and gloves [20] that must meet NFPA 1971 standards [21]. Gloves, like coats and pants, are multi-layered (outer shell, thermal liner, moisture barrier, and sometimes an inner liner). These items, especially gloves and hoods, may directly contact sensitive skin on the hands, face, and neck. Multiple studies have reported the presence of PFAS in structural firefighter gear [22-25]. By contrast, wildland firefighter gear, regulated under NFPA 1977 [26], consists of a single-layer coat, shirt, and pants. A recent NIST study [27] quantified PFAS in gloves, hoods, and wildland firefighter textiles prior to stressing.

The objective of this NIST report is to evaluate how stresses associated with firefighting alter extractable PFAS from structural firefighter gloves, hoods, and wildland firefighter coats, shirts, and pants. Using the same textiles and nearly the same PFAS target list as in TN 2313 [27], 22 textiles taken from gloves, hoods, and wildland coats, shirts, and pants were subjected to three stressing processes based on NFPA 1971 [21] performance tests: abrasion, thermal stressing, and weathering. Following these treatments, 56 PFAS were quantified and compared with concentrations in unstressed textiles. These results provide insight into how PFAS profiles in firefighter gear change during use and point toward potential mechanisms for PFAS release.

2. Materials and Methods

The experimental chemicals and consumables used in this study were consistent with those reported in NIST Technical Notes TN 2248 [24], TN 2260 [25], and TN 2313 [27] and are described in detail in Section 2.1. A total of 4 firefighter gloves (Section 2.2), 8 firefighter hoods (Section 2.3), and 4 wildland firefighter coats, shirts, and pants (Section 2.4) were acquired from various sources between 2021 and 2023. PFAS analytical standards (Sections 2.5 and A.1) and analytical methodologies (Sections 2.6 and A.2) were similar to those used in NIST TN 2313 [27], with the exception that MeFBSE was included as an additional standard. Methods used to subject textiles to abrasion (Section 2.7), thermal stressing (Section 2.8), and weathering (Section 2.9) are also detailed below.

2.1. Chemicals and Consumables

Ammonium acetate (Optima LC-MS grade), ammonium hydroxide (Optima grade), ethyl acetate (Optima HPLC and GC grade), and water (Optima LC-MS grade) were obtained from Thermo Fisher Scientific (Waltham, MA). Methanol (OmniSolv LC-MS grade) used in high-performance liquid chromatography–tandem mass spectrometry (HPLC-MS/MS) mobile phase preparations was obtained from Supelco (Bellefonte, PA), while methanol (Optima LC-MS grade) used for all other applications was obtained from Thermo Fisher Scientific. Ultra-high purity nitrogen and helium gases were supplied by Roberts Oxygen (Rockville, MD).

High-performance liquid chromatography (HPLC) vials (2 mL, amber glass) and 250 μ L glass inserts were obtained from Agilent Technologies (Santa Clara, CA). Polyethylene 2 mL vial caps for nonvolatile and semivolatile analysis were obtained from Phenomenex (Torrance, CA), while vial caps with PTFE/silicone septa for volatile analyses were obtained from Agilent Technologies. All vials, inserts, and caps were used as received from the manufacturers. Supelclean ENVI-Carb solid phase extraction (SPE) tubes (6 mL \times 500 mg) were obtained from Supelco Analytical (Bellefonte, PA). Prior to use, SPE tubes were rinsed with 20 mL (2×10^{-5} m³) of 0.1 mol/L (10^2 mol/m³) ammonium hydroxide in methanol and allowed to dry. Glass scintillation vials (20 mL), glass Pasteur pipettes, and polypropylene centrifuge tubes (15 mL) were obtained from Cole-Parmer Instrument Company (Vernon Hills, IL) and were used as received. Syringes (1 mL) and nylon syringe filters (0.22 μ m) were obtained from Thermo Fisher Scientific and rinsed with 1 mL (10^{-6} m³) of methanol prior to use.

2.2. Structural Firefighter Gloves

Structural firefighter gloves (NFPA 1971 compliant [21]) are typically constructed with multiple layers, including an outer protective layer (often leather), a moisture barrier, and an inner thermal liner. In some designs, the inner liner is a distinct layer, while in others it is integrated with the thermal liner.

This study includes 4 structural firefighter gloves (GL-A, GL-B, GL-C, and GL-D) that were commercially available and in common use as of 2023. Due to their multilayer construction,

individual fabric layers were cut from the assembled glove prior to stressing and PFAS characterization.

GL-A was constructed with a leather outer shell (not tested), an expanded polytetrafluoroethylene (ePTFE) moisture barrier (GL-A-MB), and a meta-aramid/para-aramid thermal/inner liner (GL-A-IL).

GL-B featured a dual-material outer shell comprising 100 % para-aramid knit fleece on the dorsal side (not tested) and leather on the palm (not tested). The moisture barrier was composed of a proprietary material labeled as 100 % waterproof (GL-B-MB). The thermal liner (GL-B-TL) on the dorsal side was a meta-aramid/para-aramid blend, while the palm-side inner liner (GL-B-IL) was modacrylic.

GL-C was constructed with a 100 % para-aramid outer shell on the dorsal side (not tested) and a leather palm (not tested), and an ePTFE moisture barrier (GL-C-MB). Both the thermal liner (GL-C-TL) and inner liner (GL-C-IL) were composed of para-aramid/meta-aramid fleece blends.

GL-D was constructed with a leather outer shell (not tested), an ePTFE moisture barrier (GL-D-MB), a para-aramid/meta-aramid thermal liner (GL-D-TL), and a 100 % modacrylic inner liner (GL-D-IL).

Images and area densities of all glove layers are available in NIST Technical Note 2313 [27]. Prior to experimental stressing, all textile layers were stored individually in resealable plastic bags for up to 549 days, in the dark, at room temperature to preserve material integrity.

2.3. Structural Firefighter Hoods

Structural firefighter hoods are designed to provide flame resistance and thermal protection for the head and neck. These hoods are worn beneath the helmet and, when a self-contained breathing apparatus (SCBA) is used, are typically pulled over the SCBA straps. A facial opening accommodates the firefighter's face and the SCBA facepiece, if in use, while an extended bib section covers the upper shoulders, allowing the hood to be tucked securely into the turnout coat. They are constructed from heat-resistant knitted fabrics and comply with NFPA 1971 standards [21]. This study focused exclusively on standard knitted hoods designed primarily for thermal protection. Hoods incorporating additional particulate barrier layers or enhanced filtration features were not studied.

A total of 8 different structural firefighter hoods were obtained in 2023 from three firefighter gear vendors. The hoods were labeled HD-A through HD-H. They were constructed using rib-knit fabrics but varied in material composition and color.

HD-A: Black; composed of a carbon/aramid fiber blend.

HD-B: White; made of 100 % meta-aramid.

HD-C: Black; composed of oxidized polyacrylonitrile and a tri-blend carbon mixture.

HD-D: White; composed of a meta-aramid and cellulose fiber blend derived from wood.

HD-E: Tan; composed of polybenzimidazole (PBI) synthetic fiber and regenerated cellulose.

HD-F: Tan; composed of PBI synthetic fiber and cellulose fibers derived from wood.

HD-G: Yellow; composed of polyimide derived from aromatic dianhydrides and aromatic diisocyanates, combined with wood-derived cellulose fibers and a heat-resistant, lightweight synthetic fiber.

HD-H: Yellow; identical in material composition to HD-G but produced by a different manufacturer.

Images and area density measurements of all hood textiles are provided in NIST Technical Note 2313 [27]. Prior to experimental stressing, all hood textiles were individually stored in resealable plastic bags for up to 1006 days and kept in the dark at room temperature to preserve material integrity.

2.4. Wildland Firefighter Coats, Shirts, and Pants

Wildland firefighters wear protective gear that differs from that used in structural firefighting. The structural firefighter coats, pants, and gloves are typically a three-layer system comprising an outer shell, moisture barrier, and thermal liner. Wildland firefighter coats, shirts, and pants are generally a single fabric layer. They are functionally similar to the outer shell of structural gear. Wildland textiles must meet the performance requirements outlined in NFPA 1977 [NFPA 1977], which are specifically tailored to the environmental and operational conditions encountered during wildland fire suppression.

In this study, 4 of the 9 commercially available wildland textiles previously reported in NIST Technical Note 2313 [27] were selected for stress testing. These four textile samples, designated as WL-C, WL-E, WL-F, and WL-H, were obtained in the form of fully assembled garments (brush shirts, pants, or overcoats) from three widely used wildland textile manufacturers, through three separate distributors.

WL-C: A coat labeled “non-fluorinated,” composed of a cotton and nylon blend.

WL-E: Pants made from a combination of heat-resistant, lightweight synthetic fiber and meta-aramid.

WL-F: Pants labeled “non-fluorinated,” composed of a blend of meta-aramid, para-aramid, and anti-static fibers designed for protection against electric arc hazards.

WL-H: A shirt labeled “hypoallergenic due to the exclusion of chemical finishes and coatings,” made from a blend of modacrylic, semi-synthetic lyocell fiber, and para-aramid.

Images and area density measurements for each textile are available in NIST Technical Note 2313 [27]. Prior to exposure and testing, all samples were stored individually in resealable plastic bags for up to 610 days, in the dark, at room temperature to minimize environmental degradation and preserve material integrity.

2.5. PFAS Analytical Standards

In addition to the 55 PFAS previously quantified in unstressed structural firefighter gloves, hoods, and wildland firefighter coats, shirts, and pants reported in NIST Technical Note 2313 [27], this study also reports the concentration of the perfluoroalkane sulfonamido ethanol (FASE) class: N-methyl perfluorobutane sulfonamido ethanol (MeFBSE). The selection of PFAS analyzed in this study was informed by prior literature, the professional expertise of NIST researchers, and consultations with external subject matter experts. A complete list of all PFAS analyzed, along with their corresponding reference standards, is provided in **Table 1** and Appendix A.1.

2.6. PFAS Analysis

Three analytical procedures, referred to in this report as nonvolatile, semivolatile, and volatile methods, were previously developed for the characterization of a chemically diverse range of PFAS in firefighter gear. The specific analytical methods used for each PFAS are listed in **Table 1**. Detailed methodologies were originally described in NIST Technical Notes 2248 [24], 2260 [25], and 2313 [27].

Briefly, in the nonvolatile method, PFAS were extracted from stressed textile samples via sonication in methanol at 25 °C, followed by centrifugation, filtration through graphitized carbon solid-phase extraction (SPE) cartridges (ENVI-Carb, 500 mg × 6 mL), and evaporation to dryness under a nitrogen stream at 40 °C. The dried extracts were reconstituted in methanol and analyzed using liquid chromatography–tandem mass spectrometry (LC-MS/MS). For the semivolatile and volatile methods, PFAS were co-extracted from textile samples by sonication in ethyl acetate at 25 °C, followed by centrifugation, filtration through graphitized carbon SPE tubes (500 mg × 6 mL), and evaporation under nitrogen to a final volume of 2 mL at 35 °C. Resulting extracts were analyzed by LC-MS/MS for semivolatile PFAS and by gas chromatography–mass spectrometry (GC-MS) for volatile PFAS. Prior to analysis, the samples were stored in the dark, at ambient temperature, and inside plastic resealable bags after stressing for up to 299 days.

Table 1. Class names and abbreviations as well as individual compound names, abbreviations, analytical method used for quantification (i.e., NV for nonvolatile, SV for semivolatile, or V for volatile) as well as Chemical Abstract Service Registry Numbers (CAS RN) of all PFAS analyzed in this publication.

Class	Name	Analytical Method	CAS RN
Perfluorocarboxylic acids (PFCA)	Perfluorobutanoic acid (PFBA)	NV	375-22-4
	Perfluoropentanoic acid (PFPeA)	NV	2706-90-3
	Perfluorohexanoic acid (PFHxA)	NV	307-24-4
	Perfluoroheptanoic acid (PFHpA)	NV	375-85-9
	Perfluorooctanoic acid (PFOA)	NV	335-67-1
	Perfluorononanoic acid (PFNA)	NV	375-95-1
	Perfluorodecanoic acid (PFDA)	NV	335-76-2
	Perfluoroundecanoic acid (PFUnDA)	NV	2058-94-8
	Perfluorododecanoic acid (PFDoDA)	NV	307-55-1
	Perfluorotridecanoic acid (PFTrDA)	NV	72629-94-8
	Perfluorotetradecanoic acid (PFTeDA)	NV	376-06-7
Perfluoroalkane sulfonic acids (PFSA)	Perfluoropropane sulfonic acid (PFPrS)	NV	423-41-6
	Perfluorobutane sulfonic acid (PFBS)	NV	375-73-5
	Perfluoropentane sulfonic acid (PFPeS)	NV	2706-91-4
	Perfluorohexane sulfonic acid (PFHxS)	NV	108427-53-8
	Perfluoroheptane sulfonic acid (PFHpS)	NV	375-92-8
	Perfluorooctane sulfonic acid (PFOS)	NV	45298-90-6
	Perfluorononane sulfonic acid (PFNS)	NV	68259-12-1
	Perfluorodecane sulfonic acid (PFDS)	NV	335-77-3
Perfluoroalkane sulfonamides (FASA)	Perfluorobutane sulfonamide (FBSA)	NV	30334-69-1
	Perfluorohexane sulfonamide (FHxSA)	NV	41997-13-1
	Perfluorooctane sulfonamide (FOSA)	NV	754-91-6
	<i>N</i> -Methyl perfluorobutane sulfonamide (MeFBSA)	SV	68298-12-4
	<i>N</i> -Methyl perfluorooctane sulfonamide (MeFOSA)	SV	31506-32-8
Perfluoroalkane sulfonamido acetic acids (FASAA)	<i>N</i> -Ethyl perfluorooctane sulfonamide (EtFOSA)	SV	4151-50-2
	Perfluorooctane sulfonamido acetic acid (FOSAA)	NV	2806-24-8
	<i>N</i> -Methyl perfluorooctane sulfonamido acetic acid (MeFOSAA)	NV	2355-31-9
Perfluoroalkane sulfonamido ethanols (FASE)	<i>N</i> -Ethyl perfluorooctane sulfonamido acetic acid (EtFOSAA)	NV	2991-50-6
	<i>N</i> -Methyl perfluorobutane sulfonamido ethanol (MeFBSE)	SV	34454-97-2
	<i>N</i> -Methyl perfluorooctane sulfonamido ethanol (MeFOSE)	SV	24448-09-7
Per- and polyfluoroalkyl ether acids (PPEA)	<i>N</i> -Ethyl perfluorooctane sulfonamido ethanol (EtFOSE)	SV	1691-99-2
	Perfluoro-3-methoxypropanoic acid (PF4OPeA)	NV	377-73-1
	Perfluoro-2-ethoxyethane sulfonic acid (PFEEESA)	NV	113507-82-7
	Perfluoro-4-methoxybutanoic acid (PF5OHxA)	NV	863090-89-5
	Perfluoro-3,6-dioxahexanoic acid (3-6-OPFHxA)	NV	151772-58-6
	Hexafluoropropylene oxide dimer acid (HFPO-DA)	NV	13252-13-6
	4,8-Dioxa-3H-perfluorononanoic acid (ADONA)	NV	919005-14-4
	9-Chlorohexadecafluoro-3-oxanone-1-sulfonic acid (9Cl-PF3ONS)	NV	756426-58-1
	11-Chloroeicosafuoro-3-oxaundecane-1-sulfonic acid (11Cl-PF3OUs)	NV	763051-92-9

Table 1. (Continued)

Class	Name	Analytical Method	CAS RN
n:2 Fluorotelomer acrylates (n:2 FTAc)	8:2 Fluorotelomer acrylate (8:2 FTAc)	V	27905-45-9
	10:2 Fluorotelomer acrylate (10:2 FTAc)	V	17741-60-5
n:2 Fluorotelomer methacrylates (n:2 FTMAC)	6:2 Fluorotelomer methacrylate (6:2 FTMAC)	V	2144-53-8
	8:2 Fluorotelomer methacrylate (8:2 FTMAC)	V	1996-88-9
	10:2 Fluorotelomer methacrylate (10:2 FTMAC)	V	2144-54-9
n:2 Fluorotelomer acetates (n:2 FTOAc)	8:2 Fluorotelomer acetate (8:2 FTOAc)	V	37858-04-1
	10:2 Fluorotelomer acetate (10:2 FTOAc)	V	37858-05-2
n:2 Fluorotelomer alcohols (n:2 FTOH)	4:2 Fluorotelomer alcohol (4:2 FTOH)	V	2043-47-2
	5:2 Secondary fluorotelomer alcohol (5:2 sFTOH)	V	914637-05-1
	6:2 Fluorotelomer alcohol (6:2 FTOH)	V	647-42-7
	7:2 Secondary fluorotelomer alcohol (7:2 sFTOH)	V	24015-83-6
	8:2 Fluorotelomer alcohol (8:2 FTOH)	V	678-39-7
n:2 Fluorotelomer sulfonic acids (n:2 FTS)	10:2 Fluorotelomer alcohol (10:2 FTOH)	V	87017-97-8
	4:2 Fluorotelomer sulfonic acid (4:2 FTS)	NV	757124-72-4
	6:2 Fluorotelomer sulfonic acid (6:2 FTS)	NV	27619-97-2
	8:2 Fluorotelomer sulfonic acid (8:2 FTS)	NV	39108-34-4
	10:2 Fluorotelomer sulfonic acid (10:2 FTS)	NV	120226-60-0

2.7. Abrasion

A total of 8 hoods and 4 wildland textiles were subjected to mechanical abrasion following standardized protocols outlined in ISO 12947-3, Textiles. Determination of Abrasion Resistance of Fabrics by the Martindale Method. Part 3: Determination of Mass Loss [28], and ASTM D4966, Standard Test Method for Abrasion Resistance of Textile Fabrics (Martindale Abrasion Tester Method) [29], using a Martindale abrasion tester (James Heal Co. Ltd., United Kingdom). Abrasion testing was focused on hood and wildland textiles, which have thinner constructions and surface-applied treatments that may be more susceptible to mechanical removal than the multilayer, reinforced materials used in structural firefighter gloves.

Circular textile specimens approximately 38 mm in diameter were cut from each sample using methanol-rinsed scissors, and their initial mass was recorded. Each specimen was mounted in a sample holder with a polyurethane foam backing disk and secured in the abrasion tester. A uniform pressure of 12.0 kPa \pm 0.2 kPa was applied between the test textile and a standard abradant fabric, consisting of plain-weave worsted wool supported on standard felt. To minimize cross-contamination between samples, both the abradant fabric and the polyurethane foam backing disk were replaced for each textile. Up to four textile replicates cut from the same base textile were abraded concurrently; to further prevent airborne contamination, custom clear polycarbonate dome dividers were installed within the tester. These dividers were rinsed with methanol between test runs.

Each textile specimen was subjected to abrasion cycles (“rubs”) following a translational Lissajous motion at 47.5 revolutions per minute, with a maximum stroke length of 60.5 mm. Wildland firefighter textiles were abraded for 20,000 rubs, except for textile WL-H, which was limited to 5,000 rubs due to substantial sample degradation observed at that stage. Structural firefighter hood textiles were likewise targeted for 20,000 rubs; however, HD-A (1,000 rubs), HD-C (2,000 rubs), HD-E (10,000 rubs), and HD-F (12,000 rubs) were stopped early because significant sample degradation was observed at those respective points. Following abrasion, each textile was removed from the tester and weighed. All abraded samples were stored individually in the dark at room temperature in 15 mL polypropylene centrifuge tubes for up to 88 days until chemical extraction and analysis.

2.8. Thermal Stressing

A total of 10 glove layers and 8 hood textiles were subjected to high-temperature exposure using a hot air circulating oven (Model EQ-DHG-9000JB, MTI Corporation, Richmond, CA) following procedures adapted from NFPA 1971 [21] and ASTM F2894-19, Standard Test Method for Evaluation of Materials, Protective Clothing, and Equipment for Heat Resistance Using a Hot Air Circulating Oven [30]. Wildland textiles were not subjected to thermal stressing, as these garments may not routinely be exposed to sustained high temperatures under field conditions.

Prior to sample exposure, the convection oven was preheated to a stable temperature range of 260 °C to 268 °C for at least 30 minutes. Internal oven temperature was verified using a

thermocouple suspended in the center of the oven chamber. Sections of hood textiles were cut to dimensions of approximately $152 \text{ mm} \pm 6 \text{ mm}$ by $50 \text{ mm} \pm 6 \text{ mm}$ using methanol-rinsed scissors, and their initial masses were recorded. For gloves, each individual textile layer was carefully dissected from the glove using methanol-rinsed scissors, and the mass of each layer was measured prior to exposure.

Textile sections were individually suspended inside the oven using metal hooks, ensuring that no part of the sample came into contact with oven walls or other specimens. Samples were exposed one at a time to avoid cross-contamination. To minimize thermal fluctuation, the oven door was closed within 10 seconds of opening for sample placement. Once the internal temperature returned to $260 \text{ }^\circ\text{C}$, the textile was exposed for 5 minutes under continuous air recirculation.

Following thermal stressing, each section was removed from the oven and placed on a cooling rack at ambient conditions. The mass of each section was recorded after cooling. To prevent contamination from contact with the metal hook, the portion of the fabric that had been in contact with the hook was trimmed and discarded prior to extraction. All heat-exposed textile samples were stored individually in resealable plastic bags, kept in the dark at room temperature for up to 57 days until subsequent chemical extraction and analysis.

2.9. Weathering

Four wildland textiles were subjected to accelerated weathering using a QUV Accelerated Weathering Tester (Q-Lab, Westlake, OH), in accordance with ISO 4892-3:2016, Plastics — Methods of Exposure to Laboratory Light Sources — Part 3: Fluorescent UV Lamps [31], and ASTM G154, Standard Practice for Operating Fluorescent Ultraviolet (UV) Lamp Apparatus for Exposure of Nonmetallic Materials [32]. Wildland textiles were selected for weathering exposure because these materials are expected to experience greater levels of solar radiation during field use compared with other types of firefighter gear.

Textile sections ($76 \text{ mm} \pm 6 \text{ mm}$ by $152 \text{ mm} \pm 6 \text{ mm}$) were cut using methanol-rinsed scissors and mounted individually in QUV specimen holders. Samples were exposed in a QUV tester programmed with the following cycle: 8 hours of dry UV exposure (irradiance: 0.76 W/m^2 at 340 nm; black-panel temperature: $50 \text{ }^\circ\text{C} \pm 3 \text{ }^\circ\text{C}$), followed by a 0.25 hour water spray period (UV lamps off; black-panel temperature uncontrolled), and a 3.75 hour condensation period (UV lamps off; black-panel temperature: $50 \text{ }^\circ\text{C} \pm 3 \text{ }^\circ\text{C}$). This cycle was repeated 24 additional times, resulting in a total exposure duration of 300 hours.

Up to 12 samples were weathered simultaneously; however, each was mounted in a separate QUV specimen holder to prevent water runoff or cross-contamination between samples. After weathering, the textile sections were removed, and any portion that had been shielded from UV exposure by the holder frame was trimmed away using methanol-rinsed scissors. QUV specimen holders were thoroughly cleaned with methanol between exposure runs to further minimize cross-contamination. Weathered textile samples were stored in resealable plastic bags, in the dark, at ambient temperature for up to 299 days until extraction and chemical analysis.

3. Results

Presented below are PFAS measurements in firefighter textiles after abrasion, thermal stressing, or weathering. Each sample was subjected to only one stressing process; PFAS data are not reported for textiles exposed to multiple processes. Mass changes associated with abrasion and thermal stressing are also reported.

3.1. Abrasion

3.1.1. Changes in Textile Mass with Abrasion

Only hood and wildland textiles were abraded. Minor changes in sample mass were observed during abrasion, consistent with material loss from contact with the abrasive fabric (**Table 2**). The fractional mass changes may underestimate actual mass loss, as portions of each section were shielded by the attachment device. Due to this limitation and the relatively small magnitude of the changes, PFAS concentrations in abraded textiles are reported as μg -PFAS per kg of abraded sample. One textile exhibited a slight increase in mass following abrasion, likely due to transfer of material from the abrasive fabric or polyurethane foam backing disk. No measurable PFAS was detected in either sample, confirming that PFAS detected in the abraded samples originated solely from the textiles.

Table 2. Average and standard deviation of the quadruplicate measurements of fractional mass change in textile samples after abrasion. Positive values indicate increased mass following abrasion while negative values indicate decreased mass following abrasion.

Textile	Average \pm Standard Deviation Mass Change Following Abrasion (%)	Number of Abrasion Cycles (Rubs)
HD-A	-0.84 \pm 0.13	1,000
HD-B	0.06 \pm 0.03	20,000
HD-C	-1.54 \pm 0.37	2,000
HD-D	-0.13 \pm 0.04	20,000
HD-E	-1.00 \pm 0.21	10,000
HD-F	-1.09 \pm 0.18	12,000
HD-G	-0.58 \pm 0.03	20,000
HD-H	-0.83 \pm 0.18	20,000
WL-C	-0.71 \pm 0.10	20,000
WL-E	-0.03 \pm 0.02	20,000
WL-F	-0.07 \pm 0.01	20,000
WL-H	-0.38 \pm 0.06	5,000

3.1.2. PFAS in Abraded Firefighter Hoods and Wildland Textiles

Across 8 abraded hood textiles, 5 individual PFAS were quantified above reporting limits, with between 1 and 4 PFAS detected per textile (**Figure 1; Tables 15 to 29**). Detected compounds included perfluorocarboxylic acids (PFCAs; 3 perfluorinated carbons), perfluoroalkane sulfonic acids (PFSAs; 6 and 8 perfluorinated carbons), and per- and polyfluoroalkyl ether acids (PPEAs; 3 and 6 perfluorinated carbons). The most frequently observed PFAS in abraded hood textiles were PFBA (4 textiles), PFHxS (6 textiles), and PFOS (5 textiles), though all occurred at concentrations below 2 µg/kg (**Tables 15 to 29**). The highest concentrations were observed for PFBA (1.51 µg/kg ± 0.69 µg/kg in HD-E; **Table 23**).

Across four abraded wildland textiles, 11 PFAS were quantified above reporting limits, with between 1 and 9 PFAS detected per textile (**Figure 1; Tables 31 to 37**). Detected compounds included PFCAs (3 to 6, and 9 perfluorinated carbons), PFSAs (4 and 8 perfluorinated carbons), perfluoroalkane sulfonamides (FASAs; 4 and 8 perfluorinated carbons), PPEAs (3 perfluorinated carbons), and fluorotelomers (6 perfluorinated carbons). The most frequently observed PFAS in abraded wildland textiles were PFBA (4 textiles), PFPeA (3 textiles), and PFHxA (3 textiles), though all occurred at concentrations below 70 µg/kg (**Tables 31 to 37**). One fluorotelomer alcohol, 6:2 FTOH, was quantified above reporting limits in two abraded wildland firefighter textiles and exhibited the highest concentrations of any PFAS measured: 460 µg/kg ± 110 µg/kg (mean of total concentrations from triplicate analysis ± combined standard uncertainty) in WL-E (**Table 33**) and 350 µg/kg ± 38 µg/kg in WL-F (**Table 35**).

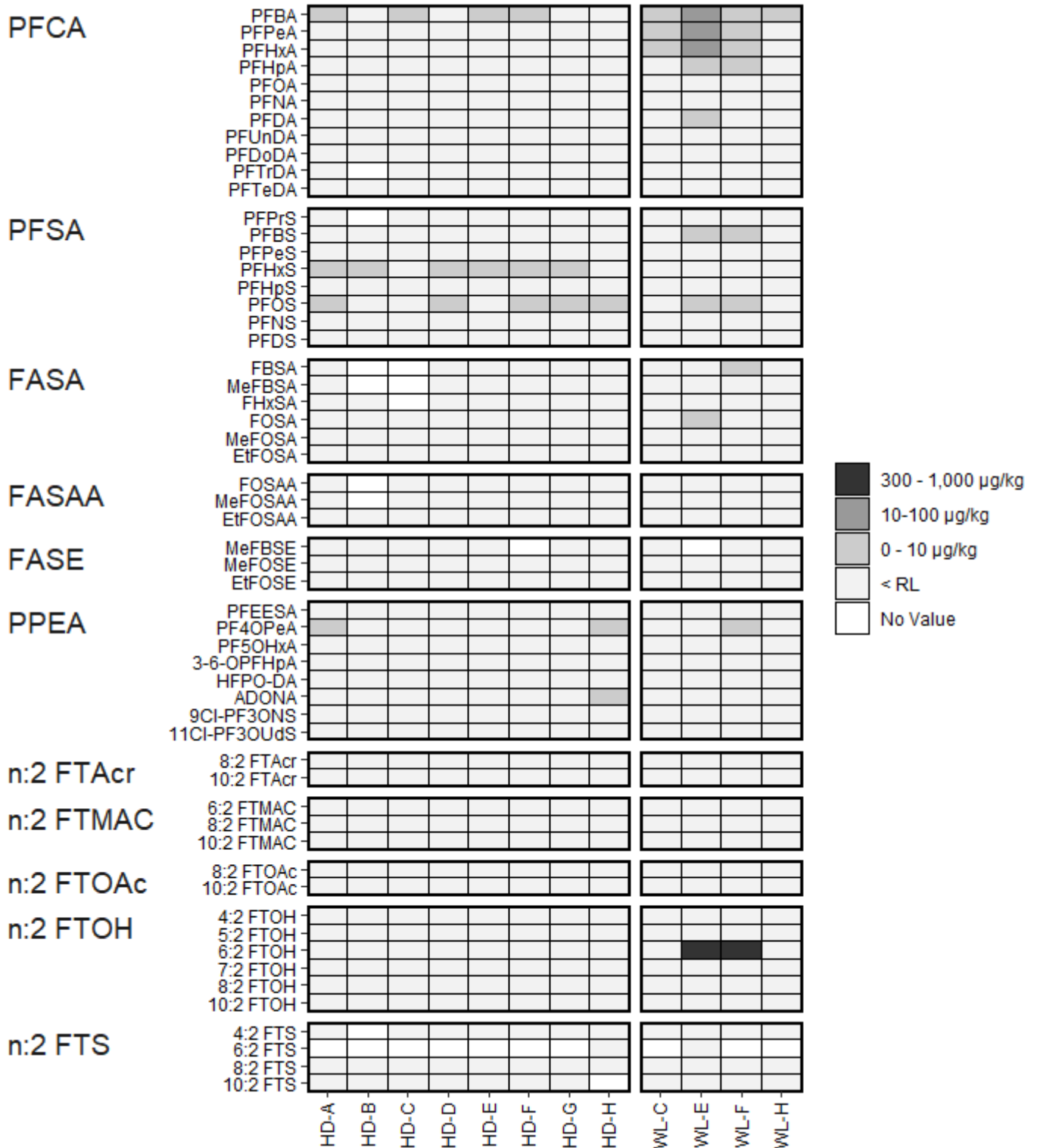


Figure 1. Average PFAS concentrations (μg PFAS/kg textile; ppb mass ratio) from triplicate analysis of structural firefighter hoods (HD-A to HD-H) and wildland firefighter coats (WL-C), pants (WL-E, -F), and shirts (WL-H) following abrasion. Values not meeting QC standards are shown in white.

Following abrasion, total PFAS concentrations in wildland textiles ranged from 2.79 $\mu\text{g}/\text{kg}$ \pm 0.19 $\mu\text{g}/\text{kg}$ (WL-H; **Table 37**) to 573 $\mu\text{g}/\text{kg}$ \pm 118 $\mu\text{g}/\text{kg}$ (WL-E; **Table 33**) (**Figure 2**). WL-F had the second highest total PFAS concentration, with a total PFAS concentration of 362 $\mu\text{g}/\text{kg}$ \pm 40 $\mu\text{g}/\text{kg}$ (**Table 35**).

In hood textiles, total PFAS concentrations following abrasion ranged from 0.041 $\mu\text{g}/\text{kg}$ \pm 0.025 $\mu\text{g}/\text{kg}$ (HD-B; **Table 17**) to 1.58 $\mu\text{g}/\text{kg}$ \pm 0.69 $\mu\text{g}/\text{kg}$ (HD-E; **Table 23**) (**Figure 2**). Previous work by Maizel et al. [25] reported low individual ($< 0.286 \mu\text{g}/\text{kg}$) and low total PFAS concentrations ($< 0.55 \mu\text{g}/\text{kg}$ in the worsted wool abradant fabric; and $< 0.278 \mu\text{g}/\text{kg}$ in the polyurethane foam). Based on those findings, these samples were not re-tested in the present study and were considered acceptable for use in abrasion stressing.

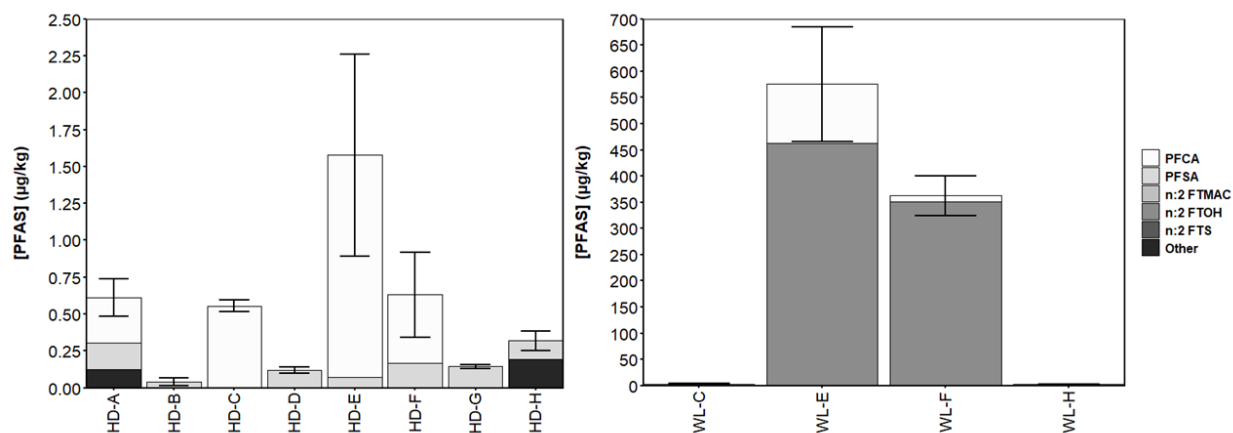


Figure 2. Total PFAS concentrations determined from triplicate analysis of firefighter hood textiles (left) and wildland textiles (right) following abrasion. Error bars indicate the combined standard uncertainty of total concentrations.

3.1.3. PFAS Changes After Abrasion

Relative to unstressed structural firefighter hood textiles, the total number of individual PFAS detected across all hood samples remained at five following abrasion (PFBS, PFOS, PFOA, FOSA, and PFTeDA); however, the specific compounds detected differed from those observed in unstressed textiles (PFBA, PFHxS, PFOS, PF4OPeA, and ADONA). The number of individual PFAS detected per hood textile ranged from 1 to 3 in unstressed textiles and from 1 to 4 following abrasion (**Figures 26 to 28**). Total PFAS concentrations were higher in 7 of 8 hood textiles following abrasion (**Figure 3**), with the median increasing by 3 $\mu\text{g}/\text{kg}$ ($1.07 \mu\text{g}/\text{kg} \pm 0.14 \mu\text{g}/\text{kg}$ to $3.96 \mu\text{g}/\text{kg} \pm 0.79 \mu\text{g}/\text{kg}$). Only HD-B showed a decrease ($0.569 \mu\text{g}/\text{kg} \pm 0.095 \mu\text{g}/\text{kg}$ to $0.041 \mu\text{g}/\text{kg} \pm 0.025 \mu\text{g}/\text{kg}$). The largest relative increase among textiles with PFAS initially above reporting limits occurred in HD-C (404 % increase; $0.110 \mu\text{g}/\text{kg} \pm 0.052 \mu\text{g}/\text{kg}$ to $0.554 \mu\text{g}/\text{kg} \pm 0.040 \mu\text{g}/\text{kg}$). Among those below reporting limits prior to abrasion, HD-E showed the largest increase in total PFAS (from below reporting limit to $1.58 \mu\text{g}/\text{kg} \pm 0.69 \mu\text{g}/\text{kg}$). PFBA and PFOS primarily drove these increases, contributing between 0 % to 100 % and 0 % to 73 % of the total concentrations,

respectively. However, total PFAS concentrations in all hood textiles both abraded or unstressed remained below 2.5 $\mu\text{g}/\text{kg}$.

Relative to unstressed wildland textiles, the total number of individual PFAS detected across all samples increased from 10 in unstressed to 11 following abrasion, with seven PFAS detected under both conditions (6:2 FTOH, PFBA, PFBS, PFHpA, PFHxA, PFOS, and PFPeA). The number of individual PFAS detected per wildland firefighter gear textile ranged from 1 to 9 in both unstressed textiles and after abrasion (**Figures 29 to 30**). Total PFAS concentrations in abraded wildland textiles generally decreased with abrasion (**Figure 3**). Median total concentrations fell from 5,520 $\mu\text{g}/\text{kg}$ in unstressed textiles to 938 $\mu\text{g}/\text{kg}$ in abraded textiles. Only WL-C showed an increase following abrasion (0.50 $\mu\text{g}/\text{kg} \pm 0.02 \mu\text{g}/\text{kg}$ to 3.02 $\mu\text{g}/\text{kg} \pm 0.38 \mu\text{g}/\text{kg}$). The greatest decreases following abrasion occurred in WL-H (99 %; 200 $\mu\text{g}/\text{kg} \pm 30 \mu\text{g}/\text{kg}$ to 2.79 $\mu\text{g}/\text{kg} \pm 0.19 \mu\text{g}/\text{kg}$) and WL-F (97 %; 4,240 $\mu\text{g}/\text{kg} \pm 890 \mu\text{g}/\text{kg}$ to 362 $\mu\text{g}/\text{kg} \pm 40 \mu\text{g}/\text{kg}$). The decreases in PFAS concentration following abrasion were largely attributable to loss of 6:2 FTMAC and 6:2 FTOH. In unstressed wildland textiles, 6:2 FTMAC accounted for 70 % (WL-F) and 81 % (WL-E) of total PFAS and 6:2 FTOH for 100 % in WL-H. After abrasion, 6:2 FTMAC fell below reporting limits in all textiles, and 6:2 FTOH was below reporting limits in WL-H. However, 6:2 FTOH remained the most abundant PFAS in WL-E and WL-F, contributing approximately 80 % and 97 % of their totals, though overall PFAS concentrations were substantially lower after abrasion. Four PFAS were newly detected in at least one abraded wildland textile (PFDA, FBSA, FOSA, and PF4OPeA), all at low levels (below 1 $\mu\text{g}/\text{kg}$), while three compounds present in unstressed textiles (PFPeS, 6:2 FTMAC, and 6:2 FTS) were not observed after abrasion.

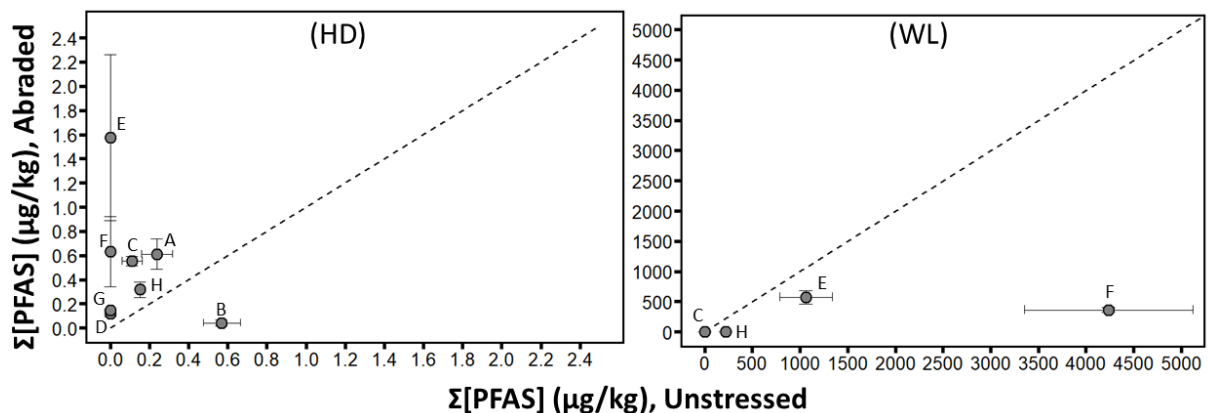


Figure 3. Total PFAS concentrations from triplicate analysis of abraded firefighter gear textiles (y-axis) versus unstressed textiles (x-axis). Error bars represent combined standard uncertainty. Panel labels denote textile type (HD = firefighter hood textiles; WL = wildland firefighter gear textiles), and individual textiles are identified by marker labels. The dashed line indicates a 1:1 ratio, where concentrations are equal in unstressed and abraded textiles.

3.2. Thermal Stressing

3.2.1. Change in Textile Mass After Thermal Stressing

Only gloves and hoods were thermally stressed. Glove and hood textile section masses were measured before and after exposure to thermal stressing, and all samples showed mass loss (**Table 3**). Although these losses were consistently greater than those observed during abrasion, PFAS concentrations are reported as μg PFAS / kg of textile post-exposure because the overall magnitude of change remained small. GL-B-MB melted within 1 min after thermal stressing in all trials; therefore, no data are reported for this sample.

Table 3. Average and standard deviation of measured fractional mass change in textile samples after thermal stressing. Negative values indicate decreasing mass. All thermal stressing results were done in triplicate.

Textile	Average \pm Standard Deviation Mass Change with Thermal stressing (%)
GL-A-MB	-6.3 \pm 1.9
GL-A-TL	-3.3 \pm 1.2
GL-B-IL	-2.2 \pm 0.6
GL-B-TL	-4.0 \pm 0.2
GL-C-IL	-36 \pm 0.5
GL-C-MB	-6.3 \pm 5.0
GL-C-TL	-4.5 \pm 2.4
GL-D-IL	-56 \pm 0.3
GL-D-MB	-0.3 \pm 3.2
GL-D-TL	-3.6 \pm 1.0
HD-A	-5.9 \pm 0.5
HD-B	-3.1 \pm 0.7
HD-C	-3.9 \pm 0.7
HD-D	-47 \pm 18
HD-E	-58 \pm 9.4
HD-F	-58 \pm 4.4
HD-G	-32 \pm 0.2
HD-H	-30 \pm 0.4

3.2.2. PFAS Changes in Thermally Stressed Gloves and Hoods Textiles

Across 10 structural glove textile layers exposed to thermal stressing, 19 individual PFAS were quantified above reporting limits, with 1 to 11 detected per sample (**Figure 4; Tables 5 to 14**). Detected compounds included PFCAs (3 to 5, 7, and 9 perfluorinated carbons), PFSAAs (4, 6, and 8 to 9 perfluorinated carbons), FASAs (4 and 8 perfluorinated carbons), FASEs (4 perfluorinated carbons), PPEAs (3 and 8 perfluorinated carbons), and fluorotelomers (4 to 10 perfluorinated carbons). The most frequently observed PFAS in thermally stressed glove textile layers were PFBA (6 textiles), PFPeA (5 textiles), PFBS (7 textiles), and MeFBSE (8 textiles). Concentrations among these PFAS were below 10 µg/kg (**Tables 5 to 14**), with the exception of PFBS (up to 24 µg/kg) and MeFBSE (up to 177 µg/kg). The highest concentrations were observed for MeFBSE (177 µg/kg ± 26 µg/kg in GL-C-MB; **Table 10**), 6:2 FTOH (360 µg/kg ± 40 µg/kg in GL-D-TL; **Table 14**), and 6:2 FTS (300 µg/kg ± 250 µg/kg in GL-B-IL; **Table 7**).

Across 8 hood textiles exposed to thermal stressing, 14 individual PFAS were quantified above reporting limits, with 7 to 12 PFAS detected per textile (**Figure 4; Tables 15 to 30**). Detected compounds included PFCAs (3 to 5, and 7 to 8 perfluorinated carbons), PFSAAs (3, 6, and 8 perfluorinated carbons), FASAs (8 perfluorinated carbons), PPEAs (3 to 4 perfluorinated carbons), and fluorotelomers (4 and 6 perfluorinated carbons). The most frequently observed PFAS in thermally stressed hood textiles were PFBA (8 textiles), PFPeA (8 textiles), PFHxA (8 textiles), PFOA (8 textiles), and 4:2 FTS (6 textiles), all occurred at concentrations below 5 µg/kg (**Tables 15 to 30**). The highest concentration was observed for 6:2 FTS (2.2 µg/kg ± 2.0 µg/kg in HD-D; **Table 22**).

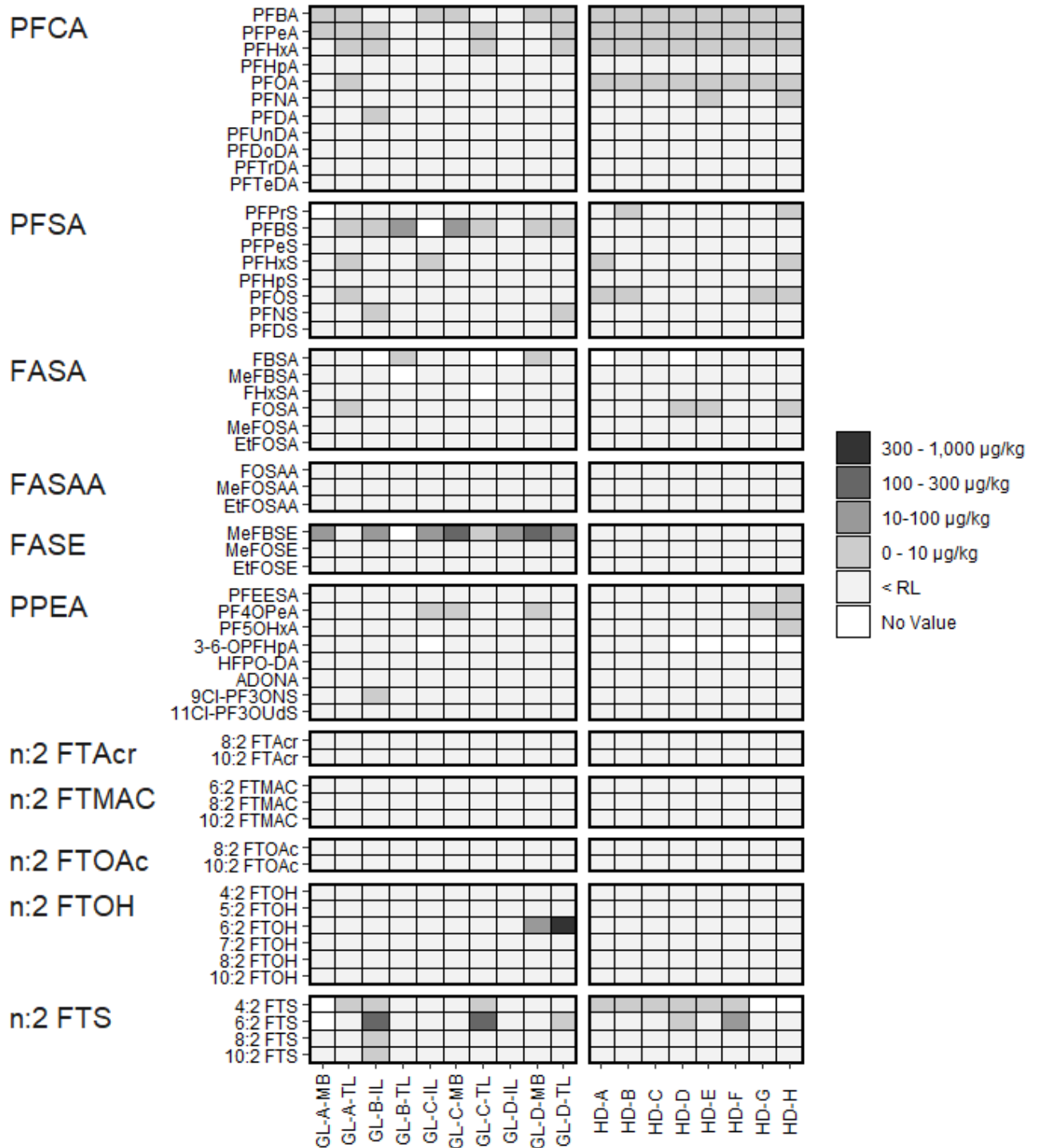


Figure 4. Average PFAS concentrations (μg PFAS/kg textile or ppb mass ratio) determined from triplicate analysis of structural firefighter glove layers (GL-A to GL-D) and hood textiles (HD-A to HD-H) after thermal stressing. Values not meeting QC standards are shown in white.

After thermal stressing, total PFAS concentrations in glove textiles (mean of total concentrations from triplicate analysis \pm combined standard uncertainty; **Figure 5**) ranged from 3.36 $\mu\text{g}/\text{kg}$ \pm 1.70 $\mu\text{g}/\text{kg}$ (GL-A-TL; **Table 6**) to 398 $\mu\text{g}/\text{kg}$ \pm 42 $\mu\text{g}/\text{kg}$ (GL-D-TL; **Table 14**). GL-B-IL had the second highest total PFAS concentration among glove textiles at 321 $\mu\text{g}/\text{kg}$ \pm 257 $\mu\text{g}/\text{kg}$ (**Table 7**).

In hood textiles, total PFAS concentrations after thermal stressing ranged from 1.18 $\mu\text{g}/\text{kg}$ \pm 0.25 $\mu\text{g}/\text{kg}$ (HD-C; **Table 20**) to 70 $\mu\text{g}/\text{kg}$ \pm 15 $\mu\text{g}/\text{kg}$ (HD-F; **Table 26**). A total of 7 of 8 thermally stressed hoods had total PFAS concentrations below 5 $\mu\text{g}/\text{kg}$ (**Figure 5**).

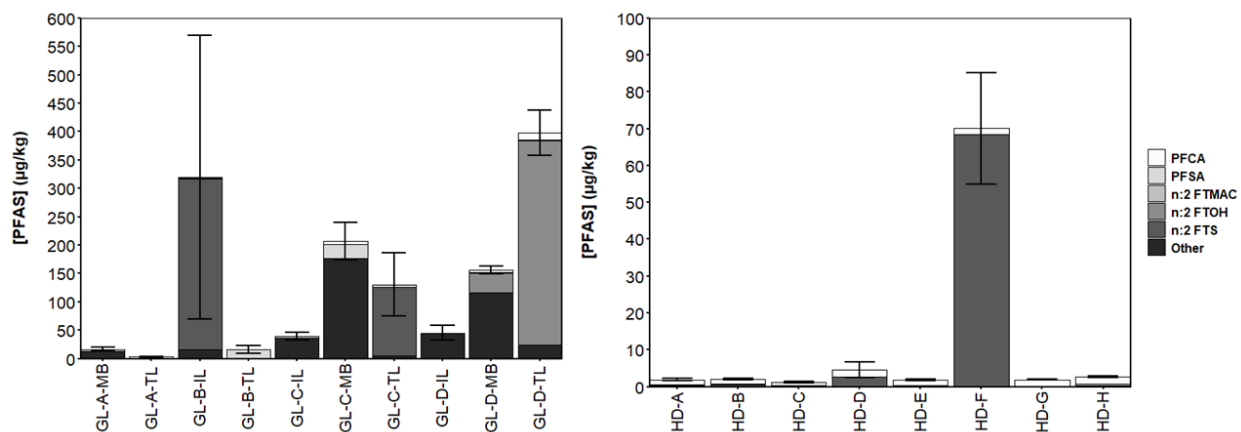


Figure 5. Total PFAS concentrations determined from triplicate analysis of structural firefighter glove layers (left) and firefighter hood textiles (right) after thermal stressing. Error bars indicate the combined standard uncertainty of total concentrations.

3.2.3. PFAS Changes After Thermal Stressing

For structural firefighter glove layer textiles, the total number of PFAS detected across all samples increased from 7 in unstressed textiles to 19 after thermal stressing. The number of individual PFAS detected per glove textile layer ranged from 2 to 6 in unstressed textiles and from 1 to 11 after thermal stressing (**Figures 22 to 25**). Total PFAS concentrations were higher in all 10 textile glove layers after thermal stressing (**Figure 6**), with the median increase of 1150 $\mu\text{g}/\text{kg}$ (from 180 $\mu\text{g}/\text{kg}$ to 1330 $\mu\text{g}/\text{kg}$). The largest relative increases among textile glove layers occurred in GL-D-TL (83900 %; 0.47 $\mu\text{g}/\text{kg}$ \pm 0.06 $\mu\text{g}/\text{kg}$ to 398 $\mu\text{g}/\text{kg}$ \pm 42 $\mu\text{g}/\text{kg}$), GL-C-TL (17200 %; 0.757 $\mu\text{g}/\text{kg}$ \pm 0.299 $\mu\text{g}/\text{kg}$ to 131 $\mu\text{g}/\text{kg}$ \pm 59 $\mu\text{g}/\text{kg}$), and GL-B-IL (16100 %; 1.98 $\mu\text{g}/\text{kg}$ \pm 0.18 $\mu\text{g}/\text{kg}$ to 321 $\mu\text{g}/\text{kg}$ \pm 257 $\mu\text{g}/\text{kg}$). The increases were primarily driven by 6:2 FTS and 6:2 FTOH, with 6:2 FTS contributing between 92 % and 93 % of the total concentrations in GL-C-TL and GL-B-IL, and 6:2 FTOH contributing 90 % in GL-D-TL. Thirteen PFAS were newly detected in textile glove layers only after thermal stressing, including short-, mid-, and long-chain PFCAs (PFHxA, PFOA, PFDA), PFSA (PFHxS, PFOS, PFNS), sulfonamide- and ether-based PFAS (MeFBSE, PF4OPeA, 9Cl-PF3ONS), and fluorotelomer sulfonates/alcohols (6:2 FTOH, 4:2 FTS, 8:2 FTS, and 10:2 FTS). MeFBSA was present only in unstressed textile layers but was not observed in thermally stressed textile layers. It should be noted that MeFBSE was a newly added analyte not

included in the unstressed glove analysis, yet it contributed between 74 % and 100 % of total PFAS concentrations in four of the glove layers (GL-C-IL, GL-C-MB, GL-D-IL, and GL-D-D-MB).

For hood textiles, the total number of PFAS detected across all samples increased from five in unstressed textiles to 14 after thermal stressing. The number of individual PFAS detected per hood textile ranged from 1 to 3 in unstressed textiles and from 5 to 12 following thermal stressing (**Figures 26 to 28**). Total PFAS concentrations were higher in all 8 structural hood textiles after thermal stressing (**Figure 7**), with the median increasing by 85 $\mu\text{g}/\text{kg}$ (1 $\mu\text{g}/\text{kg}$ to 86 $\mu\text{g}/\text{kg}$). The largest relative increases among textiles with PFAS initially above reporting limits occurred in HD-H (1700 %; 0.15 $\mu\text{g}/\text{kg} \pm 0.024 \mu\text{g}/\text{kg}$ to 2.692 $\mu\text{g}/\text{kg} \pm 0.489 \mu\text{g}/\text{kg}$) and HD-C (972 %; 0.110 $\mu\text{g}/\text{kg} \pm 0.052 \mu\text{g}/\text{kg}$ to 1.180 $\mu\text{g}/\text{kg} \pm 0.245 \mu\text{g}/\text{kg}$). Among those with all PFAS present below reporting limits prior to exposure to thermal stressing, HD-F showed the largest increase in total PFAS (from below reporting limit to 70 $\mu\text{g}/\text{kg} \pm 15 \mu\text{g}/\text{kg}$; **Table 26**). Increases in total PFAS after thermal stressing across all hood samples were primarily driven by 6:2 FTS (49 % to 97 % of total PFAS), PFBA (1 % to 44 %), and PFHxA (1 % to 44 %). Eleven PFAS were newly detected only after thermal stressing, including short- and mid-chain PFCAs (PFBA, PFPeA, PFHxA, PFNA), PFSAs (PFPrS, PFHxS), ether- and hydroxy-substituted PFAS (PFEESA, PF4OPeA, PF5OHxA), and fluorotelomer sulfonates (4:2 FTS, 6:2 FTS), while PFTeDA was observed only in unstressed hoods. Despite these changes, total PFAS concentrations in all thermally exposed remained below 100 $\mu\text{g}/\text{kg}$.

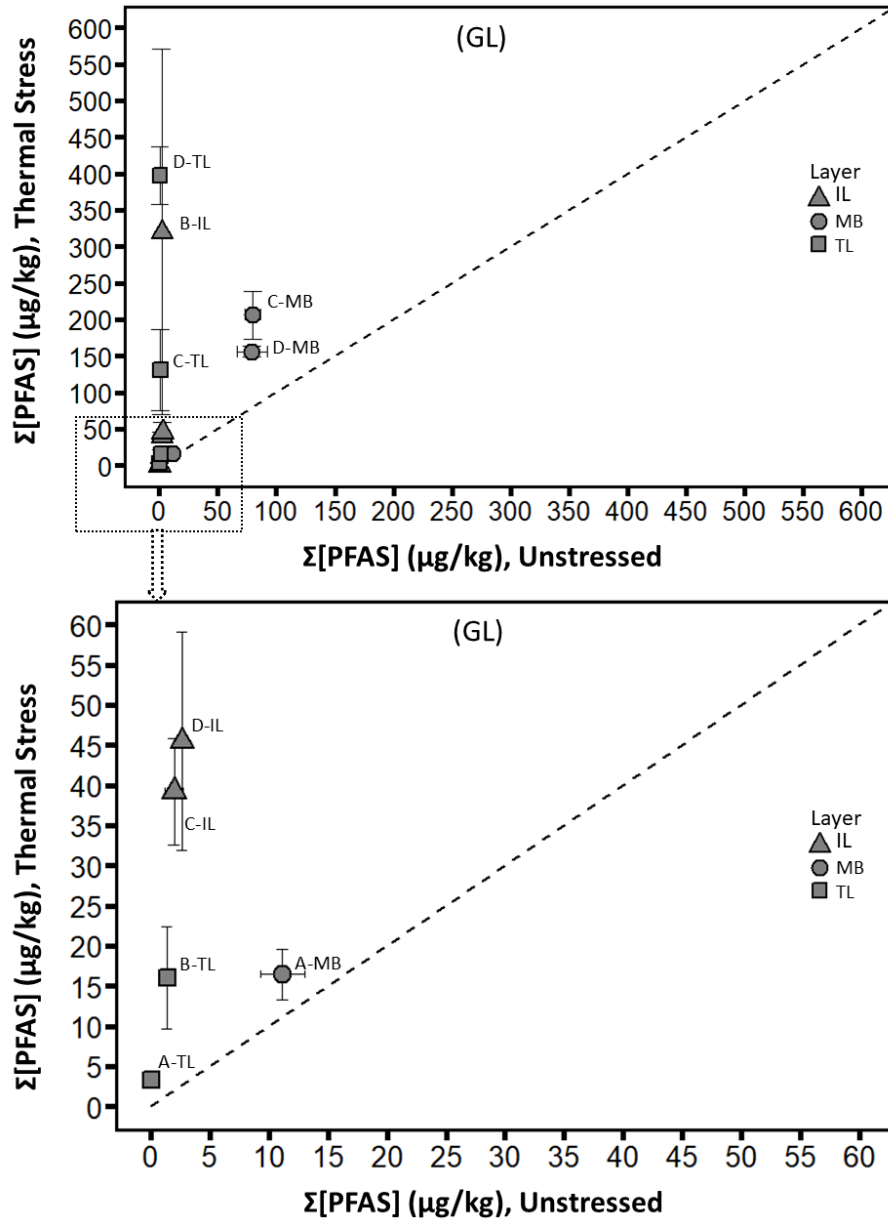


Figure 6. Total PFAS concentrations determined from triplicate analysis of firefighter glove layers following thermal stressing (y-axis) compared with corresponding unstressed textiles (x-axis). Error bars represent combined standard uncertainty. Textile type is indicated in panel label (GL = firefighter glove textiles), and individual textiles are indicated with marker labels. The dashed line denotes a 1:1 concentration ratio (i.e., equal concentrations measured in unstressed and textiles after thermal stressing). All glove layers are shown in the upper panel, with a zoomed inset displayed below.

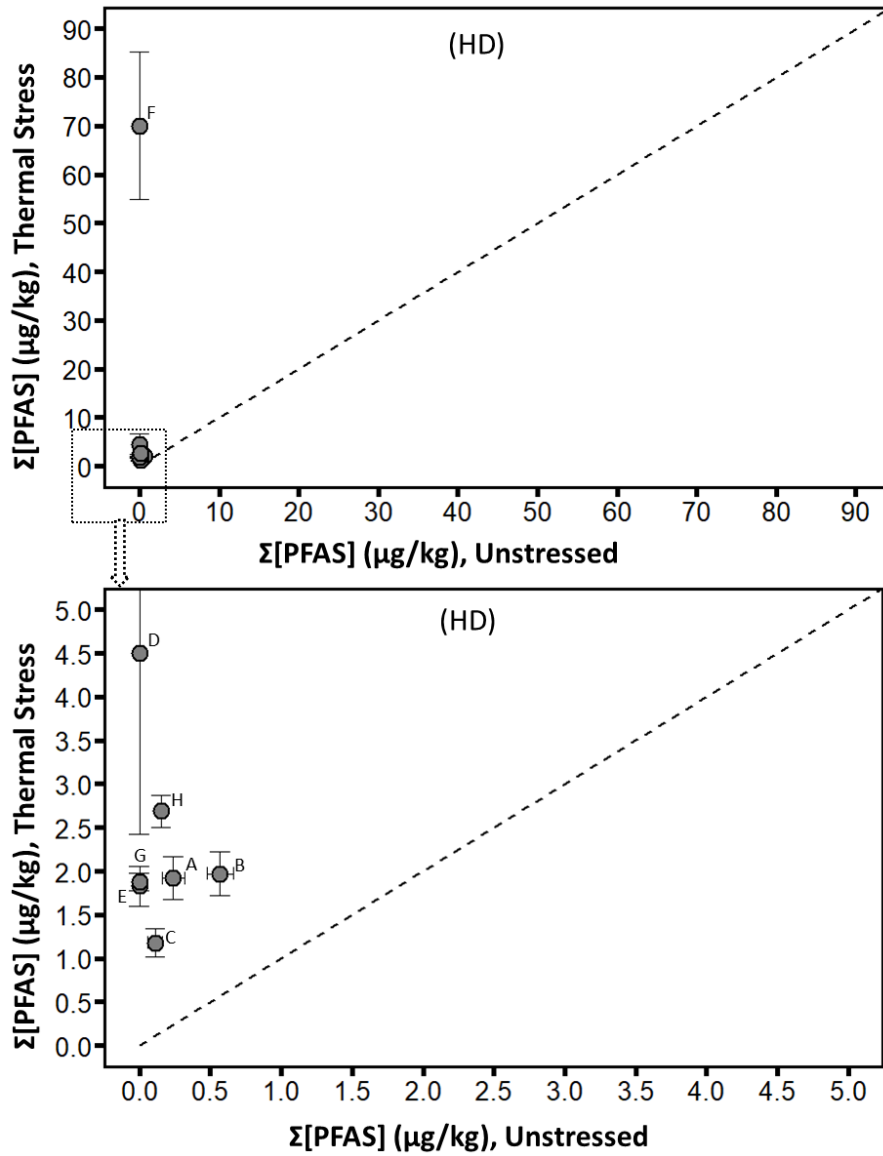


Figure 7. Total PFAS concentrations determined from triplicate analysis of firefighter hood textiles following thermal stressing (y-axis) compared with corresponding unstressed textiles (x-axis). Error bars represent combined standard uncertainty. Textile type is indicated in panel label (HD = firefighter hood textiles), and individual textiles are indicated with marker labels. The dashed line denotes a 1:1 concentration ratio (i.e., equal concentrations measured in unstressed and textiles after thermal stressing). All hood textiles are shown in the upper panel, with a zoomed inset displayed below.

3.3. Weathering

3.3.1. PFAS in Weathered Wildland Coats, Shirts, and Pants

Across the four weathered wildland firefighter gear textiles, ten PFAS were quantified above reporting limits, with between 6 and 9 PFAS detected per textile (**Figure 8; Tables 32 to 38**). Detected compounds included PFCAs (3 to 5 perfluorinated carbons), PFBS (4 perfluorinated carbons), FASAs (4 and 8 perfluorinated carbons), MeFBSE (4 perfluorinated carbons) and fluorotelomerization-derived PFAS (6 perfluorinated carbons). The most frequently identified PFAS were PFBS, FBSA, and MeFBSE which were detected in all four textiles, though all occurred at concentrations below 100 $\mu\text{g}/\text{kg}$. 6:2 FTOH and 6:2 FTMAC exhibited the highest concentrations of any PFAS measured, with 187 $\mu\text{g}/\text{kg} \pm 44$ in WL-E for 6:2 FTOH (**Table 34**), 1010 $\mu\text{g}/\text{kg} \pm 64$ $\mu\text{g}/\text{kg}$ in WL-F for 6:2 FTOH (**Table 36**), and 103 $\mu\text{g}/\text{kg} \pm 8$ $\mu\text{g}/\text{kg}$ in WL-F for 6:2 FTMAC (**Table 36**).

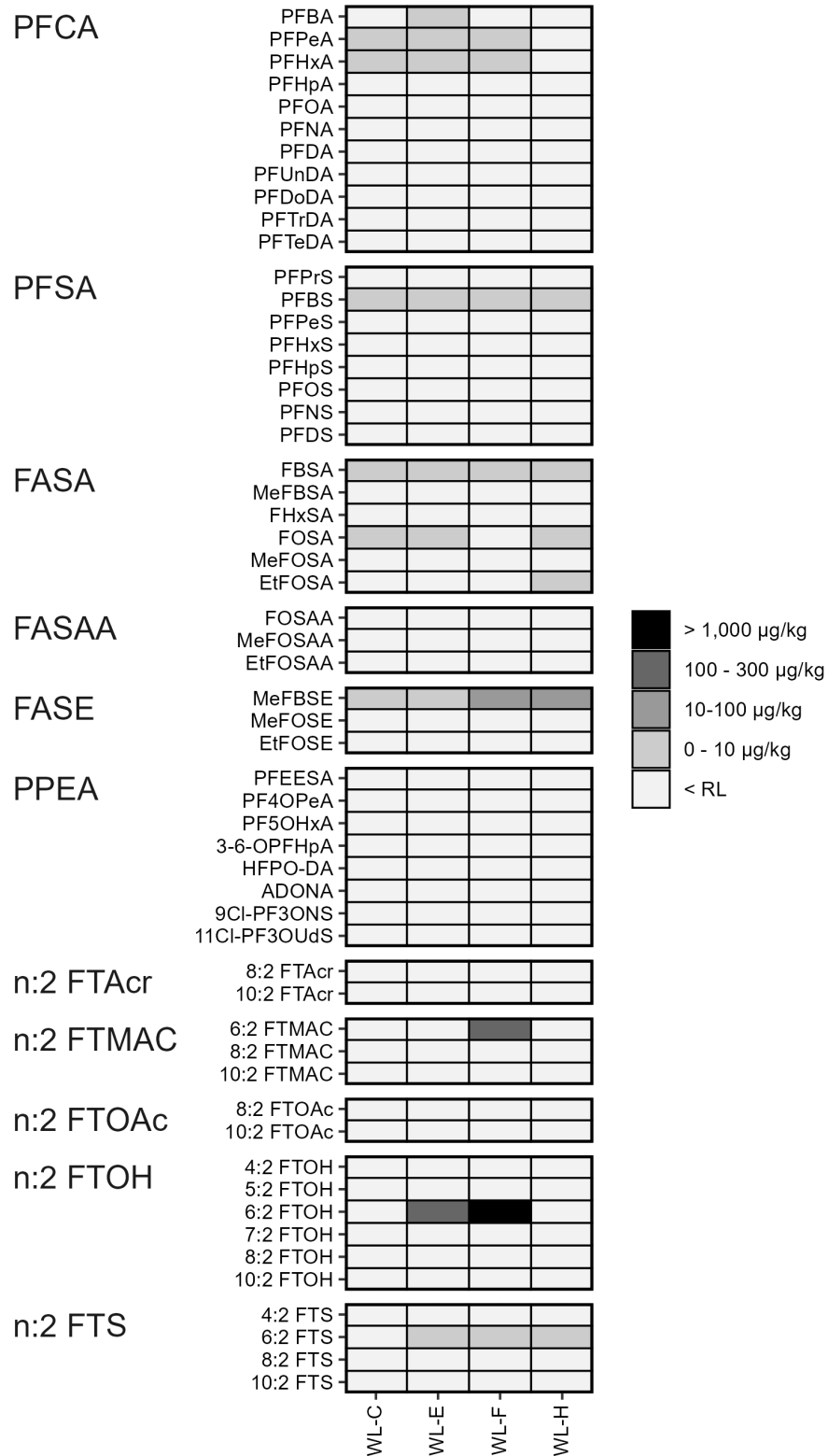


Figure 8. Average PFAS concentrations (μg PFAS/kg textile or ppb mass ratio) determined from triplicate analysis of wildland firefighter coats (WL-C), pants (WL-E, WL-F) and shirts (WL-H) following weathering.

Total PFAS concentrations in weathered wildland firefighter gear (mean of total concentrations from triplicate analysis \pm combined standard uncertainty; **Figure 9**) ranged from 6.98 $\mu\text{g}/\text{kg}$ \pm 4.27 $\mu\text{g}/\text{kg}$ (WL-C; **Table 32**) to 1140 $\mu\text{g}/\text{kg}$ \pm 73 $\mu\text{g}/\text{kg}$ (WL-F; **Table 36**). WL-E had the second highest total PFAS concentration among weathered wildland textiles at 216 $\mu\text{g}/\text{kg}$ \pm 51 $\mu\text{g}/\text{kg}$ (**Table 34**).

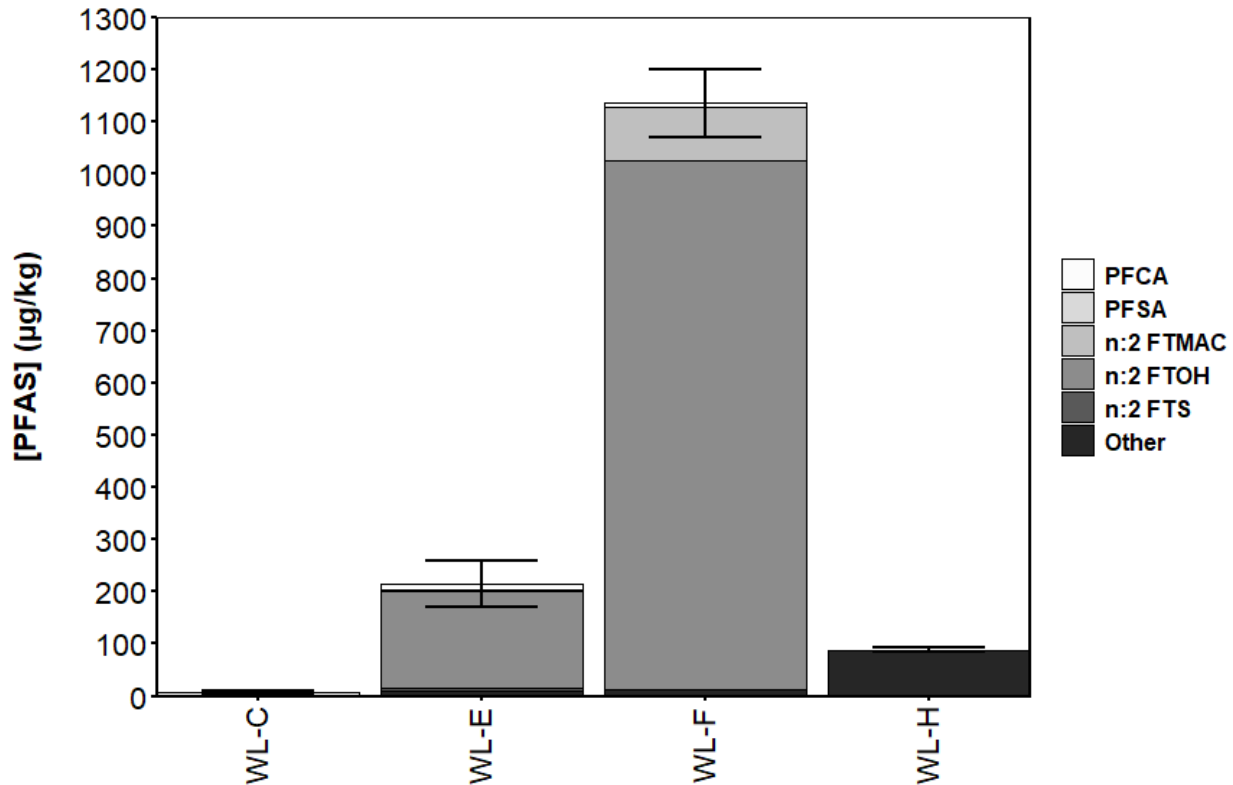


Figure 9. Total PFAS concentrations in wildland firefighter coats (WL-C), pants (WL-E, WL-F), and shirts (WL-H) following weathering. Error bars indicate the combined standard uncertainty of total concentrations. Bar color indicates PFAS class.

3.3.2. PFAS Changes in Weathered Wildland Coats, Shirts, and Pants

The total number of PFAS detected across weathered wildland textiles increased from 10 in unstressed textiles to 11 after weathering, with seven PFAS detected under both conditions (PFPeA, PFHxA, PFBA, PFBS, 6:2 FTMAC, 6:2 FTOH, and 6:2 FTS). The number of individual PFAS detected per wildland firefighter gear textile ranged from 1 to 9 in both unstressed textiles and after weathering (**Figures 29 to 30**). Total PFAS concentrations were lower in 3 of the 4 textiles after weathering (**Figure 10**), with the median decreasing by 3890 $\mu\text{g}/\text{kg}$ (from 5324 $\mu\text{g}/\text{kg}$ to 1440 $\mu\text{g}/\text{kg}$). Only WL-C showed an increase, from 0.50 $\mu\text{g}/\text{kg}$ \pm 0.02 $\mu\text{g}/\text{kg}$ to 6.98 $\mu\text{g}/\text{kg}$ \pm 4.27 $\mu\text{g}/\text{kg}$ (**Table 32**).

Decreases among textiles after weathering were observed in WL-E (80 % decrease; 1060 $\mu\text{g}/\text{kg}$ \pm 279 $\mu\text{g}/\text{kg}$ to 216 $\mu\text{g}/\text{kg}$ \pm 51 $\mu\text{g}/\text{kg}$; **Table 34**), WL-F (73 % decrease; 4240 $\mu\text{g}/\text{kg}$ \pm 890 to

1140 $\mu\text{g}/\text{kg} \pm 73 \mu\text{g}/\text{kg}$; **Table 36**), and WL-H (60 % decrease; 220 $\mu\text{g}/\text{kg} \pm 30 \mu\text{g}/\text{kg}$ to 88 $\mu\text{g}/\text{kg} \pm 4 \mu\text{g}/\text{kg}$; **Table 38**). These decreases were largely attributed to 6:2 FTMAC and 6:2 FTOH. In unstressed wildland textiles, 6:2 FTMAC accounted for 70 % in WL-F and 81 % in WL-E, while 6:2 FTOH contributed 100 % in WL-H. After weathering, 6:2 FTMAC fell below reporting limits in WL-E and decreased from 2980 $\mu\text{g}/\text{kg} \pm 820 \mu\text{g}/\text{kg}$ to 103 $\mu\text{g}/\text{kg} \pm 8 \mu\text{g}/\text{kg}$ in WL-F (**Table 36**). 6:2 FTOH also fell below reporting limits in WL-E but remained the dominant PFAS in WL-E and WL-F, contributing 87 % and 89 % of their totals, respectively, with concentrations similar to those in unstressed textiles.

The increase in WL-C was mainly due to PFHxA (0.391 $\mu\text{g}/\text{kg} \pm 0.022 \mu\text{g}/\text{kg}$ to 4.1 $\mu\text{g}/\text{kg} \pm 3.6 \mu\text{g}/\text{kg}$; **Table 32**) and MeFBSE (not reported in TN 2313 [27], but 1.86 $\mu\text{g}/\text{kg} \pm 0.22 \mu\text{g}/\text{kg}$ after weathering, **Table 32**). Three PFAS were newly detected in at least one weathered textile (FBSA, FOSA, and MeFBSE), all below 100 $\mu\text{g}/\text{kg}$, while three compounds found in unstressed textiles (PFHpA, PFPeS, and PFOS) were absent after weathering.

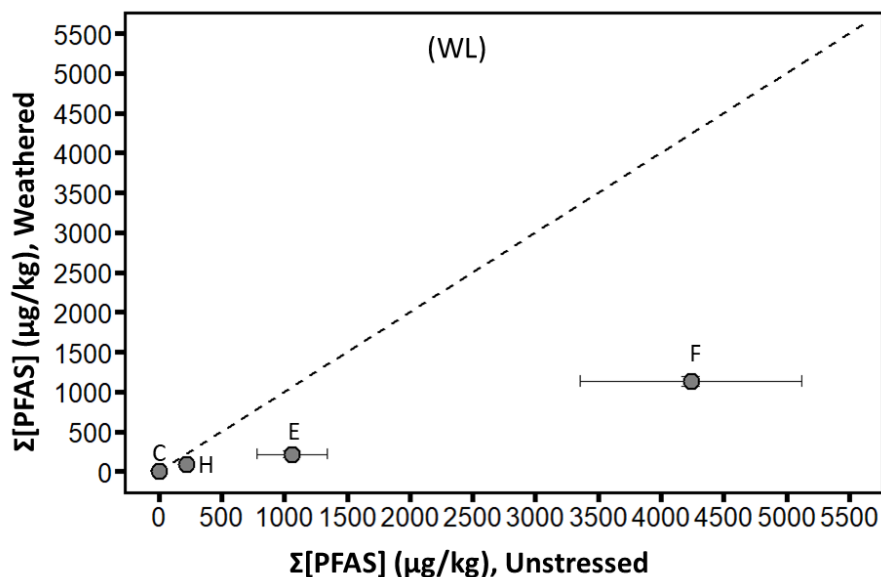


Figure 10. Total PFAS concentrations determined from triplicate analysis of wildland firefighter coats (WL-C), pants (WL-E, WL-F), and shirts (WL-H) following weathering (y-axis) compared with corresponding unstressed textiles (x-axis). Error bars represent combined standard uncertainty. Textile type is indicated in panel label (WL = wildland firefighter gear textiles), and individual textiles are indicated with marker labels. The dashed line denotes a 1:1 concentration ratio (i.e., equal concentrations measured in unstressed and textiles after weathering).

4. Discussion

Exposing firefighter gear textiles to stressing altered both individual and total PFAS concentrations, with outcomes varying by stress type and textile type (**Table 4**). Total PFAS concentrations increased in 7 of 8 firefighter hood textiles after abrasion stressing (median change: 157 % increase among samples with detectable baseline concentrations), whereas 3 of 4 wildland firefighter textiles exhibited decreases after abrasion stressing (median change: 91 % decrease). Thermal stressing increased total PFAS concentrations in all ten glove textile layers (median change: 1630 % increase among samples with detectable baseline concentrations) and all 8 hood textiles (median change: 755 % increase among samples with detectable baseline concentrations). Weathering decreased total PFAS concentrations in 3 of 4 wildland textiles (median change: 73 % decrease). These results indicate that multiple processes and differences among textile types influence how stressing influences PFAS concentrations.

The largest increases in total PFAS concentration occurred following abrasion of hood textiles and thermal stressing of glove textile layers and hood textiles (**Table 4**). In glove textile layers, increases in total PFAS concentrations after thermal stressing were primarily driven by MeFBSE (8 of 10 layers), 6:2 FTOH (2 of 10 layers), and 6:2 FTS (3 of 10 layers). MeFBSE was not previously reported in earlier reports, and neither 6:2 FTOH nor 6:2 FTS were detected in glove textile layers prior to thermal stressing, with the exception of 6:2 FTS in GL-A-MB. When totaled across all 10 glove textile layers after thermal stressing, MeFBSE (32 %), 6:2 FTOH (30 %), and 6:2 FTS (32 %) together accounted for 94 % of the total PFAS concentration.

In hood textiles, increases in total PFAS concentrations after thermal stressing were primarily driven by PFBA (8 of 8 textiles), PFHxA (8 of 8 textiles), and 6:2 FTS (2 of 8 textiles), none of which were detected in unstressed hood textiles. When totaled across all 8 hood textiles after thermal stressing, PFBA (5 %), PFHxA (6 %), and 6:2 FTS (82 %) together accounted for 93 % of the total PFAS concentration; notably, 79 % of the total 6:2 FTS was observed in HD-F. Following abrasion of hood textiles, increases in total PFAS concentrations were primarily driven by PFBA (4 of 8 textiles) and PFOS (5 of 8 textiles). When totaled across all 8 hood textiles after abrasion, PFBA (71 %) and PFOS (13 %) together accounted for 84 % of the total PFAS concentration.

Wildland textiles exhibited decreases in total PFAS concentrations following abrasion and weathering, primarily due to reductions in 6:2 FTOH and 6:2 FTMAC, which were the dominant PFAS prior to stressing. Notably, 6:2 FTMAC was not detected in any of the four wildland textiles after abrasion and was detected in only 1 of 4 textiles after weathering. Similarly, 6:2 FTOH was detected in 2 of 4 wildland textiles following both abrasion and weathering. When totaled across all four wildland textiles after abrasion, 6:2 FTOH accounted for 86 % of the total PFAS concentration, with 6:2 FTMAC below reporting limits. After weathering, 6:2 FTOH accounted for 83 % of the total, while 6:2 FTMAC accounted for 7 %.

Table 4. Median changes in total PFAS concentrations by stressing and textile type.
 ++ > + 150 %, + + 25 % to + 150 %, ≈ - 25 % to + 25 %, - < - 25 %. NS – not studied.

	Abrasion	Elevated Temp.	Weathering
Gloves	NS	++	NS
Hoods	++	++	NS
Wildland Coats	++	NS	++
Wildland Pants	-	NS	-
Wildland Shirts	-	NS	-

The targeted analytical approach used in this study provides only limited insight into the mechanisms underlying changes in PFAS concentrations with stressing. PFAS transformations can only be detected if analytes observed both before and after stressing are included in the targeted compound list, and multiple processes may occur simultaneously during stressing. As noted in prior studies of durable water repellent (DWR)-treated textiles [16,18,19], identifying the cause of analyte or concentration change is difficult. For example, changes observed during weathering may reflect fluorinated polymer degradation, PFAS transformations, volatilization of PFAS, or physical migration of water-soluble PFAS.

Nonetheless, shifts in the measured concentrations of specific PFAS subsets provide some insight into potential mechanisms. Abrasion generally decreased total PFAS concentrations in volatile PFAS in wildland textiles (**Figure 11**), but increased concentrations of nonvolatile PFAS in wildland and hood textiles (**Figure 12**). While no prior studies have examined abrasion of wildland firefighter gear or hood textiles, Schellenberger et al. [16] reported that abrasion and laundering decreased total fluorine in DWR-treated textiles, attributed to the loss of outer layers containing most of the applied treatment. In contrast, the increases observed here suggest abrasion may enhance the fraction of PFAS extractable by solvent, even as outer textile material is worn away. Similar results were reported by Maizel et al [25], who found increased total PFAS concentrations in 18 of 20 structural firefighter textiles after abrasion. However, Maizel et al [25] reported increases in both volatile and nonvolatile PFAS, whereas the present study found decreases in volatile PFAS for wildland textiles alongside increases in nonvolatile PFAS for wildland and hood textiles.

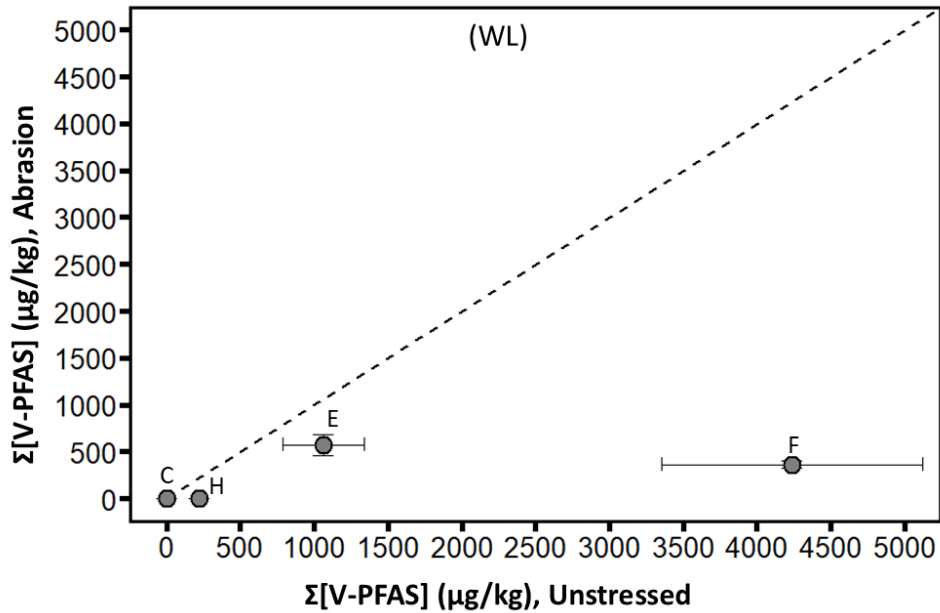


Figure 11. Average total volatile PFAS concentrations determined from triplicate analysis of wildland firefighter coats (WL-C), pants (WL-E, WL-F), and shirts (WL-H) following abrasion (y-axis) compared with corresponding unstressed textiles (x-axis). Error bars represent combined standard uncertainty. Textile type is indicated in panel label (WL = wildland firefighter gear textiles), and individual textiles are indicated with marker labels. The dashed line denotes a 1:1 concentration ratio (i.e., equal concentrations measured in unstressed and textiles after abrasion).

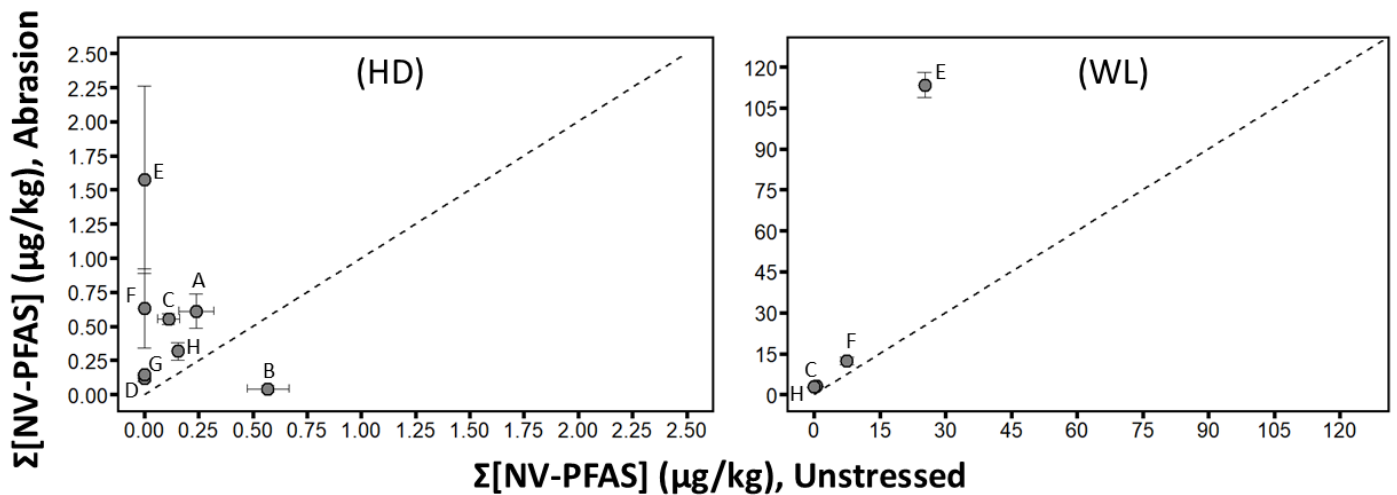


Figure 12. Average total nonvolatile PFAS concentrations determined from triplicate analysis of hood textiles (left) and wildland textiles (right) following abrasion (y-axis) compared with corresponding unstressed textiles (x-axis). Error bars represent combined standard uncertainty. Textile type is indicated in panel label (HD = firefighter hood textiles; WL = wildland firefighter gear textiles), and individual textiles are indicated with marker labels. The dashed line denoted a 1:1 concentration ratio (i.e., equal concentrations measured in unstressed and textiles after abrasion).

Thermal stressing produced increases in both total volatile (**Figure 13**) and nonvolatile (**Figure 14**) PFAS in glove textile layers and hood textiles. In contrast, Maizel et al [25] reported mixed outcomes for structural firefighter gear textiles following thermal stressing: moisture barriers showed little change (- 25 % and + 25 %), outer shells increased substantially (> 150 %), and thermal liners increased moderately (25 % to 150 %). Beyond that report, there are no other published studies on PFAS concentrations in textiles after thermal stressing. However, the predicted boiling points of 6:2 FTMAC (186 °C) [33], 6:2 FTOH (150 °C) [34], 6:2 FTS (219 °C) [35], MeFBSE (247 °C) [36], and PFBA (121 °C) [37] are all below 260 °C, and side-chain fluorinated acrylates have been shown to partially decompose below 300 °C [38]. Thus, exposure to 260 °C could lead to volatilization of PFAS, partial degradation of fluorinated polymers, and formation of new PFAS. The observed increase in volatile PFAS concentrations suggest that, beyond vaporization, thermal stressing may enhance the extractable fraction of volatile PFAS or generate PFAS through polymer degradation.

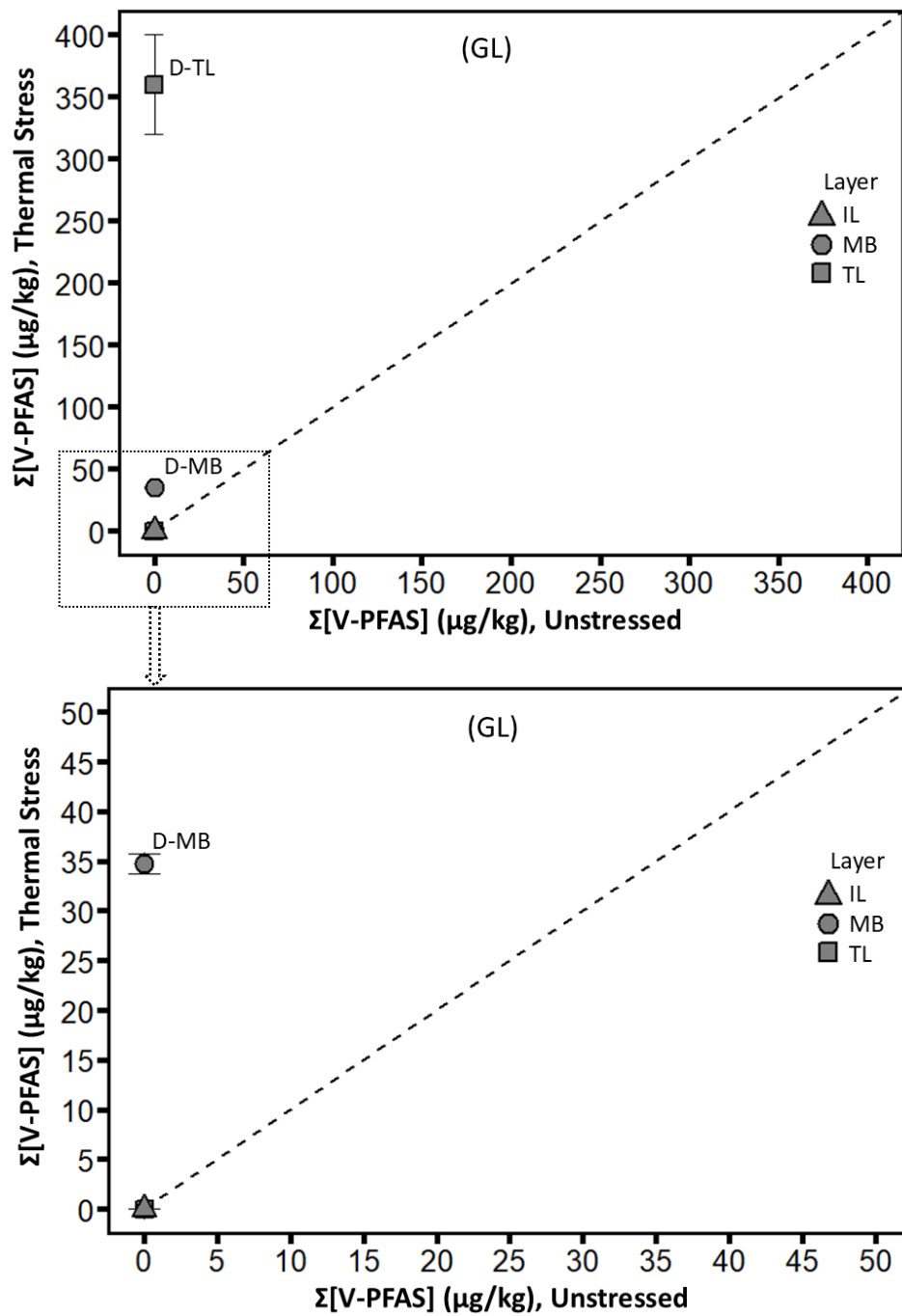


Figure 13. Average total volatile PFAS concentrations determined from triplicate analysis of firefighter glove textiles following thermal stressing (y-axis) compared with corresponding unstressed glove textiles (x-axis). Error bars represent combined standard uncertainty. Textile type is indicated in panel label (GL = firefighter glove textiles), and individual textiles are indicated with marker labels. The dashed line denotes a 1:1 concentration ratio (i.e., equal concentrations measured in unstressed and textiles after thermal stressing). All glove layers are shown in the upper panel, with a zoomed inset displayed below.

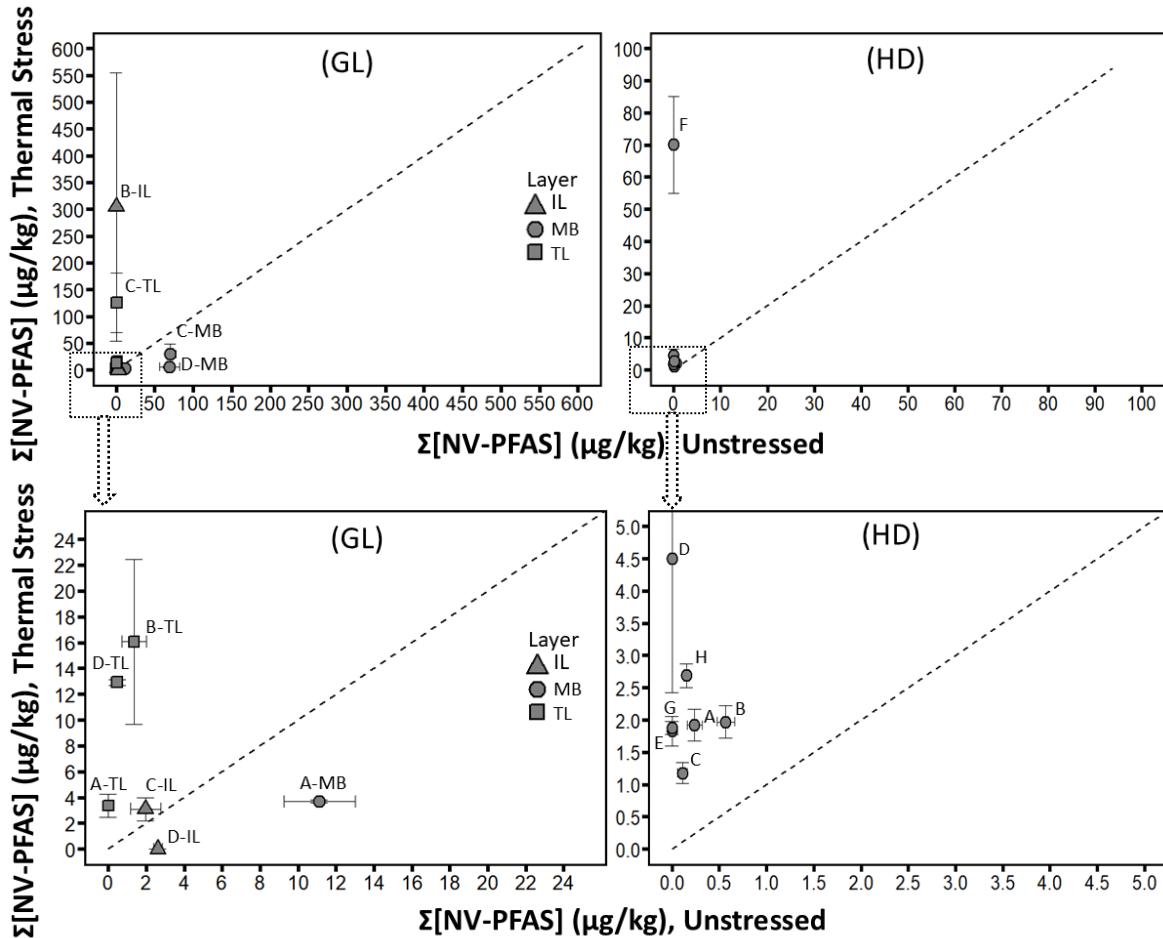


Figure 14. Average total nonvolatile PFAS concentrations determined from triplicate analysis of firefighter gloves textiles (left) and hood textiles (right) following thermal stressing (y-axis) compared with corresponding unstressed textiles (x-axis). Error bars represent combined standard uncertainty. Textile type is indicated in panel label (GL = firefighter glove textiles; HD = firefighter hood textiles), and individual textiles are indicated with marker labels. The dashed line denoted a 1:1 concentration ratio (i.e., equal concentrations measured in unstressed and textiles after thermal stressing). All glove layers and hood textiles are shown in the upper panel, with a zoomed inset displayed below.

Weathering of wildland textiles decreased total volatile PFAS concentrations relative to unstressed textiles in 3 of 4 textiles (**Figure 15**), with variable changes among nonvolatile PFAS (**Figure 16**). All weathered wildland textiles also showed visible discoloration, consistent with textile degradation. By comparison, Maizel et al. [25] observed increases in total volatile PFAS after weathering outer shell textiles, alongside inconsistent changes in nonvolatile PFAS. Similar to thermal stressing, multiple concurrent processes may drive these outcomes. Similarly, Schellenberger et al. [16] exposed polyamide textiles treated with side-chain fluorinated polymers to six months of outdoor weathering and reported large increases in perfluoroalkyl acid

(PFAA) concentrations (up to 7000 $\mu\text{g}/\text{kg}$) despite decreases in total fluorine, which they attributed to evaporation of volatile PFAS and washout of soluble PFAS and polymer-coated textile fibers Schellenberger et al. [16]. They also suggested radical driven degradation of side-chain fluoropolymers and PFAA precursors contributed to new PFAS formation. Van der Veen et al. [18] used an ATLAS weather-O-meter to stress outdoor clothing and performance outerwear. In both cases, increases in PFAAs and volatile PFAS were observed, including up to 400 $\mu\text{g}/\text{m}^2$ for multiple n:2 FTOHs and 170 $\mu\text{g}/\text{m}^2$ for 6:2 FTMAC [18]. These studies proposed mechanisms consistent with the findings here, including changes in PFAS extractability, hydrolysis of fluorinated polymers, and transformation of unmeasured PFAS into detectable species [18,19].

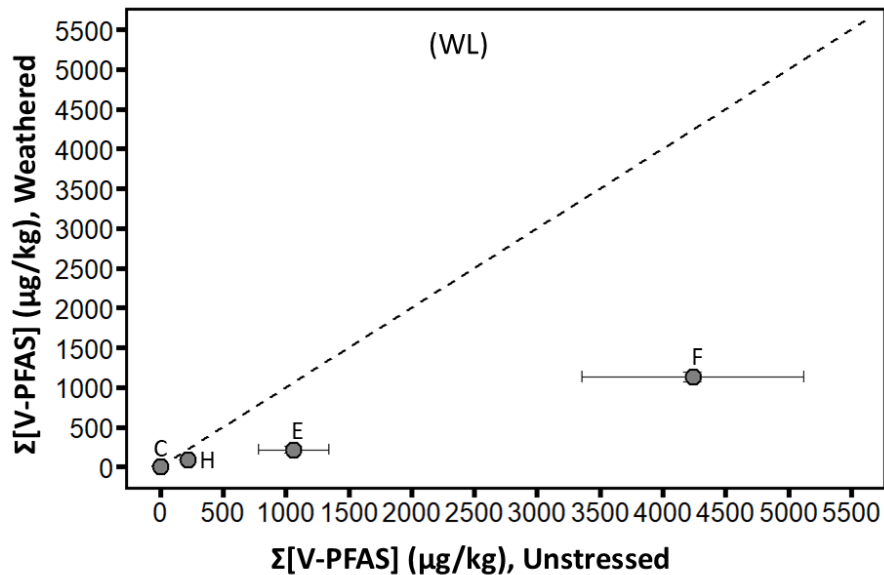


Figure 15. Average total volatile PFAS concentrations determined from triplicate analysis of wildland firefighter coats (WL-C), pants (WL-E, WL-F), and shirts (WL-H) following weathering (y-axis) compared with corresponding unstressed textiles (x-axis). Error bars represent combined standard uncertainty. Textile type is indicated in panel label (WL = wildland firefighter gear textiles), and individual textiles are indicated with marker labels. The dashed line denotes a 1:1 concentration ratio (i.e., equal concentrations measured in unstressed and textiles after weathering).

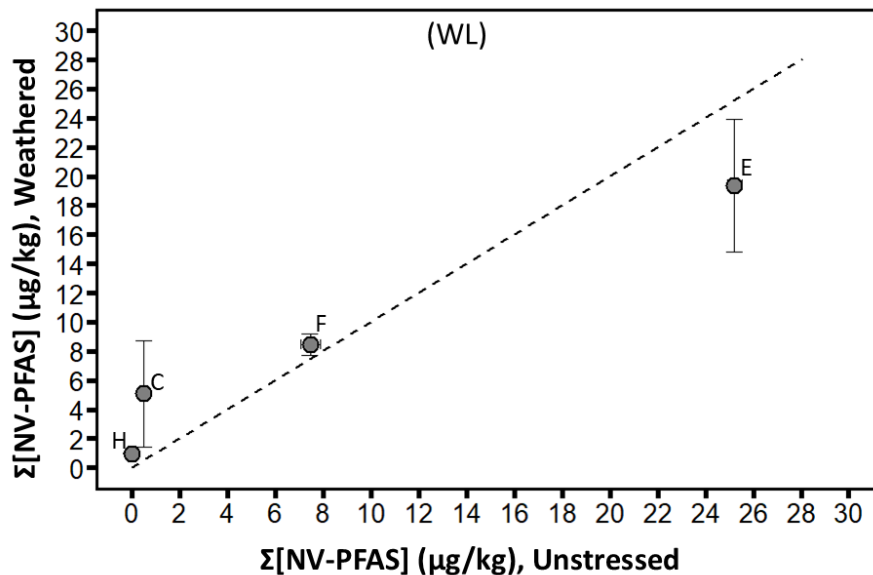


Figure 16. Average total nonvolatile PFAS concentrations determined from triplicate analysis of wildland firefighter coats (WL-C), pants (WL-E, WL-F), and shirts (WL-H) following weathering (y-axis) compared with corresponding unstressed textiles (x-axis). Error bars represent combined standard uncertainty. Textile type is indicated in panel label (WL = wildland firefighter gear textiles), and individual textiles are indicated with marker labels. The dashed line denotes a 1:1 concentration ratio (i.e., equal concentrations measured in unstressed and textiles after weathering).

Across all textiles and stressing conditions examined here, 15 PFAS were detected above reporting limits in at least one stressed textile but not in any unstressed textile. This set included five PPEAs (PFEESA, PF4OPeA, PF5OHxA, ADONA, and 9Cl-PF3ONS), a class absent from all unstressed textiles. However, all 15 detected PFAS post stressing contributed minimally to total PFAS concentrations, with none exceeding 1 µg/kg except for 4:2 FTS in thermally stressed GL-B-IL (2.3 µg/kg ± 1.8 µg/kg; **Table 7**) and GL-C-TL (1.04 µg/kg ± 0.52 µg/kg **Table 11**). Similar results were reported by Maizel et al. [25], where previously undetected PPEAs were observed in stressed textiles and at low concentrations (< 10 µg/kg). MeFBSE, which was not included in earlier unstressed textile analysis, was newly identified in thermally stressed glove textile layers at concentrations from 4.88 µg/kg ± 0.84 µg/kg (GL-C-TL; **Table 11**) up to 177 µg/kg ± 26 µg/kg (GL-C-MB; **Table 10**) and in weathered wildland textiles from 1.86 µg/kg ± 0.22 µg/kg (WL-C; **Table 32**) to 86 µg/kg ± 4 µg/kg (WL-H; **Table 38**). Given their generally low concentrations, the observation of PFAS in stressed but not in unstressed textiles could reflect differences in reporting limits or uncertainty between the two datasets rather than true concentration increases due to stressing.

Among the PFAS quantified in this study, 6:2 FTOH (weathered WL-F; 1010 µg/kg ± 64 µg/kg; **Table 36**) and 6:2 FTMAC (weathered WL-F; 103 µg/kg ± 8 µg/kg; **Table 36**) were the volatile PFAS present at the highest measured concentrations, while MeFBSE (thermally stressed GL-C-MB; 177 µg/kg ± 26 µg/kg; **Table 10**) was the semivolatile PFAS present at the highest measured

concentration, and 6:2 FTS (thermal stressed GL-B-IL; 300 µg/kg ± 250 µg/kg; **Table 7**) was the most abundant nonvolatile PFAS.

The detection of PFCAs and PFSAAs in gloves, hoods, and wildland textiles is notable given prior reports of elevated PFAA concentrations in firefighter serum compared with the general population [39-47] and reviews of PFAA exposure, dietary intake, and toxicity [48]. PFAAs were found in nearly all stressed textiles (33 of 34), spanning PFCAs and PFSAAs with 3-10 perfluorinated carbons. However, concentrations were generally much lower than those of 6:2 FTOH, 6:2 FTMAC, 6:2 FTS, and MeFBSE. For instance, PFOA and PFOS were not quantified above 1 µg/kg in any stressed textile. Total PFAA concentrations generally increased following stressing, suggesting that stressing altered the extractable PFAS fraction. Increases in total PFAAs were observed in 29 of 34 stressed textiles, most notably in WL-E after abrasion (113 µg/kg vs. 19 µg/kg; **Table 33**). Decreases occurred in five textiles, with the largest in GL-A-MB after thermal stressing (4 µg/kg vs. 8 µg/kg; **Table 5**). These decreases may reflect abrasive removal of fluoropolymer-containing layers, reaction losses with radical species, or partitioning into water during the weathering process.

This NIST Technical Note describes how stressors representative of use conditions alter measured PFAS concentrations in structural firefighter gloves, hoods, and wildland firefighter coats, shirts, and pants. Presence alone does not determine risk. Risk depends on how, and whether, exposure occurs, at what levels, and over what duration. Those questions require different types of studies beyond the scope of this work. The targeted analytical approach applied here was restricted to compounds included on the targeted analyte list, meaning PFAS outside this list would not be detected. To address this gap, Maizel et al. [49] employed a suspect screening strategy using liquid chromatography high-resolution mass spectrometry to examine 17 firefighter turnout gear textiles (moisture barriers, outer shells, and thermal liners) for more than 4,900 PFAS from the NIST PFAS Suspect List. Six PFAS were identified with high confidence in at least one textile, including four not previously reported by targeted analysis. 6:2 fluorotelomer sulfate (6:2 FTS), methyl perfluorobutane sulfonamido ethanol (MeFBSE), perfluorobutane sulfonamido diethanol (FBSEE), and perfluorobutane sulfonamido ethanol (FBSE) as well as two which were previously reported by targeted analysis: 6:2 FTS and PFBS [24]. Together, these findings expand the chemical diversity of PFAS known to be present in firefighter turnout gear and demonstrate that targeted analyses alone may overlook important compounds. Integrating targeted and non-targeted approaches provides a more complete assessment of PFAS in firefighter gear and underscores the necessity of non-targeted methods when aiming to fully characterize PFAS in consumer products.

Previous studies that measured both targeted, suspect, non-targeted, and either total fluorine or total oxidizable precursors in firefighter gear have consistently shown that targeted PFAS account for only a small fraction of the total fluorine in textiles and that agreement between targeted PFAS and total F or oxidizable precursor measurements is often poor [2, 16, 23]. This discrepancy

likely reflects that total fluorine measurements capture a broad spectrum of extractable and non-extractable organofluorine, including polymeric PFAS and precursor species, whereas targeted methods quantify only a limited subset of known, extractable compounds. In addition, stressing could release PFAS from textiles while still leaving them as potential exposure sources. For instance, fragments were visibly shed from textiles during abrasion, suggesting that physical abrasion could contribute to PFAS contaminated fire station dust, which has been documented in other work [2, 50]. Similarly, firefighter gear textiles lost up to 58 % of their original mass after exposure to thermal stressing (**Table 3**). While this mass loss may reflect volatilization or thermal degradation of certain constituents, it likely also includes the loss of retained moisture and other non-fluorinated components. If a portion of this loss represents volatilized PFAS or PFAS precursors, similar releases could occur under field conditions, potentially contributing to atmospheric emissions. Finally, because PFAS concentrations are reported here relative to the mass of stressed textiles, reductions in textile mass following abrasion or heating could lead to over- or underestimates of PFAS mass in the garments.

This report builds on NIST Technical Note 2313 [27], which characterized PFAS in unstressed structural firefighter gloves, hoods, and wildland coats, shirts, and pants and showed that the total PFAS mass in a garment could vary by up to an order of magnitude depending on the specific textiles selected for each article. Using stressed textiles, an even larger range was observed: a glove composed of the layers with the highest total PFAS concentrations present after thermal stressing (thermally stressed GL-B-IL, GL-C-MB, GL-D-TL; average total PFAS: 926 $\mu\text{g}/\text{kg}$) would contain more than 77 times the total PFAS mass of one made from the lowest concentration layers (GL-A-MB, GL-B-TL, GL-A-IL; average total PFAS: 12 $\mu\text{g}/\text{kg}$). Such a glove would also contain 8 times the PFAS mass of a garment built from the highest concentration unstressed textiles (average total PFAS: 122 $\mu\text{g}/\text{kg}$). These findings suggest that PFAS measurements in new or unstressed gear may underestimate post-use concentrations, given the wide range of total PFAS across individual layers within a firefighter garment. Consistent with this, prior studies of outdoor aging [16] and laboratory weathering [18] reported that textiles meeting European Union PFAS requirements when new sometimes exceeded limits after stressing. Because each textile here was stressed only once, it remains unclear whether repeated stressing would drive further PFAS increases, although Schellenberger et al. [16] did observe greater changes after six months of outdoor exposure compared with three months.

For glove textile layers, total PFAS concentrations were generally higher in stressed than in unstressed textiles; however, thermal liner textiles in 2 of the 4 gloves had the lowest total PFAS concentrations among the glove layers. Because thermal liners are the layer closest to the skin, this may suggest lower dermal PFAS exposure to firefighters than would be inferred from averaging PFAS concentrations measured across all glove layers. Notable exceptions were observed after thermal stressing, where total PFAS concentrations in GL-D-TL (398 $\mu\text{g}/\text{kg}$ \pm 42 $\mu\text{g}/\text{kg}$; **Table 14**) and GL-C-TL (131 $\mu\text{g}/\text{kg}$ \pm 59 $\mu\text{g}/\text{kg}$, **Table 11**) exceeded 100 $\mu\text{g}/\text{kg}$, while all other thermal liners remained below 4 $\mu\text{g}/\text{kg}$. Similarly, hoods, which directly contact the head, face, and neck, showed low total PFAS concentrations across stressors (< 5 $\mu\text{g}/\text{kg}$), with the exception of HD-F after thermal stressing (70 $\mu\text{g}/\text{kg}$ \pm 15 $\mu\text{g}/\text{kg}$).

To assess how stressing contributes to the broader variability, **Figure 17 and Figure 18** compares total PFAS concentrations before and after stressing. Depending on textile type and stressor, stressed concentrations were either higher or lower than corresponding unstressed values; however, consistent patterns remained, with total PFAS concentrations generally increasing from hood textiles to gloves textiles to wildland textiles. Stressing typically raised total PFAS in hoods and gloves, while decreasing them in wildland textiles. Importantly, thermal stressing of glove textiles substantially increased concentrations, placing them within the range of some stressed and unstressed wildland textiles.

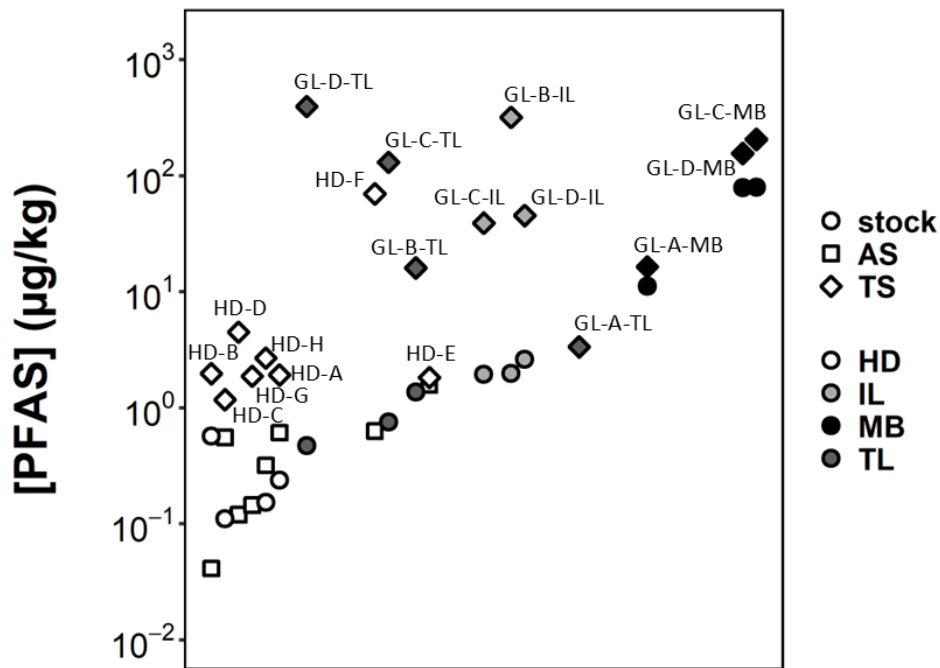


Figure 17. Total PFAS concentrations in logarithmic scale (y-axis) in firefighter glove layers (IL, MB, TL) and hood textiles (HD) following different stress conditions (unstressed = stock, circle; abrasion = AS, square; thermal stressing = TS, diamond). Textiles are ordered left to right by increasing total PFAS concentration, and labels indicate textile identity. Glove layers are shown with different grayscale shades, while all hood samples are shown in white.

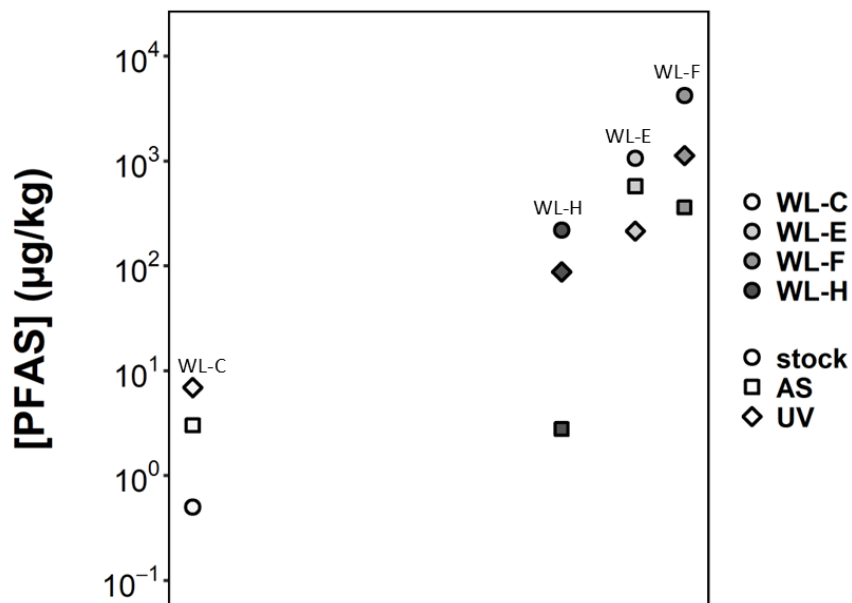


Figure 18. Total PFAS concentrations in logarithmic scale (y-axis) in wildland firefighter coats (WL-C), pants (WL-E, WL-F), and shirts (WL-H) following different stress conditions (unstressed = stock, circle; abrasion = AS, square; weathering = UV, diamond). Textiles are ordered left to right by increasing total PFAS concentration, and labels indicate textile identity. Wildland firefighter textiles are shown with different grayscale shades.

5. Summary

This NIST Technical Note quantified 56 individual PFAS in 22 firefighter textiles (glove layers, hoods, wildland coats, shirts, and pants) following exposure to abrasion, thermal stressing, or weathering, and compared results with corresponding unstressed textiles reported in NIST TN 2313 [27].

Generally, abrasion increased total PFAS concentrations in hood textiles but decreased them in wildland textiles. Thermal stressing increased total PFAS in both glove and hood textiles, while weathering reduced total PFAS in wildland textiles. The largest absolute change occurred in wildland textiles after abrasion, where median total PFAS concentrations decreased from 5520 µg/kg to 942 µg/kg. Increases in PFAS concentrations were primarily driven by MeFBSE (not reported in NIST TN 2313 [27]), 6:2 FTOH, and 6:2 FTS, which were largely absent from most unstressed glove layer textiles and hood textiles, while decreases reflected losses of volatile compounds such as 6:2 FTMAC and 6:2 FTOH, which were the dominant PFAS in unstressed wildland textiles. As with unstressed textiles, stressed wildland textiles had the highest total PFAS concentrations overall, while hoods had the lowest.

Although the targeted analytical methods cannot identify mechanisms of loss, the observed changes are consistent with shifts in the extractable fraction of PFAS. These results align with prior findings for stressed structural firefighter gear, reinforcing that PFAS concentrations in firefighter textiles can change with use, and that such changes should be considered when assessing firefighter exposure.

6. Future Work

Future work will expand PFAS analysis to additional firefighter gear marketed as containing no PFAS under both unstressed and stressed conditions. High-resolution mass spectrometry will be used to broaden analytical coverage beyond the 56 compounds quantified in this study, enabling screening for known PFAS as well as identification of additional compounds through suspect and non-targeted analysis. The suspect screening approach described in Maizel et al. [49] will also be extended to other potential firefighter exposure sources, including materials associated with fire scenes and fire stations. Non-targeted analytical approaches will further support identification of PFAS not currently included in the NIST Suspect List, including compounds exhibiting characteristic PFAS-related MS/MS fragment patterns. Additional efforts may include expanding the analyte list, evaluating the cumulative effects of repeated or combined stressing techniques, characterizing PFAS associated with fire scene exposures, and assessing PFAS transport across firefighter textile layers.

Table 5. Measured PFAS concentrations ($\mu\text{g-PFAS} / \text{kg-textile}$; \pm standard deviation of triplicate measurements) and reporting limits for GL-A-MB after thermal stressing.

PFAS	Concentration ($\mu\text{g/kg}$)	RL ($\mu\text{g/kg}$)	PFAS	Concentration ($\mu\text{g/kg}$)	RL ($\mu\text{g/kg}$)
PFCA (NV)			PPEA (NV)		
PFBA	3.58 \pm 0.11	0.661	PFEESA	<RL	0.426
PFPeA	0.098 \pm 0.002	0.092	PF4OPeA	<RL	0.109
PFHxA	<RL	0.236	PF5OHxA	<RL	0.234
PFHpA	<RL	0.531	3-6-OPFHpA	<RL	0.479
PFOA	<RL	0.126	HFPO-DA	<RL	0.260
PFNA	<RL	0.121	ADONA	<RL	0.502
PFDA	<RL	0.051	9Cl-PF3ONS	<RL	0.113
PFUnDA	<RL	0.121	11Cl-PF3OUdS	<RL	0.114
PFDoDA	<RL	0.059			
PFTTrDA	<RL	0.074	n:2 FTAc (V)		
PFTeDA	<RL	0.055	8:2 FTAc	<RL	88.7
			10:2 FTAc	<RL	33.5
PFSA (NV)			n:2 FTMAC (V)		
PFPrS	No Value		6:2 FTMAC	<RL	57.0
PFBS	<RL	0.471	8:2 FTMAC	<RL	122
PFPeS	<RL	0.500	10:2 FTMAC	<RL	64.2
PFHxS	<RL	0.486			
PFHpS	<RL	0.506	n:2 FTOAc (V)		
PFOS	<RL	0.112	8:2 FTOAc	<RL	83.9
PFNS	<RL	0.116	10:2 FTOAc	<RL	35.0
PFDS	<RL	0.117			
FASA (NV, SV)			n:2 FTOH (V)		
FBSA (NV)	<RL	0.051	4:2 FTOH	<RL	16.5
MeFBSA (SV)	<RL	1.92	5:2 FTOH	<RL	26.8
FHxSA (NV)	<RL	0.051	6:2 FTOH	<RL	36.2
FOSA (NV)	<RL	0.051	7:2 FTOH	<RL	34.1
MeFOSA (SV)	<RL	0.171	8:2 FTOH	<RL	33.2
EtFOSA (SV)	<RL	0.408	10:2 FTOH	<RL	82.1
FASAA (NV)			n:2 FTS (NV)		
FOSAA	<RL	0.045	4:2 FTS	No Value	
MeFOSAA	<RL	0.121	6:2 FTS	No Value	
EtFOSAA	<RL	0.121	8:2 FTS	<RL	0.049
			10:2 FTS	<RL	0.035
FASE (SV)					
MeFBSE	12.8 \pm 3.1	4.94			
MeFOSE	<RL	1.82			
EtFOSE	<RL	2.03			

Table 6. Measured PFAS concentrations ($\mu\text{g-PFAS} / \text{kg-textile}$; \pm standard deviation of triplicate measurements) and reporting limits for GL-A-TL after thermal stressing.

PFAS	Concentration ($\mu\text{g}/\text{kg}$)	RL ($\mu\text{g}/\text{kg}$)	PFAS	Concentration ($\mu\text{g}/\text{kg}$)	RL ($\mu\text{g}/\text{kg}$)
PFCA (NV)			PPEA (NV)		
PFBA	1.00 ± 0.78	0.052	PFEESA	<RL	0.043
PFPeA	0.22 ± 0.16	0.054	PF4OPeA	<RL	0.046
PFHxA	0.91 ± 0.34	0.262	PF5OHxA	<RL	0.058
PFHpA	<RL	0.151	3-6-OPFHpA	<RL	0.047
PFOA	0.188 ± 0.052	0.052	HFPO-DA	<RL	0.108
PFNA	<RL	0.052	ADONA	<RL	0.018
PFDA	<RL	0.105	9Cl-PF3ONS	<RL	0.024
PFUnDA	<RL	0.108	11Cl-PF3OUdS	<RL	0.018
PFDoDA	<RL	0.076			
PFTTrDA	<RL	0.044	n:2 FTAc (V)		
PFTeDA	<RL	0.052	8:2 FTAc	<RL	72.8
			10:2 FTAc	<RL	27.5
PFSA (NV)			n:2 FTMAC (V)		
PFPrS	<RL	0.033	6:2 FTMAC	<RL	46.7
PFBS	0.152 ± 0.04	0.108	8:2 FTMAC	<RL	99.9
PFPeS	<RL	0.115	10:2 FTMAC	<RL	52.7
PFHxS	0.08 ± 0.011	0.047			
PFHpS	<RL	0.018	n:2 FTOAc (V)		
PFOS	0.083 ± 0.015	0.048	8:2 FTOAc	<RL	68.8
PFNS	<RL	0.018	10:2 FTOAc	<RL	28.7
PFDS	<RL	0.042			
FASA (NV, SV)			n:2 FTOH (V)		
FBSA (NV)	<RL	0.052	4:2 FTOH	<RL	13.5
MeFBSA (SV)	<RL	1.58	5:2 FTOH	<RL	22.0
FHxSA (NV)	<RL	0.024	6:2 FTOH	<RL	29.7
FOSA (NV)	0.084 ± 0.05	0.052	7:2 FTOH	<RL	28.0
MeFOSA (SV)	<RL	0.140	8:2 FTOH	<RL	27.2
EtFOSA (SV)	<RL	0.335	10:2 FTOH	<RL	67.3
FASAA (NV)			n:2 FTS (NV)		
FOSAA	<RL	0.036	4:2 FTS	0.64 ± 0.25	0.048
MeFOSAA	<RL	0.052	6:2 FTS	<RL	0.102
EtFOSAA	<RL	0.122	8:2 FTS	<RL	0.049
			10:2 FTS	<RL	0.035
FASE (SV)					
MeFBSE	<RL	4.05			
MeFOSE	<RL	1.491			
EtFOSE	<RL	1.664			

Table 7. Measured PFAS concentrations ($\mu\text{g-PFAS} / \text{kg-textile}$; \pm standard deviation of triplicate measurements) and reporting limits for GL-B-IL after thermal stressing.

PFAS	Concentration ($\mu\text{g}/\text{kg}$)	RL ($\mu\text{g}/\text{kg}$)	PFAS	Concentration ($\mu\text{g}/\text{kg}$)	RL ($\mu\text{g}/\text{kg}$)
PFCA (NV)			PPEA (NV)		
PFBA	<RL	0.780	PFEESA	<RL	0.390
PFPeA	0.31 ± 0.22	0.084	PF4OPeA	<RL	0.100
PFHxA	1.40 ± 0.33	0.216	PF5OHxA	<RL	0.214
PFHpA	<RL	0.487	3-6-OPFHpA	<RL	0.438
PFOA	<RL	0.115	HFPO-DA	<RL	0.238
PFNA	<RL	0.111	ADONA	<RL	0.460
PFDA	0.103 ± 0.069	0.047	9Cl-PF3ONS	0.123 ± 0.015	0.103
PFUnDA	<RL	0.111	11Cl-PF3OUdS	<RL	0.105
PFDoDA	<RL	0.054			
PFTTrDA	<RL	0.068	n:2 FTAc (V)		
PFTeDA	<RL	0.050	8:2 FTAc	<RL	93.3
			10:2 FTAc	<RL	35.3
PFSA (NV)			n:2 FTMAC (V)		
PFPrS	<RL	0.129	6:2 FTMAC	<RL	59.9
PFBS	0.95 ± 0.39	0.432	8:2 FTMAC	<RL	128.1
PFPeS	<RL	0.458	10:2 FTMAC	<RL	67.5
PFHxS	<RL	0.445			
PFHpS	<RL	0.464	n:2 FTOAc (V)		
PFOS	<RL	0.103	8:2 FTOAc	<RL	88.2
PFNS	0.119 ± 0.011	0.107	10:2 FTOAc	<RL	36.8
PFDS	<RL	0.107			
FASA (NV, SV)			n:2 FTOH (V)		
FBSA (NV)	No Value		4:2 FTOH	<RL	17.3
MeFBSA (SV)	<RL	2.02	5:2 FTOH	<RL	28.2
FHxSA (NV)	<RL	0.047	6:2 FTOH	<RL	38.1
FOSA (NV)	<RL	0.047	7:2 FTOH	<RL	35.9
MeFOSA (SV)	<RL	0.179	8:2 FTOH	<RL	34.9
EtFOSA (SV)	<RL	0.428	10:2 FTOH	<RL	86.3
FASAA (NV)			n:2 FTS (NV)		
FOSAA	<RL	0.041	4:2 FTS	2.3 ± 1.8	0.158
MeFOSAA	<RL	0.111	6:2 FTS	300 ± 250	10.9
EtFOSAA	<RL	0.111	8:2 FTS	0.094 ± 0.022	0.045
			10:2 FTS	0.040 ± 0.006	0.032
FASE (SV)					
MeFBSE	15.4 ± 4.2	5.20			
MeFOSE	<RL	1.91			
EtFOSE	<RL	2.14			

Table 8. Measured PFAS concentrations ($\mu\text{g-PFAS} / \text{kg-textile}$; \pm standard deviation of triplicate measurements) and reporting limits for GL-B-TL after thermal stressing.

PFAS	Concentration ($\mu\text{g}/\text{kg}$)	RL ($\mu\text{g}/\text{kg}$)	PFAS	Concentration ($\mu\text{g}/\text{kg}$)	RL ($\mu\text{g}/\text{kg}$)
PFCA (NV)			PPEA (NV)		
PFBA	<RL	1.17	PFEESA	<RL	0.036
PFPeA	<RL	0.218	PF4OPeA	<RL	0.070
PFHxA	<RL	0.967	PF5OHxA	<RL	0.040
PFHpA	<RL	4.60	3-6-OPFHpA	<RL	0.099
PFOA	<RL	1.17	HFPO-DA	<RL	0.044
PFNA	<RL	0.056	ADONA	<RL	0.020
PFDA	<RL	0.218	9Cl-PF3ONS	<RL	0.017
PFUnDA	<RL	0.109	11Cl-PF3OUdS	<RL	0.017
PFDoDA	<RL	0.109			
PFTTrDA	<RL	0.218	n:2 FTAc (V)		
PFTeDA	<RL	0.109	8:2 FTAc	<RL	17.1
			10:2 FTAc	<RL	15.7
PFSA (NV)			n:2 FTMAC (V)		
PFPrS	<RL	0.837	6:2 FTMAC	<RL	55.7
PFBS	16.0 \pm 6.4	0.069	8:2 FTMAC	<RL	57.0
PFPeS	<RL	0.042	10:2 FTMAC	<RL	30.1
PFHxS	<RL	0.077			
PFHpS	<RL	0.042	n:2 FTOAc (V)		
PFOS	<RL	0.088	8:2 FTOAc	<RL	16.1
PFNS	<RL	0.018	10:2 FTOAc	<RL	16.4
PFDS	<RL	0.018			
FASA (NV, SV)			n:2 FTOH (V)		
FBSA (NV)	0.018 \pm 0.001	0.018	4:2 FTOH	<RL	16.1
MeFBSA (SV)	No Value		5:2 FTOH	<RL	16.1
FHxSA (NV)	<RL	0.018	6:2 FTOH	<RL	17.0
FOSA (NV)	<RL	0.126	7:2 FTOH	<RL	16.0
MeFOSA (SV)	<RL	0.541	8:2 FTOH	<RL	15.6
EtFOSA (SV)	<RL	0.318	10:2 FTOH	<RL	33.0
FASAA (NV)			n:2 FTS (NV)		
FOSAA	<RL	1.03	4:2 FTS	<RL	0.041
MeFOSAA	<RL	0.218	6:2 FTS	<RL	0.104
EtFOSAA	<RL	0.109	8:2 FTS	<RL	0.042
			10:2 FTS	<RL	0.093
FASE (SV)					
MeFBSE	No Value				
MeFOSE	<RL	0.542			
EtFOSE	<RL	0.554			

Table 9. Measured PFAS concentrations ($\mu\text{g-PFAS} / \text{kg-textile}$; \pm standard deviation of triplicate measurements) and reporting limits for GL-C-IL after thermal stressing.

PFAS	Concentration ($\mu\text{g/kg}$)	RL ($\mu\text{g/kg}$)	PFAS	Concentration ($\mu\text{g/kg}$)	RL ($\mu\text{g/kg}$)
PFCA (NV)			PPEA (NV)		
PFBA	2.77 ± 0.89	1.50	PFEESA	<RL	0.046
PFPeA	<RL	0.280	PF4OPeA	0.215 ± 0.066	0.090
PFHxA	<RL	1.25	PF5OHxA	<RL	0.052
PFHpA	<RL	5.92	3-6-OPFHpA	No Value	
PFOA	<RL	1.50	HFPO-DA	<RL	0.057
PFNA	<RL	0.073	ADONA	<RL	0.026
PFDA	<RL	0.280	9CI-PF3ONS	<RL	0.022
PFUnDA	<RL	0.141	11CI-PF3OUdS	<RL	0.022
PFDoDA	<RL	0.141			
PFTTrDA	<RL	0.280	n:2 FTAc (V)		
PFTeDA	<RL	0.141	8:2 FTAc	<RL	16.7
			10:2 FTAc	<RL	15.4
PFSA (NV)			n:2 FTMAC (V)		
PFPrS	<RL	1.08	6:2 FTMAC	<RL	54.5
PFBS	No Value		8:2 FTMAC	<RL	55.8
PFPeS	<RL	0.054	10:2 FTMAC	<RL	29.4
PFHxS	0.125 ± 0.028	0.099			
PFHpS	<RL	0.054	n:2 FTOAc (V)		
PFOS	<RL	0.113	8:2 FTOAc	<RL	15.8
PFNS	<RL	0.023	10:2 FTOAc	<RL	16.0
PFDS	<RL	0.023			
FASA (NV, SV)			n:2 FTOH (V)		
FBSA (NV)	<RL	0.024	4:2 FTOH	<RL	15.8
MeFBSA (SV)	<RL	0.913	5:2 FTOH	<RL	15.7
FHxSA (NV)	<RL	0.024	6:2 FTOH	<RL	16.6
FOSA (NV)	<RL	0.162	7:2 FTOH	<RL	15.6
MeFOSA (SV)	<RL	0.528	8:2 FTOH	<RL	15.2
EtFOSA (SV)	<RL	0.310	10:2 FTOH	<RL	32.3
FASAA (NV)			n:2 FTS (NV)		
FOSAA	<RL	1.33	4:2 FTS	<RL	0.053
MeFOSAA	<RL	0.280	6:2 FTS	<RL	0.134
EtFOSAA	<RL	0.141	8:2 FTS	<RL	0.055
			10:2 FTS	<RL	0.119
FASE (SV)					
MeFBSE	36.1 ± 6.6	2.06			
MeFOSE	<RL	0.529			
EtFOSE	<RL	0.541			

Table 10. Measured PFAS concentrations ($\mu\text{g-PFAS} / \text{kg-textile}$; \pm standard deviation of triplicate measurements) and reporting limits for GL-C-MB after thermal stressing.

PFAS	Concentration ($\mu\text{g/kg}$)	RL ($\mu\text{g/kg}$)	PFAS	Concentration ($\mu\text{g/kg}$)	RL ($\mu\text{g/kg}$)
PFCA (NV)			PPEA (NV)		
PFBA	5.7 \pm 4.9	2.10	PFEESA	<RL	0.064
PFPeA	<RL	0.392	PF4OPeA	0.24 \pm 0.11	0.126
PFHxA	<RL	1.74	PF5OHxA	<RL	0.072
PFHpA	<RL	8.28	3-6-OPFHpA	<RL	0.179
PFOA	<RL	2.101	HFPO-DA	<RL	0.080
PFNA	<RL	0.101	ADONA	<RL	0.036
PFDA	<RL	0.392	9Cl-PF3ONS	<RL	0.031
PFUnDA	<RL	0.197	11Cl-PF3OUdS	<RL	0.031
PFDoDA	<RL	0.197			
PFTTrDA	<RL	0.392	n:2 FTAc (V)		
PFTeDA	<RL	0.197	8:2 FTAc	<RL	17.6
			10:2 FTAc	<RL	16.2
PFSA (NV)			n:2 FTMAC (V)		
PFPrS	<RL	1.51	6:2 FTMAC	<RL	57.5
PFBS	24 \pm 19	0.124	8:2 FTMAC	<RL	58.8
PFPeS	<RL	0.075	10:2 FTMAC	<RL	31.0
PFHxS	<RL	0.138			
PFHpS	<RL	0.076	n:2 FTOAc (V)		
PFOS	<RL	0.159	8:2 FTOAc	<RL	16.6
PFNS	<RL	0.032	10:2 FTOAc	<RL	16.9
PFDS	<RL	0.032			
FASA (NV, SV)			n:2 FTOH (V)		
FBSA (NV)	<RL	0.033	4:2 FTOH	<RL	16.6
MeFBSA (SV)	<RL	0.650	5:2 FTOH	<RL	16.6
FHxSA (NV)	<RL	0.033	6:2 FTOH	<RL	17.5
FOSA (NV)	<RL	0.227	7:2 FTOH	<RL	16.5
MeFOSA (SV)	<RL	0.554	8:2 FTOH	<RL	16.0
EtFOSA (SV)	<RL	0.325	10:2 FTOH	<RL	34.0
FASAA (NV)			n:2 FTS (NV)		
FOSAA	<RL	1.85	4:2 FTS	<RL	0.075
MeFOSAA	<RL	0.392	6:2 FTS	<RL	0.187
EtFOSAA	<RL	0.197	8:2 FTS	<RL	0.077
			10:2 FTS	<RL	0.167
FASE (SV)					
MeFBSE	177 \pm 26	1.47			
MeFOSE	<RL	0.555			
EtFOSE	<RL	0.568			

Table 11. Measured PFAS concentrations ($\mu\text{g-PFAS} / \text{kg-textile}$; \pm standard deviation of triplicate measurements) and reporting limits for GL-C-TL after thermal stressing.

PFAS	Concentration ($\mu\text{g}/\text{kg}$)	RL ($\mu\text{g}/\text{kg}$)	PFAS	Concentration ($\mu\text{g}/\text{kg}$)	RL ($\mu\text{g}/\text{kg}$)
PFCA (NV)			PPEA (NV)		
PFBA	<RL	0.689	PFEESA	<RL	0.515
PFPeA	0.213 ± 0.048	0.111	PF4OPeA	<RL	0.132
PFHxA	0.44 ± 0.12	0.285	PF5OHxA	<RL	0.283
PFHpA	<RL	0.642	3-6-OPFHpA	<RL	0.578
PFOA	<RL	0.152	HFPO-DA	<RL	0.314
PFNA	<RL	0.146	ADONA	<RL	0.607
PFDA	<RL	0.062	9Cl-PF3ONS	<RL	0.136
PFUnDA	<RL	0.146	11Cl-PF3OUdS	<RL	0.138
PFDoDA	<RL	0.071			
PFTTrDA	<RL	0.090	n:2 FTAc (V)		
PFTeDA	<RL	0.066	8:2 FTAc	<RL	23.9
			10:2 FTAc	<RL	10.8
PFSA (NV)			n:2 FTMAC (V)		
PFPrS	<RL	0.170	6:2 FTMAC	<RL	78.1
PFBS	3.5 ± 2.4	0.569	8:2 FTMAC	<RL	39.2
PFPeS	<RL	0.604	10:2 FTMAC	<RL	20.7
PFHxS	<RL	0.587			
PFHpS	<RL	0.612	n:2 FTOAc (V)		
PFOS	<RL	0.136	8:2 FTOAc	<RL	22.6
PFNS	<RL	0.141	10:2 FTOAc	<RL	11.3
PFDS	<RL	0.141			
FASA (NV, SV)			n:2 FTOH (V)		
FBSA (NV)	No Value		4:2 FTOH	<RL	22.6
MeFBSA (SV)	<RL	1.13	5:2 FTOH	<RL	57.8
FHxSA (NV)	No Value		6:2 FTOH	<RL	11.7
FOSA (NV)	<RL	0.062	7:2 FTOH	<RL	11.0
MeFOSA (SV)	<RL	0.284	8:2 FTOH	<RL	21.8
EtFOSA (SV)	<RL	0.113	10:2 FTOH	<RL	56.9
FASAA (NV)			n:2 FTS (NV)		
FOSAA	<RL	0.054	4:2 FTS	1.04 ± 0.52	0.208
MeFOSAA	<RL	0.146	6:2 FTS	121 ± 55	14.4
EtFOSAA	<RL	0.146	8:2 FTS	<RL	0.059
			10:2 FTS	<RL	0.042
FASE (SV)					
MeFBSE	4.88 ± 0.84	1.18			
MeFOSE	<RL	0.284			
EtFOSE	<RL	0.608			

Table 12. Measured PFAS concentrations ($\mu\text{g-PFAS} / \text{kg-textile}$; \pm standard deviation of triplicate measurements) and reporting limits for GL-D-IL after thermal stressing.

PFAS	Concentration ($\mu\text{g}/\text{kg}$)	RL ($\mu\text{g}/\text{kg}$)	PFAS	Concentration ($\mu\text{g}/\text{kg}$)	RL ($\mu\text{g}/\text{kg}$)
PFCA (NV)			PPEA (NV)		
PFBA	<RL	1.23	PFEESA	<RL	0.038
PFPeA	<RL	0.229	PF4OPeA	<RL	0.074
PFHxA	<RL	1.02	PF5OHxA	<RL	0.042
PFHpA	<RL	4.84	3-6-OPFHpA	<RL	0.105
PFOA	<RL	1.23	HFPO-DA	<RL	0.047
PFNA	<RL	0.059	ADONA	<RL	0.021
PFDA	<RL	0.229	9Cl-PF3ONS	<RL	0.018
PFUnDA	<RL	0.115	11Cl-PF3OUdS	<RL	0.018
PFDoDA	<RL	0.115			
PFTTrDA	<RL	0.229	n:2 FTAc (V)		
PFTeDA	<RL	0.115	8:2 FTAc	<RL	17.3
			10:2 FTAc	<RL	15.9
PFSA (NV)			n:2 FTMAC (V)		
PFPrS	<RL	0.881	6:2 FTMAC	<RL	56.5
PFBS	<RL	0.073	8:2 FTMAC	<RL	57.8
PFPeS	<RL	0.044	10:2 FTMAC	<RL	30.5
PFHxS	<RL	0.081			
PFHpS	<RL	0.044	n:2 FTOAc (V)		
PFOS	<RL	0.093	8:2 FTOAc	<RL	16.4
PFNS	<RL	0.018	10:2 FTOAc	<RL	16.6
PFDS	<RL	0.019			
FASA (NV, SV)			n:2 FTOH (V)		
FBSA (NV)	No Value		4:2 FTOH	<RL	16.3
MeFBSA (SV)	<RL	0.956	5:2 FTOH	<RL	16.3
FHxSA (NV)	<RL	0.019	6:2 FTOH	<RL	17.2
FOSA (NV)	<RL	0.132	7:2 FTOH	<RL	16.2
MeFOSA (SV)	<RL	0.549	8:2 FTOH	<RL	15.8
EtFOSA (SV)	<RL	0.323	10:2 FTOH	<RL	33.5
FASAA (NV)			n:2 FTS (NV)		
FOSAA	<RL	1.08	4:2 FTS	<RL	0.044
MeFOSAA	<RL	0.229	6:2 FTS	<RL	0.109
EtFOSAA	<RL	0.115	8:2 FTS	<RL	0.045
			10:2 FTS	<RL	0.098
FASE (SV)					
MeFBSE	45 \pm 14	2.16			
MeFOSE	<RL	0.550			
EtFOSE	<RL	0.563			

Table 13. Measured PFAS concentrations ($\mu\text{g-PFAS} / \text{kg-textile}$; \pm standard deviation of triplicate measurements) and reporting limits for GL-D-MB after thermal stressing.

PFAS	Concentration ($\mu\text{g}/\text{kg}$)	RL ($\mu\text{g}/\text{kg}$)	PFAS	Concentration ($\mu\text{g}/\text{kg}$)	RL ($\mu\text{g}/\text{kg}$)
PFCA (NV)			PPEA (NV)		
PFBA	3.67 \pm 0.79	1.35	PFEESA	<RL	0.041
PFPeA	<RL	0.251	PF4OPeA	0.150 \pm 0.069	0.081
PFHxA	<RL	1.12	PF5OHxA	<RL	0.046
PFHpA	<RL	5.31	3-6-OPFHpA	<RL	0.115
PFOA	<RL	1.35	HFPO-DA	<RL	0.051
PFNA	<RL	0.065	ADONA	<RL	0.023
PFDA	<RL	0.251	9Cl-PF3ONS	<RL	0.020
PFUnDA	<RL	0.126	11Cl-PF3OUdS	<RL	0.020
PFDoDA	<RL	0.126			
PFTTrDA	<RL	0.251	n:2 FTAc (V)		
PFTeDA	<RL	0.126	8:2 FTAc	<RL	18.0
			10:2 FTAc	<RL	16.6
PFSA (NV)			n:2 FTMAC (V)		
PFPrS	<RL	0.966	6:2 FTMAC	<RL	59.0
PFBS	1.7 \pm 0.62	0.080	8:2 FTMAC	<RL	60.4
PFPeS	<RL	0.048	10:2 FTMAC	<RL	31.8
PFHxS	<RL	0.089			
PFHpS	<RL	0.049	n:2 FTOAc (V)		
PFOS	<RL	0.102	8:2 FTOAc	<RL	17.1
PFNS	<RL	0.020	10:2 FTOAc	<RL	17.4
PFDS	<RL	0.020			
FASA (NV, SV)			n:2 FTOH (V)		
FBSA (NV)	0.271 \pm 0.056	0.021	4:2 FTOH	<RL	17.1
MeFBSA (SV)	<RL	0.754	5:2 FTOH	<RL	17.0
FHxSA (NV)	<RL	0.021	6:2 FTOH	34.73 \pm 0.97	18.0
FOSA (NV)	<RL	0.145	7:2 FTOH	<RL	16.9
MeFOSA (SV)	<RL	0.574	8:2 FTOH	<RL	16.5
EtFOSA (SV)	<RL	0.337	10:2 FTOH	<RL	34.9
FASAA (NV)			n:2 FTS (NV)		
FOSAA	<RL	1.19	4:2 FTS	<RL	0.048
MeFOSAA	<RL	0.251	6:2 FTS	<RL	0.120
EtFOSAA	<RL	0.126	8:2 FTS	<RL	0.049
			10:2 FTS	<RL	0.107
FASE (SV)					
MeFBSE	115.6 \pm 7.1	1.70			
MeFOSE	<RL	0.575			
EtFOSE	<RL	0.588			

Table 14. Measured PFAS concentrations ($\mu\text{g-PFAS} / \text{kg-textile}$; \pm standard deviation of triplicate measurements) and reporting limits for GL-D-TL after thermal stressing.

PFAS	Concentration ($\mu\text{g/kg}$)	RL ($\mu\text{g/kg}$)	PFAS	Concentration ($\mu\text{g/kg}$)	RL ($\mu\text{g/kg}$)
<i>PFCA (NV)</i>			<i>PPEA (NV)</i>		
PFBA	2.498 \pm 0.093	1.27	PFEESA	<RL	0.039
PFPeA	2.442 \pm 0.088	0.236	PF4OPeA	<RL	0.076
PFHxA	6.46 \pm 0.15	1.05	PF5OHxA	<RL	0.044
PFHpA	<RL	4.98	3-6-OPFHpA	<RL	0.108
PFOA	<RL	1.27	HFPO-DA	<RL	0.048
PFNA	<RL	0.061	ADONA	<RL	0.022
PFDA	<RL	0.236	9Cl-PF3ONS	<RL	0.018
PFUnDA	<RL	0.119	11Cl-PF3OUdS	<RL	0.019
PFDoDA	<RL	0.119			
PFTTrDA	<RL	0.236	<i>n:2 FTAc (V)</i>		
PFTeDA	<RL	0.119	8:2 FTAc	<RL	20.4
			10:2 FTAc	<RL	18.8
<i>PFSA (NV)</i>			<i>n:2 FTMAC (V)</i>		
PFPrS	<RL	0.907	6:2 FTMAC	<RL	66.8
PFBS	1.322 \pm 0.081	0.075	8:2 FTMAC	<RL	68.3
PFPeS	<RL	0.045	10:2 FTMAC	<RL	36.0
PFHxS	<RL	0.083			
PFHpS	<RL	0.046	<i>n:2 FTOAc (V)</i>		
PFOS	<RL	0.095	8:2 FTOAc	<RL	19.3
PFNS	0.026 \pm 0.001	0.019	10:2 FTOAc	<RL	19.6
PFDS	<RL	0.019			
<i>FASA (NV, SV)</i>			<i>n:2 FTOH (V)</i>		
FBSA (NV)	<RL	0.020	4:2 FTOH	<RL	19.3
MeFBSA (SV)	<RL	0.791	5:2 FTOH	<RL	19.2
FHxSA (NV)	<RL	0.020	6:2 FTOH	360 \pm 40	20.3
FOSA (NV)	<RL	0.136	7:2 FTOH	<RL	19.1
MeFOSA (SV)	<RL	0.646	8:2 FTOH	<RL	18.6
EtFOSA (SV)	<RL	0.379	10:2 FTOH	<RL	39.5
<i>FASAA (NV)</i>			<i>n:2 FTS (NV)</i>		
FOSAA	<RL	1.12	4:2 FTS	<RL	0.045
MeFOSAA	<RL	0.236	6:2 FTS	0.172 \pm 0.045	0.113
EtFOSAA	<RL	0.119	8:2 FTS	<RL	0.046
			10:2 FTS	<RL	0.101
<i>FASE (SV)</i>					
MeFBSE	24.6 \pm 1.4	1.79			
MeFOSE	<RL	0.647			
EtFOSE	<RL	0.662			

Table 15. Measured PFAS concentrations ($\mu\text{g-PFAS} / \text{kg-textile}$; \pm standard deviation of triplicate measurements) and reporting limits for abraded HD-A.

PFAS	Concentration ($\mu\text{g}/\text{kg}$)	RL ($\mu\text{g}/\text{kg}$)	PFAS	Concentration ($\mu\text{g}/\text{kg}$)	RL ($\mu\text{g}/\text{kg}$)
PFCA (NV)			PPEA (NV)		
PFBA	0.31 \pm 0.12	0.125	PFEESA	<RL	0.015
PFPeA	<RL	0.041	PF4OPeA	0.126 \pm 0.024	0.077
PFHxA	<RL	1.35	PF5OHxA	<RL	0.017
PFHpA	<RL	0.233	3-6-OPFHpA	<RL	0.114
PFOA	<RL	0.391	HFPO-DA	<RL	0.233
PFNA	<RL	0.125	ADONA	<RL	0.039
PFDA	<RL	0.082	9Cl-PF3ONS	<RL	0.018
PFUnDA	<RL	0.125	11Cl-PF3OUdS	<RL	0.018
PFDoDA	<RL	0.125			
PFTTrDA	<RL	0.125	n:2 FTAc (V)		
PFTeDA	<RL	0.041	8:2 FTAc	<RL	12.5
			10:2 FTAc	<RL	24.1
PFSA (NV)			n:2 FTMAC (V)		
PFPrS	<RL	0.277	6:2 FTMAC	<RL	40.7
PFBS	<RL	0.046	8:2 FTMAC	<RL	41.6
PFPeS	<RL	0.039	10:2 FTMAC	<RL	21.9
PFHxS	0.058 \pm 0.012	0.017			
PFHpS	<RL	0.054	n:2 FTOAc (V)		
PFOS	0.12 \pm 0.025	0.084	8:2 FTOAc	<RL	11.8
PFNS	<RL	0.018	10:2 FTOAc	<RL	12.0
PFDS	<RL	0.018			
FASA (NV, SV)			n:2 FTOH (V)		
FBSA (NV)	<RL	0.019	4:2 FTOH	<RL	11.8
MeFBSA (SV)	<RL	4.14	5:2 FTOH	<RL	24.6
FHxSA (NV)	<RL	0.019	6:2 FTOH	<RL	26.0
FOSA (NV)	<RL	0.198	7:2 FTOH	<RL	11.7
MeFOSA (SV)	<RL	0.177	8:2 FTOH	<RL	23.8
EtFOSA (SV)	<RL	0.211	10:2 FTOH	<RL	24.2
FASAA (NV)			n:2 FTS (NV)		
FOSAA	<RL	0.110	4:2 FTS	<RL	0.117
MeFOSAA	<RL	1.29	6:2 FTS	No Value	
EtFOSAA	<RL	0.485	8:2 FTS	<RL	0.224
			10:2 FTS	<RL	0.035
FASE (SV)					
MeFBSE	<RL	5.90			
MeFOSE	<RL	0.871			
EtFOSE	<RL	0.444			

Table 16. Measured PFAS concentrations ($\mu\text{g-PFAS} / \text{kg-textile}$; \pm standard deviation of triplicate measurements) and reporting limits for HD-A after thermal stressing.

PFAS	Concentration ($\mu\text{g/kg}$)	RL ($\mu\text{g/kg}$)	PFAS	Concentration ($\mu\text{g/kg}$)	RL ($\mu\text{g/kg}$)
<i>PFCA (NV)</i>			<i>PPEA (NV)</i>		
PFBA	0.55 \pm 0.11	0.047	PFEESA	<RL	0.039
PFPeA	0.125 \pm 0.036	0.049	PF4OPeA	<RL	0.042
PFHxA	0.536 \pm 0.054	0.238	PF5OHxA	<RL	0.052
PFHpA	<RL	0.138	3-6-OPFHpA	<RL	0.043
PFOA	0.180 \pm 0.086	0.047	HFPO-DA	<RL	0.098
PFNA	<RL	0.047	ADONA	<RL	0.017
PFDA	<RL	0.096	9Cl-PF3ONS	<RL	0.022
PFUnDA	<RL	0.098	11Cl-PF3OUdS	<RL	0.016
PFDoDA	<RL	0.069			
PFTTrDA	<RL	0.040	<i>n:2 FTAc (V)</i>		
PFTeDA	<RL	0.047	8:2 FTAc	<RL	71.4
			10:2 FTAc	<RL	27.0
<i>PFSA (NV)</i>			<i>n:2 FTMAC (V)</i>		
PFPrS	<RL	0.030	6:2 FTMAC	<RL	45.8
PFBS	<RL	0.098	8:2 FTMAC	<RL	98.0
PFPeS	<RL	0.104	10:2 FTMAC	<RL	51.6
PFHxS	0.090 \pm 0.018	0.043			
PFHpS	<RL	0.017	<i>n:2 FTOAc (V)</i>		
PFOS	0.051 \pm 0.010	0.043	8:2 FTOAc	<RL	67.5
PFNS	<RL	0.017	10:2 FTOAc	<RL	28.2
PFDS	<RL	0.038			
<i>FASA (NV, SV)</i>			<i>n:2 FTOH (V)</i>		
FBSA (NV)	No Value		4:2 FTOH	<RL	13.2
MeFBSA (SV)	<RL	1.53	5:2 FTOH	<RL	21.6
FHxSA (NV)	<RL	0.022	6:2 FTOH	<RL	29.2
FOSA (NV)	<RL	0.047	7:2 FTOH	<RL	27.4
MeFOSA (SV)	<RL	0.137	8:2 FTOH	<RL	26.7
EtFOSA (SV)	<RL	0.328	10:2 FTOH	<RL	66.0
<i>FASAA (NV)</i>			<i>n:2 FTS (NV)</i>		
FOSAA	<RL	0.033	4:2 FTS	0.386 \pm 0.189	0.044
MeFOSAA	<RL	0.047	6:2 FTS	<RL	0.093
EtFOSAA	<RL	0.111	8:2 FTS	<RL	0.045
			10:2 FTS	<RL	0.032
<i>FASE (SV)</i>					
MeFBSE	<RL	3.94			
MeFOSE	<RL	1.46			
EtFOSE	<RL	1.62			

Table 17. Measured PFAS concentrations ($\mu\text{g-PFAS} / \text{kg-textile}$; \pm standard deviation of triplicate measurements) and reporting limits for abraded HD-B.

PFAS	Concentration ($\mu\text{g}/\text{kg}$)	RL ($\mu\text{g}/\text{kg}$)	PFAS	Concentration ($\mu\text{g}/\text{kg}$)	RL ($\mu\text{g}/\text{kg}$)
PFCA (NV)			PPEA (NV)		
PFBA	<RL	0.112	PFEESA	<RL	0.014
PFPeA	<RL	0.037	PF4OPeA	<RL	0.069
PFHxA	<RL	1.213	PF5OHxA	<RL	0.016
PFHpA	<RL	0.210	3-6-OPFHpA	<RL	0.102
PFOA	<RL	0.351	HFPO-DA	<RL	0.210
PFNA	<RL	0.112	ADONA	<RL	0.035
PFDA	<RL	0.074	9Cl-PF3ONS	<RL	0.016
PFUnDA	<RL	0.112	11Cl-PF3OUdS	<RL	0.016
PFDoDA	<RL	0.112			
PFTrDA	No value		n:2 FTAc (V)		
PFTeDA	<RL	0.037	8:2 FTAc	<RL	14.8
			10:2 FTAc	<RL	28.7
PFSA (NV)			n:2 FTMAC (V)		
PFPrS	No value		6:2 FTMAC	<RL	48.5
PFBS	<RL	0.041	8:2 FTMAC	<RL	49.6
PFPeS	<RL	0.035	10:2 FTMAC	<RL	26.2
PFHxS	0.041 \pm 0.025	0.016			
PFHpS	<RL	0.049	n:2 FTOAc (V)		
PFOS	<RL	0.076	8:2 FTOAc	<RL	14.0
PFNS	<RL	0.017	10:2 FTOAc	<RL	14.3
PFDS	<RL	0.017			
FASA (NV, SV)			n:2 FTOH (V)		
FBSA (NV)	No value		4:2 FTOH	<RL	14.0
MeFBSA (SV)	No value		5:2 FTOH	<RL	29.3
FHxSA (NV)	<RL	0.017	6:2 FTOH	<RL	31.0
FOSA (NV)	<RL	0.178	7:2 FTOH	<RL	13.9
MeFOSA (SV)	<RL	0.211	8:2 FTOH	<RL	28.4
EtFOSA (SV)	<RL	0.252	10:2 FTOH	<RL	28.8
FASAA (NV)			n:2 FTS (NV)		
FOSAA	No value		4:2 FTS	No value	
MeFOSAA	No value		6:2 FTS	No value	
EtFOSAA	<RL	0.436	8:2 FTS	<RL	0.201
			10:2 FTS	<RL	0.031
FASE (SV)					
MeFBSE	<RL	7.03			
MeFOSE	<RL	1.04			
EtFOSE	<RL	0.529			

Table 18. Measured PFAS concentrations ($\mu\text{g-PFAS} / \text{kg-textile}$; \pm standard deviation of triplicate measurements) and reporting limits for HD-B after thermal stressing.

PFAS	Concentration ($\mu\text{g}/\text{kg}$)	RL ($\mu\text{g}/\text{kg}$)	PFAS	Concentration ($\mu\text{g}/\text{kg}$)	RL ($\mu\text{g}/\text{kg}$)
PFCA (NV)			PPEA (NV)		
PFBA	0.332 \pm 0.060	0.059	PFEESA	<RL	0.049
PFPeA	0.103 \pm 0.015	0.062	PF4OPeA	<RL	0.053
PFHxA	0.665 \pm 0.092	0.301	PF5OHxA	<RL	0.066
PFHpA	<RL	0.158	3-6-OPFHpA	<RL	0.050
PFOA	0.172 \pm 0.022	0.059	HFPO-DA	<RL	0.112
PFNA	<RL	0.059	ADONA	<RL	0.019
PFDA	<RL	0.110	9Cl-PF3ONS	<RL	0.028
PFUnDA	<RL	0.112	11Cl-PF3OUdS	<RL	0.019
PFDoDA	<RL	0.088			
PFTTrDA	<RL	0.046	n:2 FTAc (V)		
PFTeDA	<RL	0.059	8:2 FTAc	<RL	61.3
			10:2 FTAc	<RL	23.2
PFSA (NV)			n:2 FTMAC (V)		
PFPrS	0.046 \pm 0.006	0.038	6:2 FTMAC	<RL	39.4
PFBS	<RL	0.125	8:2 FTMAC	<RL	84.2
PFPeS	<RL	0.132	10:2 FTMAC	<RL	44.4
PFHxS	<RL	0.054			
PFHpS	<RL	0.019	n:2 FTOAc (V)		
PFOS	0.095 \pm 0.027	0.055	8:2 FTOAc	<RL	58.0
PFNS	<RL	0.019	10:2 FTOAc	<RL	24.2
PFDS	<RL	0.044			
FASA (NV, SV)			n:2 FTOH (V)		
FBSA (NV)	<RL	0.059	4:2 FTOH	<RL	11.4
MeFBSA (SV)	<RL	1.32	5:2 FTOH	<RL	18.5
FHxSA (NV)	<RL	0.028	6:2 FTOH	<RL	25.1
FOSA (NV)	<RL	0.059	7:2 FTOH	<RL	23.6
MeFOSA (SV)	<RL	0.117	8:2 FTOH	<RL	23.0
EtFOSA (SV)	<RL	0.280	10:2 FTOH	<RL	56.8
FASAA (NV)			n:2 FTS (NV)		
FOSAA	<RL	0.042	4:2 FTS	0.56 \pm 0.22	0.056
MeFOSAA	<RL	0.059	6:2 FTS	<RL	0.107
EtFOSAA	<RL	0.140	8:2 FTS	<RL	0.057
			10:2 FTS	<RL	0.039
FASE (SV)					
MeBFSE	<RL	3.38			
MeFOSE	<RL	1.25			
EtFOSE	<RL	1.39			

Table 19. Measured PFAS concentrations ($\mu\text{g-PFAS} / \text{kg-textile}$; \pm standard deviation of triplicate measurements) and reporting limits for abraded HD-C.

PFAS	Concentration ($\mu\text{g/kg}$)	RL ($\mu\text{g/kg}$)	PFAS	Concentration ($\mu\text{g/kg}$)	RL ($\mu\text{g/kg}$)
PFCA (NV)			PPEA (NV)		
PFBA	0.554 \pm 0.040	0.122	PFEESA	<RL	0.015
PFPeA	<RL	0.040	PF4OPeA	<RL	0.075
PFHxA	<RL	1.32	PF5OHxA	<RL	0.017
PFHpA	<RL	0.228	3-6-OPFHpA	<RL	0.111
PFOA	<RL	0.383	HFPO-DA	<RL	0.228
PFNA	<RL	0.122	ADONA	<RL	0.038
PFDA	<RL	0.080	9Cl-PF3ONS	<RL	0.017
PFUnDA	<RL	0.122	11Cl-PF3OUdS	<RL	0.018
PFDoDA	<RL	0.122			
PFTrDA	<RL	0.122	n:2 FTAc (V)		
PFTeDA	<RL	0.040	8:2 FTAc	<RL	16.5
			10:2 FTAc	<RL	31.9
PFSA (NV)			n:2 FTMAC (V)		
PFPrS	<RL	0.271	6:2 FTMAC	<RL	54.0
PFBS	<RL	0.045	8:2 FTMAC	<RL	55.2
PFPeS	<RL	0.038	10:2 FTMAC	<RL	29.1
PFHxS	<RL	0.017			
PFHpS	<RL	0.053	n:2 FTOAc (V)		
PFOS	<RL	0.082	8:2 FTOAc	<RL	15.6
PFNS	<RL	0.018	10:2 FTOAc	<RL	15.9
PFDS	<RL	0.018			
FASA (NV, SV)			n:2 FTOH (V)		
FBSA (NV)	No Value		4:2 FTOH	<RL	15.6
MeFBSA (SV)	No Value		5:2 FTOH	<RL	32.6
FHxSA (NV)	No Value		6:2 FTOH	<RL	34.5
FOSA (NV)	<RL	0.194	7:2 FTOH	<RL	15.5
MeFOSA (SV)	<RL	0.236	8:2 FTOH	<RL	31.6
EtFOSA (SV)	<RL	0.281	10:2 FTOH	<RL	32.1
FASAA (NV)			n:2 FTS (NV)		
FOSAA	<RL	0.108	4:2 FTS	<RL	0.115
MeFOSAA	<RL	1.27	6:2 FTS	No Value	
EtFOSAA	<RL	0.475	8:2 FTS	<RL	0.219
			10:2 FTS	<RL	0.034
FASE (SV)					
MeFBSE	<RL	7.84			
MeFOSE	<RL	1.16			
EtFOSE	<RL	0.591			

Table 20. Measured PFAS concentrations ($\mu\text{g-PFAS} / \text{kg-textile}$; \pm standard deviation of triplicate measurements) and reporting limits for HD-C after thermal stressing.

PFAS	Concentration ($\mu\text{g}/\text{kg}$)	RL ($\mu\text{g}/\text{kg}$)	PFAS	Concentration ($\mu\text{g}/\text{kg}$)	RL ($\mu\text{g}/\text{kg}$)
PFCA (NV)			PPEA (NV)		
PFBA	0.062 \pm 0.004	0.058	PFEESA	<RL	0.048
PFPeA	0.081 \pm 0.009	0.061	PF4OPeA	<RL	0.052
PFHxA	0.52 \pm 0.15	0.295	PF5OHxA	<RL	0.065
PFHpA	<RL	0.145	3-6-OPFHpA	<RL	0.046
PFOA	0.145 \pm 0.031	0.058	HFPO-DA	<RL	0.103
PFNA	<RL	0.058	ADONA	<RL	0.017
PFDA	<RL	0.101	9Cl-PF3ONS	<RL	0.027
PFUnDA	<RL	0.103	11Cl-PF3OUdS	<RL	0.017
PFDoDA	<RL	0.086			
PFTTrDA	<RL	0.042	n:2 FTAc (V)		
PFTeDA	<RL	0.058	8:2 FTAc	<RL	80.9
			10:2 FTAc	<RL	30.6
PFSA (NV)			n:2 FTMAC (V)		
PFPrS	<RL	0.037	6:2 FTMAC	<RL	51.9
PFBS	<RL	0.122	8:2 FTMAC	<RL	111
PFPeS	<RL	0.129	10:2 FTMAC	<RL	58.5
PFHxS	<RL	0.053			
PFHpS	<RL	0.018	n:2 FTOAc (V)		
PFOS	<RL	0.054	8:2 FTOAc	<RL	76.5
PFNS	<RL	0.018	10:2 FTOAc	<RL	31.9
PFDS	<RL	0.040			
FASA (NV, SV)			n:2 FTOH (V)		
FBSA (NV)	<RL	0.058	4:2 FTOH	<RL	15.0
MeFBSA (SV)	<RL	1.74	5:2 FTOH	<RL	24.4
FHxSA (NV)	<RL	0.027	6:2 FTOH	<RL	33.1
FOSA (NV)	<RL	0.058	7:2 FTOH	<RL	31.1
MeFOSA (SV)	<RL	0.155	8:2 FTOH	<RL	30.3
EtFOSA (SV)	<RL	0.372	10:2 FTOH	<RL	74.9
FASAA (NV)			n:2 FTS (NV)		
FOSAA	<RL	0.041	4:2 FTS	0.371 \pm 0.051	0.054
MeFOSAA	<RL	0.058	6:2 FTS	<RL	0.098
EtFOSAA	<RL	0.137	8:2 FTS	<RL	0.056
			10:2 FTS	<RL	0.036
FASE (SV)					
MeFBSE	<RL	4.48			
MeFOSE	<RL	1.65			
EtFOSE	<RL	1.84			

Table 21. Measured PFAS concentrations ($\mu\text{g-PFAS} / \text{kg-textile}$; \pm standard deviation of triplicate measurements) and reporting limits for abraded HD-D.

PFAS	Concentration ($\mu\text{g}/\text{kg}$)	RL ($\mu\text{g}/\text{kg}$)	PFAS	Concentration ($\mu\text{g}/\text{kg}$)	RL ($\mu\text{g}/\text{kg}$)
PFCA (NV)			PPEA (NV)		
PFBA	<RL	0.108	PFEESA	<RL	0.013
PFPeA	<RL	0.036	PF4OPeA	<RL	0.066
PFHxA	<RL	1.16	PF5OHxA	<RL	0.015
PFHpA	<RL	0.201	3-6-OPFHpA	<RL	0.098
PFOA	<RL	0.337	HFPO-DA	<RL	0.201
PFNA	<RL	0.108	ADONA	<RL	0.034
PFDA	<RL	0.071	9Cl-PF3ONS	<RL	0.015
PFUnDA	<RL	0.108	11Cl-PF3OUdS	<RL	0.016
PFDoDA	<RL	0.108			
PFTTrDA	<RL	0.108	n:2 FTAc (V)		
PFTeDA	<RL	0.036	8:2 FTAc	<RL	15.4
			10:2 FTAc	<RL	29.7
PFSA (NV)			n:2 FTMAC (V)		
PFPrS	<RL	0.238	6:2 FTMAC	<RL	50.2
PFBS	<RL	0.039	8:2 FTMAC	<RL	51.4
PFPeS	<RL	0.033	10:2 FTMAC	<RL	27.1
PFHxS	0.032 ± 0.013	0.015			
PFHpS	<RL	0.047	n:2 FTOAc (V)		
PFOS	0.088 ± 0.018	0.072	8:2 FTOAc	<RL	14.5
PFNS	<RL	0.016	10:2 FTOAc	<RL	14.8
PFDS	<RL	0.016			
FASA (NV, SV)			n:2 FTOH (V)		
FBSA (NV)	<RL	0.016	4:2 FTOH	<RL	14.5
MeFBSA (SV)	<RL	5.10	5:2 FTOH	<RL	30.3
FHxSA (NV)	<RL	0.016	6:2 FTOH	<RL	32.1
FOSA (NV)	<RL	0.170	7:2 FTOH	<RL	14.4
MeFOSA (SV)	<RL	0.219	8:2 FTOH	<RL	29.4
EtFOSA (SV)	<RL	0.261	10:2 FTOH	<RL	29.8
FASAA (NV)			n:2 FTS (NV)		
FOSAA	<RL	0.095	4:2 FTS	<RL	0.101
MeFOSAA	<RL	1.11	6:2 FTS	No Value	
EtFOSAA	<RL	0.418	8:2 FTS	<RL	0.193
			10:2 FTS	<RL	0.030
FASE (SV)					
MeFBSE	<RL	7.27			
MeFOSE	<RL	1.074			
EtFOSE	<RL	0.548			

Table 22. Measured PFAS concentrations ($\mu\text{g-PFAS} / \text{kg-textile}$; \pm standard deviation of triplicate measurements) and reporting limits for HD-D after thermal stressing.

PFAS	Concentration ($\mu\text{g/kg}$)	RL ($\mu\text{g/kg}$)	PFAS	Concentration ($\mu\text{g/kg}$)	RL ($\mu\text{g/kg}$)
PFCA (NV)			PPEA (NV)		
PFBA	0.345 \pm 0.093	0.056	PFEESA	<RL	0.046
PFPeA	0.53 \pm 0.25	0.058	PF4OPeA	<RL	0.050
PFHxA	0.81 \pm 0.24	0.283	PF5OHxA	<RL	0.062
PFHpA	<RL	0.138	3-6-OPFHpA	No Value	
PFOA	0.186 \pm 0.074	0.056	HFPO-DA	<RL	0.099
PFNA	<RL	0.056	ADONA	<RL	0.017
PFDA	<RL	0.097	9Cl-PF3ONS	<RL	0.026
PFUnDA	<RL	0.099	11Cl-PF3OUdS	<RL	0.017
PFDoDA	<RL	0.082			
PFTTrDA	<RL	0.040	n:2 FTAc (V)		
PFTeDA	<RL	0.056	8:2 FTAc	<RL	71.9
			10:2 FTAc	<RL	27.2
PFSA (NV)			n:2 FTMAC (V)		
PFPrS	<RL	0.036	6:2 FTMAC	<RL	46.2
PFBS	<RL	0.117	8:2 FTMAC	<RL	98.8
PFPeS	<RL	0.124	10:2 FTMAC	<RL	52.0
PFHxS	<RL	0.051			
PFHpS	<RL	0.017	n:2 FTOAc (V)		
PFOS	<RL	0.052	8:2 FTOAc	<RL	68.0
PFNS	<RL	0.017	10:2 FTOAc	<RL	28.4
PFDS	<RL	0.039			
FASA (NV, SV)			n:2 FTOH (V)		
FBSA (NV)	No Value		4:2 FTOH	<RL	13.3
MeFBSA (SV)	<RL	1.55	5:2 FTOH	<RL	21.7
FHxSA (NV)	<RL	0.026	6:2 FTOH	<RL	29.4
FOSA (NV)	0.068 \pm 0.023	0.056	7:2 FTOH	<RL	27.7
MeFOSA (SV)	<RL	0.138	8:2 FTOH	<RL	26.9
EtFOSA (SV)	<RL	0.330	10:2 FTOH	<RL	66.6
FASAA (NV)			n:2 FTS (NV)		
FOSAA	<RL	0.039	4:2 FTS	0.35 \pm 0.15	0.052
MeFOSAA	<RL	0.056	6:2 FTS	2.2 \pm 2.0	0.094
EtFOSAA	<RL	0.132	8:2 FTS	<RL	0.054
			10:2 FTS	<RL	0.034
FASE (SV)					
MeFBSE	<RL	3.98			
MeFOSE	<RL	1.47			
EtFOSE	<RL	1.63			

Table 23. Measured PFAS concentrations ($\mu\text{g-PFAS} / \text{kg-textile}$; \pm standard deviation of triplicate measurements) and reporting limits for abraded HD-E.

PFAS	Concentration ($\mu\text{g}/\text{kg}$)	RL ($\mu\text{g}/\text{kg}$)	PFAS	Concentration ($\mu\text{g}/\text{kg}$)	RL ($\mu\text{g}/\text{kg}$)
PFCA (NV)			PPEA (NV)		
PFBA	1.51 \pm 0.69	0.110	PFEESA	<RL	0.014
PFPeA	<RL	0.036	PF4OPeA	<RL	0.068
PFHxA	<RL	1.19	PF5OHxA	<RL	0.015
PFHpA	<RL	0.205	3-6-OPFHpA	<RL	0.100
PFOA	<RL	0.344	HFPO-DA	<RL	0.205
PFNA	<RL	0.110	ADONA	<RL	0.034
PFDA	<RL	0.072	9Cl-PF3ONS	<RL	0.016
PFUnDA	<RL	0.110	11Cl-PF3OUdS	<RL	0.016
PFDoDA	<RL	0.110			
PFTrDA	<RL	0.110	n:2 FTAc (V)		
PFTeDA	<RL	0.036	8:2 FTAc	<RL	14.5
			10:2 FTAc	<RL	28.0
PFSA (NV)			n:2 FTMAC (V)		
PFPrS	<RL	0.243	6:2 FTMAC	<RL	47.5
PFBS	<RL	0.040	8:2 FTMAC	<RL	48.6
PFPeS	<RL	0.034	10:2 FTMAC	<RL	25.6
PFHxS	0.071 \pm 0.001	0.015			
PFHpS	<RL	0.048	n:2 FTOAc (V)		
PFOS	<RL	0.074	8:2 FTOAc	<RL	13.7
PFNS	<RL	0.016	10:2 FTOAc	<RL	14.0
PFDS	<RL	0.016			
FASA (NV, SV)			n:2 FTOH (V)		
FBSA (NV)	<RL	0.017	4:2 FTOH	<RL	13.7
MeFBSA (SV)	<RL	4.83	5:2 FTOH	<RL	28.7
FHxSA (NV)	<RL	0.017	6:2 FTOH	<RL	30.3
FOSA (NV)	<RL	0.174	7:2 FTOH	<RL	13.6
MeFOSA (SV)	<RL	0.207	8:2 FTOH	<RL	27.8
EtFOSA (SV)	<RL	0.246	10:2 FTOH	<RL	28.2
FASAA (NV)			n:2 FTS (NV)		
FOSAA	<RL	0.097	4:2 FTS	<RL	0.103
MeFOSAA	<RL	1.14	6:2 FTS	No Value	
EtFOSAA	<RL	0.426	8:2 FTS	<RL	0.197
			10:2 FTS	<RL	0.031
FASE (SV)					
MeFBSE	<RL	6.88			
MeFOSE	<RL	1.02			
EtFOSE	<RL	0.518			

Table 24. Measured PFAS concentrations ($\mu\text{g-PFAS} / \text{kg-textile}$; \pm standard deviation of triplicate measurements) and reporting limits for HD-E after thermal stressing.

PFAS	Concentration ($\mu\text{g}/\text{kg}$)	RL ($\mu\text{g}/\text{kg}$)	PFAS	Concentration ($\mu\text{g}/\text{kg}$)	RL ($\mu\text{g}/\text{kg}$)
PFCA (NV)			PPEA (NV)		
PFBA	0.338 \pm 0.040	0.053	PFEESA	<RL	0.044
PFPeA	0.259 \pm 0.096	0.056	PF4OPeA	<RL	0.048
PFHxA	0.62 \pm 0.15	0.272	PF5OHxA	<RL	0.060
PFHpA	<RL	0.167	3-6-OPFHpA	No Value	
PFOA	0.166 \pm 0.016	0.053	HFPO-DA	<RL	0.119
PFNA	0.079 \pm 0.001	0.053	ADONA	<RL	0.020
PFDA	<RL	0.117	9Cl-PF3ONS	<RL	0.025
PFUnDA	<RL	0.119	11Cl-PF3OUdS	<RL	0.020
PFDoDA	<RL	0.079			
PFTTrDA	<RL	0.048	n:2 FTAc (V)		
PFTeDA	<RL	0.053	8:2 FTAc	<RL	91.2
			10:2 FTAc	<RL	34.5
PFSA (NV)			n:2 FTMAC (V)		
PFPrS	<RL	0.035	6:2 FTMAC	<RL	58.5
PFBS	<RL	0.112	8:2 FTMAC	<RL	125
PFPeS	<RL	0.119	10:2 FTMAC	<RL	66.0
PFHxS	<RL	0.049			
PFHpS	<RL	0.020	n:2 FTOAc (V)		
PFOS	<RL	0.050	8:2 FTOAc	<RL	86.2
PFNS	<RL	0.020	10:2 FTOAc	<RL	36.0
PFDS	<RL	0.047			
FASA (NV, SV)			n:2 FTOH (V)		
FBSA (NV)	<RL	0.053	4:2 FTOH	<RL	16.9
MeFBSA (SV)	<RL	1.966	5:2 FTOH	<RL	27.5
FHxSA (NV)	<RL	0.025	6:2 FTOH	<RL	37.2
FOSA (NV)	0.059 \pm 0.006	0.053	7:2 FTOH	<RL	35.1
MeFOSA (SV)	<RL	0.174	8:2 FTOH	<RL	34.1
EtFOSA (SV)	<RL	0.417	10:2 FTOH	<RL	84.4
FASAA (NV)			n:2 FTS (NV)		
FOSAA	<RL	0.038	4:2 FTS	0.31 \pm 0.14	0.050
MeFOSAA	<RL	0.053	6:2 FTS	<RL	0.113
EtFOSAA	<RL	0.127	8:2 FTS	<RL	0.051
			10:2 FTS	<RL	0.036
FASE (SV)					
MeFBSE	<RL	5.05			
MeFOSE	<RL	1.85			
EtFOSE	<RL	2.08			

Table 25. Measured PFAS concentrations ($\mu\text{g-PFAS} / \text{kg-textile}$; \pm standard deviation of triplicate measurements) and reporting limits for abraded HD-F.

PFAS	Concentration ($\mu\text{g/kg}$)	RL ($\mu\text{g/kg}$)	PFAS	Concentration ($\mu\text{g/kg}$)	RL ($\mu\text{g/kg}$)
<i>PFCA (NV)</i>			<i>PPEA (NV)</i>		
PFBA	0.46 \pm 0.29	0.109	PFEESA	<RL	0.013
PFPeA	<RL	0.036	PF4OPeA	<RL	0.067
PFHxA	<RL	1.18	PF5OHxA	<RL	0.015
PFHpA	<RL	0.203	3-6-OPFHpA	<RL	0.099
PFOA	<RL	0.341	HFPO-DA	<RL	0.203
PFNA	<RL	0.109	ADONA	<RL	0.034
PFDA	<RL	0.071	9Cl-PF3ONS	<RL	0.016
PFUnDA	<RL	0.109	11Cl-PF3OUdS	<RL	0.016
PFDoDA	<RL	0.109			
PFTTrDA	<RL	0.109	<i>n:2 FTAc (V)</i>		
PFTeDA	<RL	0.036	8:2 FTAc	<RL	16.1
			10:2 FTAc	<RL	31.0
<i>PFSA (NV)</i>			<i>n:2 FTMAC (V)</i>		
PFPrS	<RL	0.241	6:2 FTMAC	<RL	52.5
PFBS	<RL	0.040	8:2 FTMAC	<RL	53.7
PFPeS	<RL	0.034	10:2 FTMAC	<RL	28.3
PFHxS	0.079 \pm 0.021	0.015			
PFHpS	<RL	0.047	<i>n:2 FTOAc (V)</i>		
PFOS	0.090 \pm 0.015	0.073	8:2 FTOAc	<RL	15.2
PFNS	<RL	0.016	10:2 FTOAc	<RL	15.4
PFDS	<RL	0.016			
<i>FASA (NV, SV)</i>			<i>n:2 FTOH (V)</i>		
FBSA (NV)	<RL	0.017	4:2 FTOH	<RL	15.2
MeFBSA (SV)	<RL	5.326	5:2 FTOH	<RL	31.7
FHxSA (NV)	<RL	0.017	6:2 FTOH	<RL	33.5
FOSA (NV)	<RL	0.172	7:2 FTOH	<RL	15.0
MeFOSA (SV)	<RL	0.228	8:2 FTOH	<RL	30.7
EtFOSA (SV)	<RL	0.272	10:2 FTOH	<RL	31.2
<i>FASAA (NV)</i>			<i>n:2 FTS (NV)</i>		
FOSAA	<RL	0.096	4:2 FTS	<RL	0.102
MeFOSAA	<RL	1.13	6:2 FTS	No Value	
EtFOSAA	<RL	0.423	8:2 FTS	<RL	0.195
			10:2 FTS	<RL	0.031
<i>FASE (SV)</i>					
MeFBSE	No Value				
MeFOSE	<RL	1.12			
EtFOSE	<RL	0.572			

Table 26. Measured PFAS concentrations ($\mu\text{g-PFAS} / \text{kg-textile}$; \pm standard deviation of triplicate measurements) and reporting limits for HD-F after thermal stressing.

PFAS	Concentration ($\mu\text{g}/\text{kg}$)	RL ($\mu\text{g}/\text{kg}$)	PFAS	Concentration ($\mu\text{g}/\text{kg}$)	RL ($\mu\text{g}/\text{kg}$)
PFCA (NV)			PPEA (NV)		
PFBA	0.79 \pm 0.23	0.048	PFEESA	<RL	0.040
PFPeA	0.12 \pm 0.045	0.051	PF4OPeA	<RL	0.044
PFHxA	0.51 \pm 0.13	0.246	PF5OHxA	<RL	0.054
PFHpA	<RL	0.146	3-6-OPFHpA	No Value	
PFOA	0.132 \pm 0.022	0.048	HFPO-DA	<RL	0.104
PFNA	<RL	0.048	ADONA	<RL	0.017
PFDA	<RL	0.102	9Cl-PF3ONS	<RL	0.023
PFUnDA	<RL	0.104	11Cl-PF3OUdS	<RL	0.017
PFDoDA	<RL	0.072			
PFTTrDA	<RL	0.042	n:2 FTAc (V)		
PFTeDA	<RL	0.048	8:2 FTAc	<RL	68.2
			10:2 FTAc	<RL	25.8
PFSA (NV)			n:2 FTMAC (V)		
PFPrS	<RL	0.031	6:2 FTMAC	<RL	43.8
PFBS	<RL	0.102	8:2 FTMAC	<RL	93.6
PFPeS	<RL	0.108	10:2 FTMAC	<RL	49.3
PFHxS	<RL	0.044			
PFHpS	<RL	0.018	n:2 FTOAc (V)		
PFOS	<RL	0.045	8:2 FTOAc	<RL	64.5
PFNS	<RL	0.018	10:2 FTOAc	<RL	26.9
PFDS	<RL	0.041			
FASA (NV, SV)			n:2 FTOH (V)		
FBSA (NV)	<RL	0.048	4:2 FTOH	<RL	12.7
MeFBSA (SV)	<RL	1.46	5:2 FTOH	<RL	20.6
FHxSA (NV)	<RL	0.023	6:2 FTOH	<RL	27.8
FOSA (NV)	<RL	0.048	7:2 FTOH	<RL	26.2
MeFOSA (SV)	<RL	0.130	8:2 FTOH	<RL	25.5
EtFOSA (SV)	<RL	0.312	10:2 FTOH	<RL	63.1
FASAA (NV)			n:2 FTS (NV)		
FOSAA	<RL	0.034	4:2 FTS	0.513 \pm 0.061	0.045
MeFOSAA	<RL	0.048	6:2 FTS	68 \pm 15	0.479
EtFOSAA	<RL	0.115	8:2 FTS	<RL	0.046
			10:2 FTS	<RL	0.033
FASE (SV)					
MeFBSE	<RL	3.75			
MeFOSE	<RL	1.39			
EtFOSE	<RL	1.54			

Table 27. Measured PFAS concentrations ($\mu\text{g-PFAS} / \text{kg-textile}$; \pm standard deviation of triplicate measurements) and reporting limits for abraded HD-G.

PFAS	Concentration ($\mu\text{g/kg}$)	RL ($\mu\text{g/kg}$)	PFAS	Concentration ($\mu\text{g/kg}$)	RL ($\mu\text{g/kg}$)
PFCA (NV)			PPEA (NV)		
PFBA	<RL	0.108	PFEESA	<RL	0.013
PFPeA	<RL	0.036	PF4OPeA	<RL	0.067
PFHxA	<RL	1.17	PF5OHxA	<RL	0.015
PFHpA	<RL	0.202	3-6-OPFHpA	<RL	0.098
PFOA	<RL	0.338	HFPO-DA	<RL	0.202
PFNA	<RL	0.108	ADONA	<RL	0.034
PFDA	<RL	0.071	9Cl-PF3ONS	<RL	0.015
PFUnDA	<RL	0.108	11Cl-PF3OUdS	<RL	0.016
PFDoDA	<RL	0.108			
PFTTrDA	<RL	0.108	n:2 FTAc (V)		
PFTeDA	<RL	0.036	8:2 FTAc	<RL	15.3
			10:2 FTAc	<RL	29.5
PFSA (NV)			n:2 FTMAC (V)		
PFPrS	<RL	0.239	6:2 FTMAC	<RL	50.0
PFBS	<RL	0.039	8:2 FTMAC	<RL	51.1
PFPeS	<RL	0.034	10:2 FTMAC	<RL	26.9
PFHxS	0.050 ± 0.012	0.015			
PFHpS	<RL	0.047	n:2 FTOAc (V)		
PFOS	0.095 ± 0.007	0.073	8:2 FTOAc	<RL	14.5
PFNS	<RL	0.016	10:2 FTOAc	<RL	14.7
PFDS	<RL	0.016			
FASA (NV, SV)			n:2 FTOH (V)		
FBSA (NV)	<RL	0.017	4:2 FTOH	<RL	14.4
MeFBSA (SV)	<RL	5.07	5:2 FTOH	<RL	30.2
FHxSA (NV)	<RL	0.017	6:2 FTOH	<RL	31.9
FOSA (NV)	<RL	0.171	7:2 FTOH	<RL	14.3
MeFOSA (SV)	<RL	0.217	8:2 FTOH	<RL	29.2
EtFOSA (SV)	<RL	0.259	10:2 FTOH	<RL	29.7
FASAA (NV)			n:2 FTS (NV)		
FOSAA	<RL	0.095	4:2 FTS	<RL	0.101
MeFOSAA	<RL	1.12	6:2 FTS	No Value	
EtFOSAA	<RL	0.419	8:2 FTS	<RL	0.194
			10:2 FTS	<RL	0.030
FASE (SV)					
MeFBSE	<RL	7.22			
MeFOSE	<RL	1.07			
EtFOSE	<RL	0.544			

Table 28. Measured PFAS concentrations ($\mu\text{g-PFAS} / \text{kg-textile}$; \pm standard deviation of triplicate measurements) and reporting limits for HD-G after thermal stressing.

PFAS	Concentration ($\mu\text{g}/\text{kg}$)	RL ($\mu\text{g}/\text{kg}$)	PFAS	Concentration ($\mu\text{g}/\text{kg}$)	RL ($\mu\text{g}/\text{kg}$)
PFCA (NV)			PPEA (NV)		
PFBA	0.831 ± 0.067	0.056	PFEESA	<RL	0.046
PFPeA	0.092 ± 0.019	0.059	PF4OPeA	0.152 ± 0.039	0.051
PFHxA	0.555 ± 0.059	0.286	PF5OHxA	<RL	0.063
PFHpA	<RL	0.147	3-6-OPFHpA	No Value	
PFOA	0.173 ± 0.016	0.056	HFPO-DA	<RL	0.105
PFNA	<RL	0.056	ADONA	<RL	0.018
PFDA	<RL	0.103	9Cl-PF3ONS	<RL	0.026
PFUnDA	<RL	0.105	11Cl-PF3OUdS	<RL	0.018
PFDoDA	<RL	0.083			
PFTTrDA	<RL	0.043	n:2 FTAc (V)		
PFTeDA	<RL	0.056	8:2 FTAc	<RL	81.5
			10:2 FTAc	<RL	30.8
PFSA (NV)			n:2 FTMAC (V)		
PFPrS	<RL	0.036	6:2 FTMAC	<RL	52.3
PFBS	<RL	0.118	8:2 FTMAC	<RL	111.9
PFPeS	<RL	0.125	10:2 FTMAC	<RL	59.0
PFHxS	<RL	0.051			
PFHpS	<RL	0.018	n:2 FTOAc (V)		
PFOS	0.076 ± 0.019	0.052	8:2 FTOAc	<RL	77.1
PFNS	<RL	0.018	10:2 FTOAc	<RL	32.2
PFDS	<RL	0.041			
FASA (NV, SV)			n:2 FTOH (V)		
FBSA (NV)	<RL	0.056	4:2 FTOH	<RL	15.1
MeFBSA (SV)	<RL	1.76	5:2 FTOH	<RL	24.6
FHxSA (NV)	<RL	0.027	6:2 FTOH	<RL	33.3
FOSA (NV)	<RL	0.056	7:2 FTOH	<RL	31.3
MeFOSA (SV)	<RL	0.156	8:2 FTOH	<RL	30.5
EtFOSA (SV)	<RL	0.374	10:2 FTOH	<RL	75.4
FASAA (NV)			n:2 FTS (NV)		
FOSAA	<RL	0.040	4:2 FTS	No Value	
MeFOSAA	<RL	0.056	6:2 FTS	<RL	0.100
EtFOSAA	<RL	0.133	8:2 FTS	<RL	0.101
			10:2 FTS	<RL	0.036
FASE (SV)					
MeFBSE	<RL	4.52			
MeFOSE	<RL	1.66			
EtFOSE	<RL	1.86			

Table 29. Measured PFAS concentrations ($\mu\text{g-PFAS} / \text{kg-textile}$; \pm standard deviation of triplicate measurements) and reporting limits for abraded HD-H.

PFAS	Concentration ($\mu\text{g}/\text{kg}$)	RL ($\mu\text{g}/\text{kg}$)	PFAS	Concentration ($\mu\text{g}/\text{kg}$)	RL ($\mu\text{g}/\text{kg}$)
PFCA (NV)			PPEA (NV)		
PFBA	<RL	1.26	PFEESA	<RL	0.039
PFPeA	<RL	0.235	PF4OPeA	0.162 ± 0.064	0.075
PFHxA	<RL	1.04	PF5OHxA	<RL	0.043
PFHpA	<RL	4.96	3-6-OPFHpA	<RL	0.107
PFOA	<RL	1.26	HFPO-DA	<RL	0.048
PFNA	<RL	0.061	ADONA	0.030 ± 0.001	0.022
PFDA	<RL	0.235	9Cl-PF3ONS	<RL	0.018
PFUnDA	<RL	0.118	11Cl-PF3OUdS	<RL	0.019
PFDoDA	<RL	0.118			
PFTTrDA	<RL	0.235	n:2 FTAc (V)		
PFTeDA	<RL	0.118	8:2 FTAc	<RL	15.1
			10:2 FTAc	<RL	13.9
PFSA (NV)			n:2 FTMAC (V)		
PFPrS	<RL	0.902	6:2 FTMAC	<RL	49.3
PFBS	<RL	0.074	8:2 FTMAC	<RL	50.4
PFPeS	<RL	0.045	10:2 FTMAC	<RL	26.6
PFHxS	<RL	0.083			
PFHpS	<RL	0.045	n:2 FTOAc (V)		
PFOS	0.126 ± 0.013	0.095	8:2 FTOAc	<RL	14.3
PFNS	<RL	0.019	10:2 FTOAc	<RL	14.5
PFDS	<RL	0.019			
FASA (NV, SV)			n:2 FTOH (V)		
FBSA (NV)	<RL	0.020	4:2 FTOH	<RL	14.2
MeFBSA (SV)	<RL	0.834	5:2 FTOH	<RL	14.2
FHxSA (NV)	<RL	0.020	6:2 FTOH	<RL	15.0
FOSA (NV)	<RL	0.136	7:2 FTOH	<RL	14.1
MeFOSA (SV)	<RL	0.477	8:2 FTOH	<RL	13.8
EtFOSA (SV)	<RL	0.280	10:2 FTOH	<RL	29.2
FASAA (NV)			n:2 FTS (NV)		
FOSAA	<RL	1.11	4:2 FTS	<RL	0.045
MeFOSAA	<RL	0.235	6:2 FTS	<RL	0.112
EtFOSAA	<RL	0.118	8:2 FTS	<RL	0.046
			10:2 FTS	No Value	
FASE (SV)					
MeFBSE	<RL	1.30			
MeFOSE	<RL	0.478			
EtFOSE	<RL	0.489			

Table 30. Measured PFAS concentrations ($\mu\text{g-PFAS} / \text{kg-textile}$; \pm standard deviation of triplicate measurements) and reporting limits for HD-H after thermal stressing.

PFAS	Concentration ($\mu\text{g}/\text{kg}$)	RL ($\mu\text{g}/\text{kg}$)	PFAS	Concentration ($\mu\text{g}/\text{kg}$)	RL ($\mu\text{g}/\text{kg}$)
PFCA (NV)			PPEA (NV)		
PFBA	0.85 \pm 0.14	0.051	PFEESA	0.056 \pm 0.023	0.042
PFPeA	0.16 \pm 0.035	0.053	PF4OPeA	0.224 \pm 0.031	0.046
PFHxA	0.719 \pm 0.081	0.259	PF5OHxA	0.075 \pm 0.005	0.057
PFHpA	<RL	0.145	3-6-OPFHpA	No Value	
PFOA	0.192 \pm 0.025	0.051	HFPO-DA	<RL	0.104
PFNA	0.067 \pm 0.018	0.051	ADONA	<RL	0.017
PFDA	<RL	0.101	9Cl-PF3ONS	<RL	0.024
PFUnDA	<RL	0.104	11Cl-PF3OUdS	<RL	0.017
PFDoDA	<RL	0.075			
PFTTrDA	<RL	0.042	n:2 FTAc (V)		
PFTeDA	<RL	0.051	8:2 FTAc	<RL	89.3
			10:2 FTAc	<RL	33.7
PFSA (NV)			n:2 FTMAC (V)		
PFPrS	0.053 \pm 0.022	0.033	6:2 FTMAC	<RL	57.3
PFBS	<RL	0.107	8:2 FTMAC	<RL	122.6
PFPeS	<RL	0.114	10:2 FTMAC	<RL	64.6
PFHxS	0.080 \pm 0.036	0.047			
PFHpS	<RL	0.018	n:2 FTOAc (V)		
PFOS	0.133 \pm 0.037	0.047	8:2 FTOAc	<RL	84.4
PFNS	<RL	0.018	10:2 FTOAc	<RL	35.2
PFDS	<RL	0.041			
FASA (NV, SV)			n:2 FTOH (V)		
FBSA (NV)	<RL	0.051	4:2 FTOH	<RL	16.6
MeFBSA (SV)	<RL	1.92	5:2 FTOH	<RL	27.0
FHxSA (NV)	<RL	0.024	6:2 FTOH	<RL	36.5
FOSA (NV)	0.083 \pm 0.036	0.051	7:2 FTOH	<RL	34.3
MeFOSA (SV)	<RL	0.174	8:2 FTOH	<RL	33.4
EtFOSA (SV)	<RL	0.416	10:2 FTOH	<RL	82.6
FASAA (NV)			n:2 FTS (NV)		
FOSAA	<RL	0.036	4:2 FTS	No Value	
MeFOSAA	<RL	0.051	6:2 FTS	<RL	0.098
EtFOSAA	<RL	0.121	8:2 FTS	<RL	0.099
			10:2 FTS	<RL	0.036
FASE (SV)					
MeFBSE	<RL	4.94			
MeFOSE	<RL	1.85			
EtFOSE	<RL	2.03			

Table 31. Measured PFAS concentrations ($\mu\text{g-PFAS} / \text{kg-textile}$; \pm standard deviation of triplicate measurements) and reporting limits for abraded WL-C.

PFAS	Concentration ($\mu\text{g/kg}$)	RL ($\mu\text{g/kg}$)	PFAS	Concentration ($\mu\text{g/kg}$)	RL ($\mu\text{g/kg}$)
PFCA (NV)			PPEA (NV)		
PFBA	0.31 \pm 0.17	0.154	PFEESA	<RL	0.019
PFPeA	0.146 \pm 0.049	0.051	PF4OPeA	<RL	0.095
PFHxA	2.56 \pm 0.16	1.66	PF5OHxA	<RL	0.021
PFHpA	<RL	0.287	3-6-OPFHpA	<RL	0.140
PFOA	<RL	0.482	HFPO-DA	<RL	0.287
PFNA	<RL	0.154	ADONA	<RL	0.048
PFDA	<RL	0.101	9Cl-PF3ONS	<RL	0.022
PFUnDA	<RL	0.154	11Cl-PF3OUdS	<RL	0.022
PFDoDA	<RL	0.154			
PFTTrDA	<RL	0.154	n:2 FTAc (V)		
PFTeDA	<RL	0.051	8:2 FTAc	<RL	22.0
			10:2 FTAc	<RL	42.6
PFSA (NV)			n:2 FTMAC (V)		
PFPrS	<RL	0.341	6:2 FTMAC	<RL	72.0
PFBS	<RL	0.056	8:2 FTMAC	<RL	73.7
PFPeS	<RL	0.048	10:2 FTMAC	<RL	38.8
PFHxS	<RL	0.022			
PFHpS	<RL	0.067	n:2 FTOAc (V)		
PFOS	<RL	0.104	8:2 FTOAc	<RL	20.8
PFNS	<RL	0.023	10:2 FTOAc	<RL	21.2
PFDS	<RL	0.023			
FASA (NV, SV)			n:2 FTOH (V)		
FBSA (NV)	<RL	0.024	4:2 FTOH	<RL	20.8
MeFBSA (SV)	<RL	7.25	5:2 FTOH	<RL	43.5
FHxSA (NV)	<RL	0.024	6:2 FTOH	<RL	46.0
FOSA (NV)	<RL	0.243	7:2 FTOH	<RL	20.6
MeFOSA (SV)	<RL	0.311	8:2 FTOH	<RL	42.2
EtFOSA (SV)	<RL	0.370	10:2 FTOH	<RL	42.8
FASAA (NV)			n:2 FTS (NV)		
FOSAA	<RL	0.136	4:2 FTS	<RL	0.144
MeFOSAA	<RL	1.59	6:2 FTS	No Value	
EtFOSAA	<RL	0.597	8:2 FTS	<RL	0.276
			10:2 FTS	<RL	0.043
FASE (SV)					
MeFBSE	<RL	10.3			
MeFOSE	<RL	1.52			
EtFOSE	<RL	0.778			

Table 32. Measured PFAS concentrations ($\mu\text{g-PFAS} / \text{kg-textile}$; \pm standard deviation of triplicate measurements) and reporting limits for WL-C following controlled weathering.

PFAS	Concentration ($\mu\text{g/kg}$)	RL ($\mu\text{g/kg}$)	PFAS	Concentration ($\mu\text{g/kg}$)	RL ($\mu\text{g/kg}$)
PFCA (NV)			PPEA (NV)		
PFBA	<RL	1.07	PFEESA	<RL	0.033
PFPeA	0.41 ± 0.30	0.200	PF4OPeA	<RL	0.064
PFHxA	4.1 ± 3.6	0.886	PF5OHxA	<RL	0.037
PFHpA	<RL	4.21	3-6-OPFHpA	<RL	0.091
PFOA	<RL	1.07	HFPO-DA	<RL	0.041
PFNA	<RL	0.052	ADONA	<RL	0.019
PFDA	<RL	0.200	9Cl-PF3ONS	<RL	0.016
PFUnDA	<RL	0.100	11Cl-PF3OUdS	<RL	0.016
PFDoDA	<RL	0.100			
PFTrDA	<RL	0.200	n:2 FTAc (V)		
PFTeDA	<RL	0.100	8:2 FTAc	<RL	18.5
			10:2 FTAc	<RL	17.0
PFSA (NV)			n:2 FTMAC (V)		
PFPrS	<RL	0.767	6:2 FTMAC	<RL	60.5
PFBS	0.123 ± 0.041	0.063	8:2 FTMAC	<RL	61.9
PFPeS	<RL	0.038	10:2 FTMAC	<RL	32.6
PFHxS	<RL	0.070			
PFHpS	<RL	0.039	n:2 FTOAc (V)		
PFOS	<RL	0.081	8:2 FTOAc	<RL	17.5
PFNS	<RL	0.016	10:2 FTOAc	<RL	17.8
PFDS	<RL	0.016			
FASA (NV, SV)			n:2 FTOH (V)		
FBSA (NV)	0.323 ± 0.078	0.017	4:2 FTOH	<RL	17.5
MeFBSA (SV)	<RL	0.634	5:2 FTOH	<RL	17.4
FHxSA (NV)	<RL	0.017	6:2 FTOH	<RL	18.4
FOSA (NV)	0.160 ± 0.031	0.115	7:2 FTOH	<RL	17.3
MeFOSA (SV)	<RL	0.588	8:2 FTOH	<RL	16.9
EtFOSA (SV)	<RL	0.346	10:2 FTOH	<RL	35.8
FASAA (NV)			n:2 FTS (NV)		
FOSAA	<RL	0.943	4:2 FTS	<RL	0.038
MeFOSAA	<RL	0.200	6:2 FTS	<RL	0.095
EtFOSAA	<RL	0.100	8:2 FTS	<RL	0.039
			10:2 FTS	<RL	0.085
FASE (SV)					
MeFBSE	1.86 ± 0.22	1.43			
MeFOSE	<RL	0.589			
EtFOSE	<RL	0.603			

Table 33. Measured PFAS concentrations ($\mu\text{g-PFAS} / \text{kg-textile}$; \pm standard deviation of triplicate measurements) and reporting limits for abraded WL-E.

PFAS	Concentration ($\mu\text{g}/\text{kg}$)	RL ($\mu\text{g}/\text{kg}$)	PFAS	Concentration ($\mu\text{g}/\text{kg}$)	RL ($\mu\text{g}/\text{kg}$)
PFCA (NV)			PPEA (NV)		
PFBA	21.4 \pm 2.8	0.145	PFEESA	<RL	0.018
PFPeA	24.7 \pm 3.5	0.048	PF4OPeA	<RL	0.089
PFHxA	59.3 \pm 1.4	1.57	PF5OHxA	<RL	0.020
PFHpA	7.33 \pm 0.27	0.271	3-6-OPFHpA	<RL	0.132
PFOA	<RL	0.454	HFPO-DA	<RL	0.271
PFNA	<RL	0.145	ADONA	<RL	0.045
PFDA	0.110 \pm 0.015	0.095	9Cl-PF3ONS	<RL	0.021
PFUnDA	<RL	0.145	11Cl-PF3OUdS	<RL	0.021
PFDoDA	<RL	0.145			
PFTTrDA	<RL	0.145	n:2 FTAc (V)		
PFTeDA	<RL	0.048	8:2 FTAc	<RL	21.4
			10:2 FTAc	<RL	41.4
PFSA (NV)			n:2 FTMAC (V)		
PFPrS	<RL	0.321	6:2 FTMAC	<RL	70.0
PFBS	0.195 \pm 0.082	0.053	8:2 FTMAC	<RL	71.6
PFPeS	<RL	0.045	10:2 FTMAC	<RL	37.8
PFHxS	<RL	0.020			
PFHpS	<RL	0.063	n:2 FTOAc (V)		
PFOS	0.138 \pm 0.021	0.098	8:2 FTOAc	<RL	20.3
PFNS	<RL	0.021	10:2 FTOAc	<RL	20.6
PFDS	<RL	0.021			
FASA (NV, SV)			n:2 FTOH (V)		
FBSA (NV)	<RL	0.022	4:2 FTOH	<RL	20.2
MeFBSA (SV)	<RL	7.07	5:2 FTOH	<RL	42.3
FHxSA (NV)	<RL	0.022	6:2 FTOH	460 \pm 110	44.7
FOSA (NV)	0.287 \pm 0.019	0.230	7:2 FTOH	<RL	20.1
MeFOSA (SV)	<RL	0.303	8:2 FTOH	<RL	41.0
EtFOSA (SV)	<RL	0.361	10:2 FTOH	<RL	41.6
FASAA (NV)			n:2 FTS (NV)		
FOSAA	<RL	0.128	4:2 FTS	<RL	0.136
MeFOSAA	<RL	1.50	6:2 FTS	<RL	1.43
EtFOSAA	<RL	0.563	8:2 FTS	<RL	0.260
			10:2 FTS	<RL	0.041
FASE (SV)					
MeFBSE	No Value				
MeFOSE	<RL	1.49			
EtFOSE	<RL	0.759			

Table 34. Measured PFAS concentrations ($\mu\text{g-PFAS} / \text{kg-textile}$; \pm standard deviation of triplicate measurements) and reporting limits for WL-E following exposure to controlled weathering.

PFAS	Concentration ($\mu\text{g/kg}$)	RL ($\mu\text{g/kg}$)	PFAS	Concentration ($\mu\text{g/kg}$)	RL ($\mu\text{g/kg}$)
PFCA (NV)			PPEA (NV)		
PFBA	1.56 \pm 0.29	1.23	PFEESA	<RL	0.038
PFPeA	1.34 \pm 0.44	0.229	PF4OPeA	<RL	0.074
PFHxA	9.8 \pm 4.5	1.02	PF5OHxA	<RL	0.042
PFHpA	<RL	4.83	3-6-OPFHpA	<RL	0.104
PFOA	<RL	1.23	HFPO-DA	<RL	0.047
PFNA	<RL	0.059	ADONA	<RL	0.021
PFDA	<RL	0.229	9Cl-PF3ONS	<RL	0.018
PFUnDA	<RL	0.115	11Cl-PF3OUdS	<RL	0.018
PFDoDA	<RL	0.115			
PFTTrDA	<RL	0.229	n:2 FTAc (V)		
PFTeDA	<RL	0.115	8:2 FTAc	<RL	20.5
			10:2 FTAc	<RL	18.9
PFSA (NV)			n:2 FTMAC (V)		
PFPrS	<RL	0.879	6:2 FTMAC	<RL	67.0
PFBS	1.256 \pm 0.021	0.072	8:2 FTMAC	<RL	68.5
PFPeS	<RL	0.044	10:2 FTMAC	<RL	36.1
PFHxS	<RL	0.081			
PFHpS	<RL	0.044	n:2 FTOAc (V)		
PFOS	<RL	0.093	8:2 FTOAc	<RL	19.4
PFNS	<RL	0.018	10:2 FTOAc	<RL	19.7
PFDS	<RL	0.019			
FASA (NV, SV)			n:2 FTOH (V)		
FBSA (NV)	1.38 \pm 0.20	0.019	4:2 FTOH	<RL	19.4
MeFBSA (SV)	<RL	0.908	5:2 FTOH	<RL	19.3
FHxSA (NV)	<RL	0.019	6:2 FTOH	187 \pm 44	20.4
FOSA (NV)	0.214 \pm 0.026	0.132	7:2 FTOH	<RL	19.2
MeFOSA (SV)	<RL	0.650	8:2 FTOH	<RL	18.7
EtFOSA (SV)	<RL	0.382	10:2 FTOH	<RL	39.6
FASAA (NV)			n:2 FTS (NV)		
FOSAA	<RL	1.08	4:2 FTS	<RL	0.044
MeFOSAA	<RL	0.229	6:2 FTS	3.90 \pm 0.25	0.109
EtFOSAA	<RL	0.115	8:2 FTS	<RL	0.045
			10:2 FTS	<RL	0.097
FASE (SV)					
MeFBSE	9.46 \pm 0.96	2.05			
MeFOSE	<RL	0.652			
EtFOSE	<RL	0.667			

Table 35. Measured PFAS concentrations ($\mu\text{g-PFAS / kg-textile}$; \pm standard deviation of triplicate measurements) and reporting limits for abraded WL-F.

PFAS	Concentration ($\mu\text{g/kg}$)	RL ($\mu\text{g/kg}$)	PFAS	Concentration ($\mu\text{g/kg}$)	RL ($\mu\text{g/kg}$)
PFCA (NV)			PPEA (NV)		
PFBA	1.06 \pm 0.13	0.165	PFEESA	<RL	0.020
PFPeA	0.942 \pm 0.076	0.054	PF4OPeA	0.339 \pm 0.070	0.101
PFHxA	8.9 \pm 1.4	1.78	PF5OHxA	<RL	0.023
PFHpA	0.395 \pm 0.056	0.308	3-6-OPFHpA	<RL	0.150
PFOA	<RL	0.516	HFPO-DA	<RL	0.308
PFNA	<RL	0.165	ADONA	<RL	0.051
PFDA	<RL	0.108	9Cl-PF3ONS	<RL	0.024
PFUnDA	<RL	0.165	11Cl-PF3OUdS	<RL	0.024
PFDoDA	<RL	0.165			
PFTTrDA	<RL	0.165	n:2 FTAc (V)		
PFTeDA	<RL	0.054	8:2 FTAc	<RL	23.0
			10:2 FTAc	<RL	44.5
PFSA (NV)			n:2 FTMAC (V)		
PFPrS	<RL	0.365	6:2 FTMAC	<RL	75.2
PFBS	0.586 \pm 0.032	0.060	8:2 FTMAC	<RL	77.0
PFPeS	<RL	0.051	10:2 FTMAC	<RL	40.6
PFHxS	<RL	0.023			
PFHpS	<RL	0.072	n:2 FTOAc (V)		
PFOS	0.124 \pm 0.006	0.111	8:2 FTOAc	<RL	21.8
PFNS	<RL	0.024	10:2 FTOAc	<RL	22.1
PFDS	<RL	0.024			
FASA (NV, SV)			n:2 FTOH (V)		
FBSA (NV)	0.033 \pm 0.002	0.025	4:2 FTOH	<RL	21.8
MeFBSA (SV)	<RL	7.59	5:2 FTOH	<RL	45.5
FHxSA (NV)	<RL	0.025	6:2 FTOH	350 \pm 38	48.1
FOSA (NV)	<RL	0.261	7:2 FTOH	<RL	21.6
MeFOSA (SV)	<RL	0.325	8:2 FTOH	<RL	44.1
EtFOSA (SV)	<RL	0.387	10:2 FTOH	<RL	44.7
FASAA (NV)			n:2 FTS (NV)		
FOSAA	<RL	0.145	4:2 FTS	<RL	0.154
MeFOSAA	<RL	1.70	6:2 FTS	No Value	
EtFOSAA	<RL	0.639	8:2 FTS	<RL	0.295
			10:2 FTS	<RL	0.046
FASE (SV)					
MeFBSE	<RL	10.8			
MeFOSE	<RL	1.60			
EtFOSE	<RL	0.814			

Table 36. Measured PFAS concentrations ($\mu\text{g-PFAS} / \text{kg-textile}$; \pm standard deviation of triplicate measurements) and reporting limits for WL-F following exposure to controlled weathering.

PFAS	Concentration ($\mu\text{g/kg}$)	RL ($\mu\text{g/kg}$)	PFAS	Concentration ($\mu\text{g/kg}$)	RL ($\mu\text{g/kg}$)
PFCA (NV)			PPEA (NV)		
PFBA	<RL	1.35	PFEESA	<RL	0.041
PFPeA	0.56 ± 0.14	0.251	PF4OPeA	<RL	0.081
PFHxA	5.80 ± 0.68	1.117	PF5OHxA	<RL	0.046
PFHpA	<RL	5.310	3-6-OPFHpA	<RL	0.115
PFOA	<RL	1.347	HFPO-DA	<RL	0.051
PFNA	<RL	0.065	ADONA	<RL	0.023
PFDA	<RL	0.251	9Cl-PF3ONS	<RL	0.020
PFUnDA	<RL	0.126	11Cl-PF3OUdS	<RL	0.020
PFDoDA	<RL	0.126			
PFTTrDA	<RL	0.251	n:2 FTAc (V)		
PFTeDA	<RL	0.126	8:2 FTAc	<RL	17.7
			10:2 FTAc	<RL	16.3
PFSA (NV)			n:2 FTMAC (V)		
PFPrS	<RL	0.966	6:2 FTMAC	102.8 ± 7.5	57.8
PFBS	0.361 ± 0.024	0.080	8:2 FTMAC	<RL	59.2
PFPeS	<RL	0.048	10:2 FTMAC	<RL	31.2
PFHxS	<RL	0.089			
PFHpS	<RL	0.049	n:2 FTOAc (V)		
PFOS	<RL	0.102	8:2 FTOAc	<RL	16.7
PFNS	<RL	0.020	10:2 FTOAc	<RL	17.0
PFDS	<RL	0.020			
FASA (NV, SV)			n:2 FTOH (V)		
FBSA (NV)	1.44 ± 0.13	0.021	4:2 FTOH	<RL	16.7
MeFBSA (SV)	<RL	0.985	5:2 FTOH	<RL	16.7
FHxSA (NV)	<RL	0.021	6:2 FTOH	1014 ± 64	17.6
FOSA (NV)	<RL	0.145	7:2 FTOH	<RL	16.6
MeFOSA (SV)	<RL	0.565	8:2 FTOH	<RL	16.1
EtFOSA (SV)	<RL	0.332	10:2 FTOH	<RL	34.2
FASAA (NV)			n:2 FTS (NV)		
FOSAA	<RL	1.19	4:2 FTS	<RL	0.048
MeFOSAA	<RL	0.251	6:2 FTS	0.289 ± 0.055	0.120
EtFOSAA	<RL	0.126	8:2 FTS	<RL	0.049
			10:2 FTS	<RL	0.107
FASE (SV)					
MeFBSE	10.22 ± 0.86	2.22			
MeFOSE	<RL	0.566			
EtFOSE	<RL	0.579			

Table 37. Measured PFAS concentrations ($\mu\text{g-PFAS} / \text{kg-textile}$; \pm standard deviation of triplicate measurements) and reporting limits for abraded WL-H.

PFAS	Concentration ($\mu\text{g/kg}$)	RL ($\mu\text{g/kg}$)	PFAS	Concentration ($\mu\text{g/kg}$)	RL ($\mu\text{g/kg}$)
PFCA (NV)			PPEA (NV)		
PFBA	2.79 \pm 0.19	0.218	PFEESA	<RL	0.027
PFPeA	<RL	0.072	PF4OPeA	<RL	0.135
PFHxA	<RL	2.36	PF5OHxA	<RL	0.030
PFHpA	<RL	0.408	3-6-OPFHpA	<RL	0.198
PFOA	<RL	0.683	HFPO-DA	<RL	0.408
PFNA	<RL	0.218	ADONA	<RL	0.068
PFDA	<RL	0.143	9Cl-PF3ONS	<RL	0.031
PFUnDA	<RL	0.218	11Cl-PF3OUdS	<RL	0.032
PFDoDA	<RL	0.218			
PFTrDA	<RL	0.218	n:2 FTAc (V)		
PFTeDA	<RL	0.072	8:2 FTAc	<RL	30.8
			10:2 FTAc	<RL	59.5
PFSA (NV)			n:2 FTMAC (V)		
PFPrS	<RL	0.484	6:2 FTMAC	<RL	100
PFBS	<RL	0.080	8:2 FTMAC	<RL	103
PFPeS	<RL	0.068	10:2 FTMAC	<RL	54.2
PFHxS	<RL	0.031			
PFHpS	<RL	0.095	n:2 FTOAc (V)		
PFOS	<RL	0.147	8:2 FTOAc	<RL	29.1
PFNS	<RL	0.032	10:2 FTOAc	<RL	29.6
PFDS	<RL	0.032			
FASA (NV, SV)			n:2 FTOH (V)		
FBSA (NV)	<RL	0.033	4:2 FTOH	<RL	29.1
MeFBSA (SV)	<RL	10.2	5:2 FTOH	<RL	60.8
FHxSA (NV)	<RL	0.033	6:2 FTOH	<RL	64.3
FOSA (NV)	<RL	0.345	7:2 FTOH	<RL	28.8
MeFOSA (SV)	<RL	0.437	8:2 FTOH	<RL	58.9
EtFOSA (SV)	<RL	0.521	10:2 FTOH	<RL	59.8
FASAA (NV)			n:2 FTS (NV)		
FOSAA	<RL	0.193	4:2 FTS	<RL	0.205
MeFOSAA	<RL	2.26	6:2 FTS	No Value	
EtFOSAA	<RL	0.847	8:2 FTS	<RL	0.391
			10:2 FTS	<RL	0.061
FASE (SV)					
MeFBSE	<RL	14.5			
MeFOSE	<RL	2.15			
EtFOSE	<RL	1.10			

Table 38. Measured PFAS concentrations ($\mu\text{g-PFAS} / \text{kg-textile}$; \pm standard deviation of triplicate measurements) and reporting limits for WL-H following exposure to controlled weathering.

PFAS	Concentration ($\mu\text{g/kg}$)	RL ($\mu\text{g/kg}$)	PFAS	Concentration ($\mu\text{g/kg}$)	RL ($\mu\text{g/kg}$)
PFCA (NV)			PPEA (NV)		
PFBA	<RL	1.19	PFEESA	<RL	0.037
PFPeA	<RL	0.222	PF4OPeA	<RL	0.071
PFHxA	<RL	0.986	PF5OHxA	<RL	0.041
PFHpA	<RL	4.69	3-6-OPFHpA	<RL	0.101
PFOA	<RL	1.19	HFPO-DA	<RL	0.045
PFNA	<RL	0.057	ADONA	<RL	0.021
PFDA	<RL	0.222	9Cl-PF3ONS	<RL	0.017
PFUnDA	<RL	0.111	11Cl-PF3OUdS	<RL	0.018
PFDoDA	<RL	0.111			
PFTTrDA	<RL	0.222	n:2 FTAc (V)		
PFTeDA	<RL	0.111	8:2 FTAc	<RL	20.7
			10:2 FTAc	<RL	19.1
PFSA (NV)			n:2 FTMAC (V)		
PFPrS	<RL	0.853	6:2 FTMAC	<RL	67.7
PFBS	0.146 ± 0.034	0.070	8:2 FTMAC	<RL	69.3
PFPeS	<RL	0.042	10:2 FTMAC	<RL	36.5
PFHxS	<RL	0.078			
PFHpS	<RL	0.043	n:2 FTOAc (V)		
PFOS	<RL	0.090	8:2 FTOAc	<RL	19.6
PFNS	<RL	0.018	10:2 FTOAc	<RL	19.9
PFDS	<RL	0.018			
FASA (NV, SV)			n:2 FTOH (V)		
FBSA (NV)	0.354 ± 0.016	0.019	4:2 FTOH	<RL	19.6
MeFBSA (SV)	<RL	0.864	5:2 FTOH	<RL	19.5
FHxSA (NV)	<RL	0.019	6:2 FTOH	<RL	20.6
FOSA (NV)	0.338 ± 0.029	0.128	7:2 FTOH	<RL	19.4
MeFOSA (SV)	<RL	0.658	8:2 FTOH	<RL	18.9
EtFOSA (SV)	0.75 ± 0.16	0.386	10:2 FTOH	<RL	40.1
FASAA (NV)			n:2 FTS (NV)		
FOSAA	<RL	1.05	4:2 FTS	<RL	0.042
MeFOSAA	<RL	0.222	6:2 FTS	0.138 ± 0.025	0.106
EtFOSAA	<RL	0.111	8:2 FTS	<RL	0.043
			10:2 FTS	<RL	0.095
FASE (SV)					
MeFBSE	86.1 ± 4.1	1.95			
MeFOSE	<RL	0.659			
EtFOSE	<RL	0.674			

7. References

- [1] Gluge J, Scheringer M, Cousins IT, DeWitt JC, Goldenman G, Herzke D, Lohmann R, Ng CA, Trier X, Wang Z (2020) An overview of the uses of per- and polyfluoroalkyl substances (PFAS). *Environmental Science: Processes & Impacts* 22(12):2345-2373. <https://doi.org/10.1039/d0em00291g>.
- [2] Peaslee GF, Wilkinson JT, McGuinness SR, Tighe M, Caterisano N, Lee S, Gonzales A, Roddy M, Mills S, Mitchell K (2020) Another pathway for firefighter exposure to per- and polyfluoroalkyl substances: Firefighter textiles. *Environmental Science & Technology Letters* 7(8):594-599. <https://doi.org/10.1021/acs.estlett.0c00410>.
- [3] Holmquist H, Schellenberger S, Van der Veen I, Peters GM, Leonards PEG, Cousins IT (2016) Properties, performance and associated hazards of state-of-the-art durable water repellent (DWR) chemistry for textile finishing. *Environ. Int.* 91, 251-264. <https://doi.org/10.1016/j.envint.2016.02.035>.
- [4] de Vos MG, Huijbregts MAJ, Van den Heuvel-Greve MJ, Vethaak AD, Van de Vijver KI, Leonards PEG, van Leeuwen SPJ, de Voogt P, Hendriks AJ (2008) Accumulation of perfluorooctane sulfonate (PFOS) in the food chain of the Western Scheldt estuary: comparing field measurements with kinetic modeling. *Chemosphere* 70, 1766-1773. <https://doi.org/10.1016/j.chemosphere.2007.08.038>.
- [5] Stahl T, Mattern D, Brunn H (2011) Toxicology of perfluorinated compounds. *Environ. Sci. Eur.* 23, 38. <https://doi.org/10.1186/2190-4715-23-38>.
- [6] Hekster FM, Laane RWPM, de Voogt P (2003) Environmental and Toxicity Effects of Perfluoroalkylated Substances. *Rev. Environ. Contam. T.* Springer, New York, New York, NY, pp. 99-121. https://doi.org/10.1007/0-387-21731-2_4.
- [7] Olsen GW, Burris JM, Ehresman DJ, Froehlich JW, Seacat AM, Butenhoff JL, Zobel LR (2007) Half-life of serum elimination of perfluorooctanesulfonate, perfluorohexanesulfonate, and perfluorooctanoate in retired fluorochemical production workers. *Environ. Health Perspect.* 115, 1298-1305. doi:10.1289/ehp.10009.
- [8] Lopez-Espinosa MJ, Fletcher T, Armstrong B, Genser B, Dhatariya K, Mondal D, Ducatman A, Leonardi G (2011) Association of Perfluorooctanoic Acid (PFOA) and Perfluorooctane Sulfonate (PFOS) with age of puberty among children living near a chemical plant. *Environ. Sci. Technol.* 45, 8160-8166. <https://doi.org/10.1021/es1038694>.
- [9] Corsini E, Sangiovanni E, Avogadro A, Galbiati V, Viviani B, Marinovich M, Galli CL, Dell'Agli M, Germolec DR (2012) In vitro characterization of the immunotoxic potential of several perfluorinated compounds (PFCs). *Toxicol. Appl. Pharmacol.* 258, 248-255. <https://doi.org/10.1016/j.taap.2011.11.004>.
- [10] Liu C, Chang VWC, Gin KYH (2014) Oxidative toxicity of perfluorinated chemicals in green mussel and bioaccumulation factor dependent quantitative structure-activity relationship. *Environ. Toxicol. Chem.* 33, 2323-2332. <https://doi.org/10.1002/etc.2679>.
- [11] Panieri E, Baralic K, Djukic-Cosic D, Djordjevic AB, Saso L (2022) PFAS Molecules: A Major Concern for the Human Health and the Environment. *Toxics* 10(2):44. <https://doi.org/10.3390/toxics10020044>.

- [12] Schellenberger S, Gillgard P, Stare A, Hanning A, Levenstam O, Roos S, Cousins IT (2018) Facing the Rain after the Phase out: Performance Evaluation of Alternative Fluorinated and Non-Fluorinated Durable Water Repellents for Outdoor Fabrics. *Chemosphere* 193 675–684. <https://doi.org/10.1016/j.chemosphere.2017.11.027>.
- [13] Carney Almroth BM, Åström L, Roslund S, Petersson H, Johansson M, Persson NK (2018) Quantifying Shedding of Synthetic Fibers from Textiles; a Source of Microplastics Released into the Environment. *Environ. Sci. Pollut. Res.* 25 (2), 1191–1199. <https://doi.org/10.1007/s11356-017-0528-7>.
- [14] Davis R, Chin J, Lin CC, Petit S (2010) Accelerated weathering of polyaramid and polybenzimidazole firefighter protective clothing fabrics. *Polymer Degradation and Stability* 95(9):1642-1654. <https://doi.org/10.1016/j.polymdegradstab.2010.05.029>.
- [15] Nazaré S, Davis RD, Peng JS, Chin J (2012) Accelerated weathering of firefighter protective clothing: delineating the impact of thermal, moisture, and ultraviolet light exposures. (National Institute of Standards and Technology), *NIST TN 1746*. <https://doi.org/10.6028/nist.Tn.1746>.
- [16] Schellenberger S, Liagkouridis I, Awad R, Khan S, Plassmann M, Peters G, Benskin JP, Cousins IT (2022) An outdoor aging study to investigate the release of per- and polyfluoroalkyl substances (PFAS) from functional textiles. *Environmental Science & Technology* 56(6):3471-3479. <https://doi.org/10.1021/acs.est.1c06812>.
- [17] van der Veen I, Weiss JM, Hanning AC, de Boer J, Leonards PE (2016) Development and validation of a method for the quantification of extractable perfluoroalkyl acids (PFAAs) and perfluorooctane sulfonamide (FOSA) in textiles. *Talanta* 147:8-15. <https://doi.org/10.1016/j.talanta.2015.09.021>
- [18] van der Veen I, Hanning AC, Stare A, Leonards PEG, de Boer J, Weiss JM (2020) The effect of weathering on per- and polyfluoroalkyl substances (PFASs) from durable water repellent (DWR) clothing. *Chemosphere* 249:126100. <https://doi.org/10.1016/j.chemosphere.2020.126100>
- [19] van der Veen I, Schellenberger S, Hanning AC, Stare A, de Boer J, Weiss JM, Leonards PEG (2022) Fate of per- and polyfluoroalkyl substances from durable water-repellent clothing during use. *Environmental Science & Technology* 56(9):5886-5897. <https://doi.org/10.1021/acs.est.1c07876>.
- [20] Boorady LM, Lin SH, Barker J, Cho E, Lee YA, Ashdown SP (2013) Exploration of firefighter turnout gear Part 1: Identifying male firefighter user needs. *Journal of Textile and Apparel, Technology and Management* 8(1). <https://jstatm.textiles.ncsu.edu/index.php/JTATM/article/view/3762>.
- [21] National Fire Protection Agency 1971. Standard on Protective ensembles for structural fire fighting and proximity fire fighting, 2018 Edition. (National Fire Protection Association).
- [22] Mazumder NUS, Hossain MT, Jahura FT, Girase A, Hall AS, Lu J, Ormond RB (2023) Firefighters' exposure to per-and polyfluoroalkyl substances (PFAS) as an occupational hazard: A review. *Frontiers in Materials* 10. <https://doi.org/10.3389/fmats.2023.1143411>.
- [23] Muensterman DJ, Titaley IA, Peaslee GF, Minc LD, Cahuas L, Rodowa AE, Horiuchi Y, Yamane S, Fouquet TNJ, Kissel JC, Carignan CC, Field JA (2022) Disposition of fluorine on

- new firefighter turnout gear. *Environmental Science & Technology* 56(2):974-983.
<https://doi.org/10.1021/acs.est.1c06322>.
- [24] Maizel AC, Thompson A, Tighe M, Escobar Veras S, Rodowa AE, Falkenstein-Smith F, Benner B, Hoffman K, Donnelly M, Hernandez O, Wetzler N, Ngu T, Reiner J, Place B, Kucklick J, Rimmer C, Davis RD (2023) Per- and Polyfluoroalkyl Substances in New Firefighter Turnout Gear Textiles. (National Institute of Standards and Technology), *NIST TN 2248*. <https://doi.org/10.6028/nist.Tn.2248>.
- [25] Maizel AC, Thompson A, Tighe M, Escobar Veras S, Rodowa AE, Falkenstein-Smith F, Benner B, Hoffman K, Donnelly M, Hernandez O, Wetzler N, Ngu T, Reiner J, Place B, Kucklick J, Rimmer C, Davis RD (2024) Per- and Polyfluoroalkyl Substances in Firefighter Turnout Gear Textiles Exposed to Abrasion, Elevated Temperature, Laundering, or Weathering (National Institute of Standards and Technology), *NIST TN 2260*.
<https://doi.org/10.6028/NIST.TN.2260>.
- [26] National Fire Protection Agency 1977. Standard on Protective Clothing and Equipment for Wildland Fire Fighting and Urban Interface Fire Fighting, 2016 Edition. (National Fire Protection Association).
- [27] Thompson AL, Maizel AC, Tighe M, Escobar-Veras S, Rodowa AE, Benner B, Tombaugh AF, Reiner J, Donnelly M, Falkenstein-Smith R, Kucklick J, Rimmer C, Davis RD (2024) Per- and Polyfluoroalkyl Substances in Textiles Present in Firefighter Gloves, Hoods, and Wildland Gear (National Institute of Standards and Technology), *NIST TN 2313*.
<https://doi.org/10.6028/NIST.TN.2313>.
- [28] International Organization for Standardization (1998) ISO 12947-3 – Textiles - Determination of the Abrasion Resistance of Fabrics by the Martindale Method (International Organization for Standardization, Switzerland).
- [29] ASTM International (2016) D4966-12 – Standard Test Method for Abrasion Resistance of Textile Fabrics (Martindale Abrasion Tester Method) (ASTM International, West Conchohocken, PA). <https://doi.org/10.1520/d4966-12r16>.
- [30] ASTM International (2019) F2894-19 – Standard Test Method for Evaluation of Materials, Protective Clothing, and Equipment for Heat Resistance Using a Hot Air Circulating Oven (ASTM International, West Conchohocken, PA).
<https://doi.org/10.1520/f2894-19>.
- [31] International Organization for Standardization (2016) ISO 4892-3:2016 – Plastics - Methods of Exposure to Laboratory Light Sources (International Organization for Standardization, Switzerland).
- [32] ASTM International (2000) G154-00a – Standard Practice for Operating Fluorescent Light Apparatus for UV Exposure of Nonmetallic Materials (ASTM International, West Conchohocken, PA).
- [33] U.S. Environmental Protection Agency (2025) *Comptox Chemicals Dashboard. 2-(Perfluorohexyl)ethyl methacrylate*. Available at
<https://comptox.epa.gov/dashboard/chemical/details/DTXSID3047558>.
- [34] U.S. Environmental Protection Agency (2025) *Comptox Chemical Dashboard 2-(Perfluorohexyl)ethanol*. Available at
<https://comptox.epa.gov/dashboard/chemical/details/DTXSID5044572>.

- [35] U.S. Environmental Protection Agency (2025) *Comptox Chemical Dashboard 2-(Perfluorohexyl)ethanol*. Available at <https://comptox.epa.gov/dashboard/chemical/details/DTXSID40873417>.
- [36] U.S. Environmental Protection Agency (2025) *Comptox Chemical Dashboard 2-(Perfluorohexyl)ethanol*. Available at <https://comptox.epa.gov/dashboard/chemical/properties/DTXSID0067848>.
- [37] U.S. Environmental Protection Agency (2025) *Comptox Chemical Dashboard 2-(Perfluorohexyl)ethanol*. Available at <https://comptox.epa.gov/dashboard/chemical/details/DTXSID4059916>.
- [38] Zuev VV, Bertini F, Audisio G (2006) Investigation on the thermal degradation of acrylic polymers with fluorinated side-chains. *Polymer Degradation and Stability* 91(3):512-516. <https://doi.org/10.1016/j.polymdegradstab.2005.03.025>.
- [39] Trowbridge J, Gerona RR, Lin T, Rudel RA, Bessonneau V, Buren H, Morello-Frosch R (2020) Exposure to perfluoroalkyl substances in a cohort of women firefighters and office workers in San Francisco. *Environmental Science & Technology* 54(6):3363-3374. <https://doi.org/10.1021/acs.est.9b05490>.
- [40] Graber JM, Black TM, Shah NN, Caban-Martinez AJ, Lu SE, Brancard T, Yu CH, Turyk ME, Black K, Steinberg MB, Fan Z, Burgess JL (2021) Prevalence and predictors of per- and polyfluoroalkyl substances (PFAS) serum levels among members of a suburban US volunteer fire department. *International Journal of Environmental Research and Public Health* 18(7):3730. <https://doi.org/10.3390/ijerph18073730>.
- [41] Nilsson S, Smurthwaite K, Aylward LL, Kay M, Toms LM, King L, Marrington S, Barnes C, Kirk MD, Mueller JF, Braunig J (2022) Serum concentration trends and apparent half-lives of per- and polyfluoroalkyl substances (PFAS) in Australian firefighters. *International Journal of Hygiene and Environmental Health* 246:114040. <https://doi.org/10.1016/j.ijheh.2022.114040>.
- [42] Rotander A, Toms LM, Aylward L, Kay M, Mueller JF (2015) Elevated levels of PFOS and PFHxS in firefighters exposed to aqueous film forming foam (AFFF). *Environment International* 82:28-34. <https://doi.org/10.1016/j.envint.2015.05.005>.
- [43] Khalil N, Ducatman AM, Sinari S, Billheimer D, Hu C, Littau S, Burgess JL (2020) Per- and polyfluoroalkyl substance and cardio metabolic markers in firefighters. *Journal of Occupational and Environmental Medicine* 62(12):1076-1081. <https://doi.org/10.1097/JOM.0000000000002062>.
- [44] Leary DB, Takazawa M, Kannan K, Khalil N (2020) Perfluoroalkyl substances and metabolic syndrome in firefighters: A pilot study. *Journal of Occupational and Environmental Medicine* 62(1):52-57. <https://doi.org/10.1097/JOM.0000000000001756>.
- [45] Jin C, Sun Y, Islam A, Qian Y, Ducatman A (2011) Perfluoroalkyl acids including perfluorooctane sulfonate and perfluorohexane sulfonate in firefighters. *Journal of Occupational and Environmental Medicine* 53(3):324-328. <https://doi.org/10.1097/JOM.0b013e31820d1314>.
- [46] Goodrich JM, Calkins MM, Caban-Martinez AJ, Stueckle T, Grant C, Calafat AM, Nematollahi A, Jung AM, Graber JM, Jenkins T, Slitt AL, Dewald A, Cook Botelho J, Beitel S, Littau S, Gulotta J, Wallentine D, Hughes J, Popp C, Burgess JL (2021) Per- and

- polyfluoroalkyl substances, epigenetic age and DNA methylation: a cross-sectional study of firefighters. *Epigenomics* 13(20):1619-1636. <https://doi.org/10.2217/epi-2021-0225>.
- [47] Laitinen JA, Koponen J, Koikkalainen J, Kiviranta H (2014) Firefighters' exposure to perfluoroalkyl acids and 2-butoxyethanol present in firefighting foams. *Toxicology Letters* 231(2):227-232. <https://doi.org/10.1016/j.toxlet.2014.09.007>.
- [48] Sznajder-Katarzynska K, Surma M, Cieslik I (2019) A Review of Perfluoroalkyl Acids (PFAAs) in terms of Sources, Applications, Human Exposure, Dietary Intake, Toxicity, Legal Regulation, and Methods of Determination. *Journal of Chemistry*. 2019: 1-20. <https://doi.org/10.1155/2019/2717528>.
- [49] Maizel A, Thompson A, Place B, Rodowa A, Reiner J, Tombaugh A, Solomon H, Stinger B, Donnelly M, Davis R (2025) Suspect Screening of Per- and Polyfluoroalkyl Substances in New Firefighter Turnout Gear Textiles (National Institute of Standards and Technology), *NIST TN 2334*. <https://doi.org/10.6028/NIST.TN.2334>.
- [50] Hall SM, Patton S, Petreas M, Zhang S, Phillips AL, Hoffman K, Stapleton HM (2020) Per- and polyfluoroalkyl substances in dust collected from residential homes and fire stations in North America. *Environ Sci Technol* 54(22):14558-14567. <https://doi.org/10.1021/acs.est.0c04869>.

Appendix A. Experimental Details

A.1. PFAS Analytical Standards and NIST Reference Materials

Analytical standards (**Table 39**) and isotopically labeled standards (**Table 40**) for nonvolatile PFAS as well as semivolatile PFAS (**Table 41** and **Table 42**) were obtained from Wellington Laboratories (Guelph, Ontario, Canada). Analytical standards and isotopically labeled standards for volatile PFAS (**Table 43** and **Table 44**) were obtained from Wellington Laboratories and Synquest Laboratories (Alachua, FL).

Table 39. Nonvolatile PFAS analytical standards obtained from Wellington Laboratories, with full analyte names, CAS RN, and abbreviations (**bold**), and analyte concentrations with expanded maximum combined percent relative uncertainty. PFHxS, PFOS, MeFOSAA, and EtFOSAA in PFAC30PAR were present as a mixture of structural isomers.

Standard	Contents	Concentration
PFAC30PAR	Perfluoro-n-butanoic acid (375-22-4; PFBA), Perfluoro-n-pentanoic acid (2706-90-3; PFPeA), Perfluoro-n-hexanoic acid (307-24-4; PFHxA), Perfluoro-n-heptanoic acid (375-85-9; PFHpA), Perfluoro-n-octanoic acid (335-67-1; PFOA), Perfluoro-n-nonanoic acid (375-95-1; PFNA), Perfluoro-n-decanoic acid (335-76-2; PFDA), Perfluoro-n-undecanoic acid (2058-94-8; PFUnDA), Perfluoro-n-dodecanoic acid (307-55-1; PFDoDA), Perfluoro-n-tridecanoic acid (72629-94-8; PFTTrDA), Perfluoro-n-tetradecanoic acid (376-06-7; PFTeDA), Perfluoro-1-butanefulfonamide (30334-69-1; FBSA), Perfluoro-1-hexanesulfonamide (41997-13-1; FHxSA), Perfluoro-1-octanesulfonamide (754-91-6; FOSA), Tetrafluoro-2-(1,1,2,2,3,3,3-heptafluoropropoxy)-propanoic acid (13252-13-6; HFPO-DA), N-methylperfluoro-1-octanesulfonamidoacetic acid (2355-31-9; N-MeFOSAA), N-ethylperfluoro-1-octanesulfonamidoacetic acid (2991-50-6, N-EtFOSAA), Potassium perfluorobutanesulfonate (29420-49-3; PFBS), Sodium perfluoropentanesulfonate (630402-22-1; PFPeS), Potassium perfluorohexanesulfonate (3871-99-6; PFHxS), Sodium perfluoroheptanesulfonate (21934-50-9; PFHpS), Potassium perfluorooctanesulfonate (2795-39-3; PFOS), Sodium perfluorononanesulfonate (98789-57-2; PFNS), Sodium perfluorodecanesulfonate (2806-15-7; PFDS), Sodium 1H,1H,2H,2H,-perfluoro-1-hexanesulfonate (27619-93-8; 4:2 FTS), Sodium 1H,1H,2H,2H,-perfluoro-1-octanesulfonate (27619-94-9; 6:2 FTS), Sodium 1H,1H,2H,2H,-perfluoro-1-decanesulfonate (27619-96-1; 8:2 FTS), Sodium dodecafluoro-3H-4,8-dioxanonatoate; NaDONA), Potassium 9-chlorohexadecafluoro-3-oxanonane-1-sulfonate (73606-19-6; 9Cl-PF3ONS), Potassium 11-chloroeicosafuoro-3-oxaundecane-1-sulfonate (83329-89-9; 11Cl-PF3OUdS)	1.00 µg/mL ± 0.05 µg/mL in methanol/isopropanol (6 %)/water (<1 %)
PFAC-MXG	Perfluoro-4-oxapentenoic acid (377-73-1; PF4OPeA), Perfluoro-5-oxahexanoic acid (863090-89-5; PF5OHxA), Perfluoro-3,6-dioxahexanoic acid (151772-58-6; 3,6-OPFHxA), Potassium perfluoro(2-ethoxyethane)sulfonic acid (PFEESA)	2.0 µg/mL ± 0.1 µg/mL in methanol/water (<1 %)
L-PFPrS	Sodium perfluoropropanesulfonate (359868-82-9; PFPrS)	50.0 µg/mL ± 2.5 µg/mL in methanol
FOSAA	Perfluorooctane sulfonamidoacetic acid (2806-24-6; FOSAA)	50.0 µg/mL ± 2.5 µg/mL in

		methanol/water (<1 %)
10:2FTS	Sodium 1H,1H,2H,2H,-perfluoro-1-dodecanesulfonate (10:2 FTS)	50.0 µg/mL ± 2.5 µg/mL in methanol

Table 40. Nonvolatile isotopically labeled PFAS internal and injection standards obtained from Wellington Laboratories, with full analyte names, and analyte concentrations with expanded maximum combined percent relative uncertainty where provided.

Standard	Contents	Concentration
MPFAC-24ES	Perfluoro-n-[13C4]-butanoic acid, Perfluoro-n-[13C5]-pentanoic acid, Perfluoro-n-[1,2,3,4,6-13C5]-hexanoic acid, Perfluoro-n-[1,2,3,4-13C4]-heptanoic acid, Perfluoro-n-[13C8]-octanoic acid, Perfluoro-n-[13C9]-nonanoic acid, Perfluoro-n-[1,2,3,4,5,6-13C5]decanoic acid, Perfluoro-n-[1,2,3,4,5,6,7-13C7]undecanoic acid, Perfluoro-n-[1,2-13C2]dodecanoic acid, Perfluoro-n-[1,2-13C2]tetradecanoic acid, Sodium perfluoro-1-[2,3,4-13C3]-butanesulfonate, Sodium perfluoro-1-[1,2,3-13C3]-hexanesulfonate, Sodium perfluoro-1-[13C8]-octanesulfonate, Perfluoro-1-[13C8]octanesulfonamide, N-methyl-d3-perfluoro-1-octanesulfonamid acetic acid, N-ethyl-d5-perfluoro-1-octanesulfonamido acetic acid, Sodium 1H, 1H, 2H, 2H-perfluoro-1-[1,2-13C2]-hexane sulfonate, Sodium 1H, 1H, 2H, 2H-perfluoro-1-[1,2-13C2]-octane sulfonate, Sodium 1H, 1H, 2H, 2H-perfluoro-1-[1,2-13C2]-decane sulfonate	1.00 µg/mL ± 0.05 µg/mL in methanol/isopropanol (2 %)/water (<1 %)
M3HFPO-DA	Tetrafluoro(heptafluoropropoxy)[¹³ C ₃]-propanoic acid	50.0 µg/mL ± 2.5 µg/mL in methanol
MPFAC-C-IS	Perfluoro-n-[2,3,4-13C3]-butanoic acid (PFBA-INJ), Perfluoro-n-[1,2,3,4-13C4]-octanoic acid (PFOA -INJ), Perfluoro-n-[1,2-13C2]decanoic acid (PFDA -INJ), Sodium perfluoro-1-[1,2,3,4-13C4]-octanesulfonate (PFOS -INJ)	50.0 µg/mL ± 2.5 µg/mL in methanol/water (<1 %)

Table 41. Semivolatile PFAS analytical standards purchased from Wellington Laboratories including full analyte names, CAS RN, abbreviations (bold), and analyte concentrations with expanded maximum combined percent relative uncertainty where provided.

Standard	Contents	Concentration
N-MeFBSA-M	Nonafluoro-N-methylbutanesulfonamide (6829-12-4; MeFBSA)	50 µg/mL ± 2.5 µg/mL
N-MeFOSA-M	Heptadecafluoro-N-methyloctanesulfonamide (31506-32-8; MeFOSA)	50 µg/mL ± 2.5 µg/mL
N-EtFOSA-M	Heptadecafluoro-N-ethyloctanesulfonamide (4151-50-2; EtFOSA)	50 µg/mL ± 2.5 µg/mL
N-MeFBSE-M	2-(N-methylperfluoro-1-butan-sulfonamido)-ethanol (252-043-1; MeFBSE)	50 µg/mL ± 2.5 µg/mL
N-MeFOSE-M	2-(N-methylperfluoro-1-octanesulfonamido)-ethanol (24448-09-7; MeFOSE)	50 µg/mL ± 2.5 µg/mL
N-EtFOSE-M	2-(N-ethylperfluoro-1-octanesulfonamido)-ethanol (1691-99-2; EtFOSE)	50 µg/mL ± 2.5 µg/mL

Table 42. Semivolatile isotopically labeled PFAS internal standards obtained from Wellington Laboratories, with full analyte names, and analyte concentrations with expanded maximum combined percent relative uncertainty where provided.

Standard	Contents	Concentration
d-N-MeFOSA-M	N-methyl-d3-perfluoro-1-octanesulfonamide	50 µg/mL ± 2.5 µg/mL
d-N-EtFOSA	N-ethyl-d5-perfluoro-1-octanesulfonamide	50 µg/mL ± 2.5 µg/mL
d7-N-MeFOSE-M	2-(N-methyl-d3-perfluoro-1-octanesulfonamido)ethan-d4-ol	50 µg/mL ± 2.5 µg/mL
d9-N-EtFOSE-M	2-(N-ethyl-d5-perfluoro-1-octanesulfonamido)ethan-d4-ol	50 µg/mL ± 2.5 µg/mL

Table 43. Volatile target PFAS analytical standards, supplier, full analyte names, CAS RN, abbreviations (**bold**), and analyte concentrations with expanded maximum combined percent relative uncertainty where provided.

Standard	Contents	Concentration
8:2FTAc (Wellington Laboratories)	1H, 1H, 2H, 2H-Perfluorodecyl acrylate (27905-45-9; 8:2 FTAc)	50.0 µg/mL ± 2.5 µg/mL in isooctane
10:2 FTAc (Wellington Laboratories)	1H, 1H, 2H, 2H-Pefluorododecyl acrylate (17741-60-5; 10:2 FTAc)	47.9 µg/mL ± 2.4 µg/mL in isooctane
FBET (Wellington Laboratories)	2-Perflourobutyl ethanol (2043-47-2; 4:2 FTOH)	50.0 µg/mL ± 2.5 µg/mL in methanol
5:2sFTOH (Wellington Laboratories)	1-Perfluoropentyl ethanol (914637-05-1; 5:2 FTOH)	50.0 µg/mL ± 2.5 µg/mL in methanol
FHET (Wellington Laboratories)	2-Perfluorohexyl ethanol (647-42-7; 6:2 FTOH)	50.0 µg/mL ± 2.5 µg/mL in methanol
7:2sFTOH (Wellington Laboratories)	1-Perfluoroheptyl ethanol (24015-83-6; 7:2 FTOH)	50.0 µg/mL ± 2.5 µg/mL in methanol
FOET (Wellington Laboratories)	2-Perfluorooctyl ethanol (678-39-7; 8:2 FTOH)	50.0 µg/mL ± 2.5 µg/mL in methanol
FDET (Wellington Laboratories)	2-Perfluorodecyl ethanol (865-86-1; 10:2 FTOH)	50.0 µg/mL ± 2.5 µg/mL in methanol
8:2 FTOAc (Wellington Laboratories)	1H, 1H, 2H, 2H-Perfluorodecyl acetate (37858-04-1; 8:2 FTOAc)	48.5 µg/mL ± 2.4 µg/mL in isooctane
10:2FTOAc (Wellington Laboratories)	1H, 1H, 2H, 2H-Perfluorododecyl acetate (37858-05-2; 10:2 FTOAc)	50.0 µg/mL ± 2.5 µg/mL in isooctane
8:2 FTAc (Wellington Laboratories)	1H, 1H, 2H, 2H-Perfluorodecyl acrylate (27905-45-9; 8:2 FTAc)	50.0 µg/mL ± 2.5 µg/mL in isooctane
10:2 FTAc (Wellington Laboratories)	1H, 1H, 2H, 2H-Perfluorododecyl acrylate (17741-60-5; 10:2 FTAc)	47.9 µg/mL ± 2.4 µg/mL in isooctane
2324-3-46 (Synquest Laboratories)	1H, 1H, 2H, 2H-Perfluorooctyl methacrylate (2144-53-8; 6:2 FTMAC)	Neat (97 % Purity)
2324-3-42 (Synquest Laboratories)	1H, 1H, 2H, 2H-Perfluorodecyl methacrylate (1996-88-9; 8:2 FTMAC)	Neat (97 % Purity)
2324-3-Y5 (Synquest Laboratories)	1H, 1H, 2H, 2H-Perfluorododecyl methacrylate (2144-54-9; 10:2 FTMAC)	Neat (97 % Purity)

Table 44. Volatile internal standard PFAS purchased from Wellington Laboratories, including full analyte names, and analyte concentrations with expanded maximum combined percent relative uncertainty where provided.

Standard	Contents	Concentration
MF BET	2-Perfluorobutyl-[1,1,2,2- ² H ₄]-ethanol	48.5 µg/mL ± 2.4 µg/mL in methanol
MF HET	2-Perfluorohexyl-[1,1- ² H ₂]-[1,2- ¹³ C ₂]-ethanol	50 µg/mL ± 2.5 µg/mL in methanol
MF OET	2-Perfluorooctyl-[1,1- ² H ₂]-[1,2- ¹³ C ₂]-ethanol	50 µg/mL ± 2.5 µg/mL in methanol
MF DET	2-Perfluorodecyl-[1,1- ² H ₂]-[1,2- ¹³ C ₂]-ethanol	50 µg/mL ± 2.5 µg/mL in methanol

NIST Reference Materials (RMs) 8446 Perfluorinated Carboxylic Acids and Perfluorooctane Sulfonamide in Methanol (8446) and 8447 Perfluorinated Sulfonic Acids in Methanol (8447) were obtained for use as quality control samples (**Table 45 and Table 46**).

Table 45. Reference mass fractions for NIST Reference Material 8446 including mean value and expanded uncertainty with 95 % confidence.

PFAS	Mass Fraction (mg/kg)
PFHxA	59.1 ± 1.4
PFHpA	76.0 ± 7.2
PFOA	54.8 ± 2.2
PFNA	63.0 ± 1.4
PFDA	58.1 ± 4.0
PFUdA	62.8 ± 6.5
PFDoDA	59.5 ± 7.0
PFTTrDA	62.9 ± 2.8
PFTeDA	58.0 ± 3.8
PFBA	43 ± 11
PFPeA	60.9 ± 0.9
FOSA	66.9 ± 1.7

Table 46. Reference mass fractions NIST Reference Material 8447 including mean value and expanded uncertainty with 95 % confidence.

PFAS	Mass Fraction (mg/kg)
PFBS	42.3 ± 2.3
PFHxS	55.2 ± 1.7
PFOS	56.6 ± 2.5

A.2. PFAS Analysis

PFAS analytical methods, including quality control limits, for GC-MS analysis of volatile PFAS as well as LC-MS/MS analysis of semivolatile and nonvolatile PFAS were performed similarly as described in NIST TN 2248 [24].

A.3. Quality Control Results

With each analytical sequence a range of quality control (QC) results were obtained. Reporting limits determined with each measurement (Section A.3.1), NIST RM 8446 and 8447 recovery (Section A.3.2), as well as OS-FRM recovery (Section A.3.3) are detailed below.

A.3.1. Reporting Limits

Reporting limits determined for each PFAS measurement in stressed firefighter gear textiles are above in **Tables 5 to 38**. Histograms of the reporting limits for measurements made with each of the three analytical methods are shown in **Figure 19**. Most of the determined reporting limits for nonvolatile (2247 out of 2328) and semivolatile (267 out of 358) PFAS measurements were < 1 $\mu\text{g}/\text{kg}$. Reporting limits for volatile PFAS were much higher; out of a total of 858 reported volatile GC measurements, no reporting limit was under 7.7 $\mu\text{g}/\text{kg}$ and 146 were over 100 $\mu\text{g}/\text{kg}$.

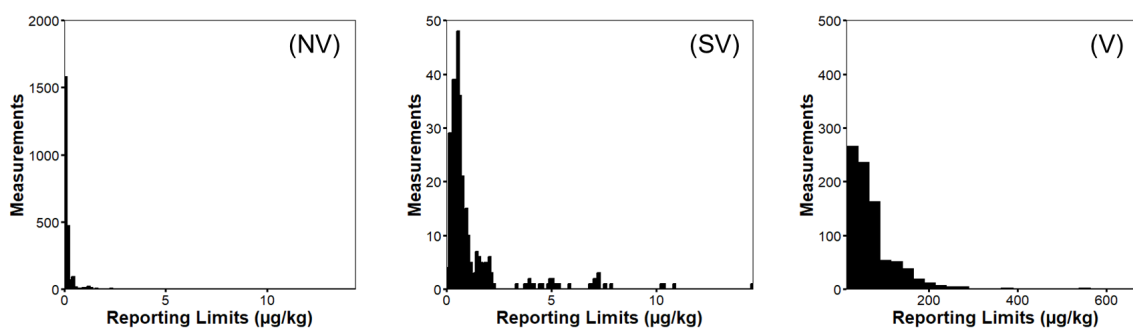


Figure 19. Histograms of reporting limits for individual measurements of nonvolatile (NV; binwidth = 0.125 $\mu\text{g}/\text{kg}$), semivolatile (SV; binwidth = 0.1 $\mu\text{g}/\text{kg}$), and volatile PFAS (V; binwidth = 25 $\mu\text{g}/\text{kg}$).

A.3.2. NIST Reference Materials 8446 and 8447

Nonvolatile PFAS concentrations in extracts of firefighter turnout gear textiles were determined across 9 analytical sequences. Gravimetric dilutions of NIST RMs 8446 Perfluorinated Carboxylic Acids and Perfluorooctane Sulfonamide in Methanol as well as 8447 Perfluorinated Sulfonic Acids in Methanol were prepared and analyzed with each sequence and measured concentrations were between 70 % to 130 % of the reference values for all analytes, except for a single analysis of PFBA which recovered 145 % (**Figure 20**) The recovery of all NIST RM 8446 and 8447 analytes suggests that calibration regressions determined with each nonvolatile analytical sequence were consistent and accurate.

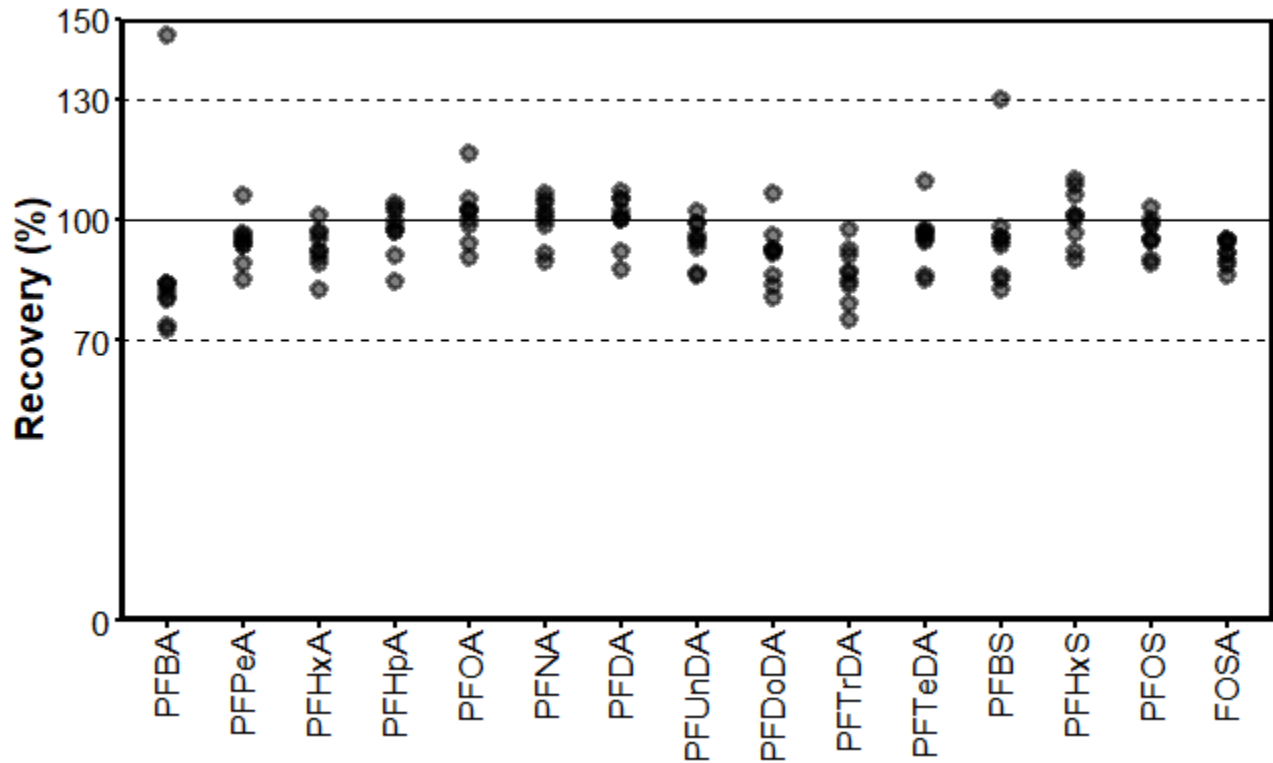


Figure 20. Recoveries of reference PFAS in NIST reference materials 8446 and 8447 across 16 nonvolatile PFAS analytical sequences. 100 % recovery is indicated by a solid line while 70 % and 130 % recoveries are indicated by dashed lines.

A.3.3. Method Reproducibility Materials (OS-FRM)

As described in NIST TN 2248 [24], NIST TN 2260 [25], and NIST TN 2313 [27], 400 firefighter gear outer shell textile OS-F samples were cut, weighed, and stored in 15 mL polypropylene centrifuge tubes as a reproducibility material (OS-FRM). Each extraction batch of 11 FFG samples was extracted with a randomly-selected OS-FRM textile replicate to demonstrate extraction consistency and calibration accuracy. Recoveries are shown in **Figure 21**. Some recoveries are not shown because the measured concentration was below the sample and analyte specific reporting limit.

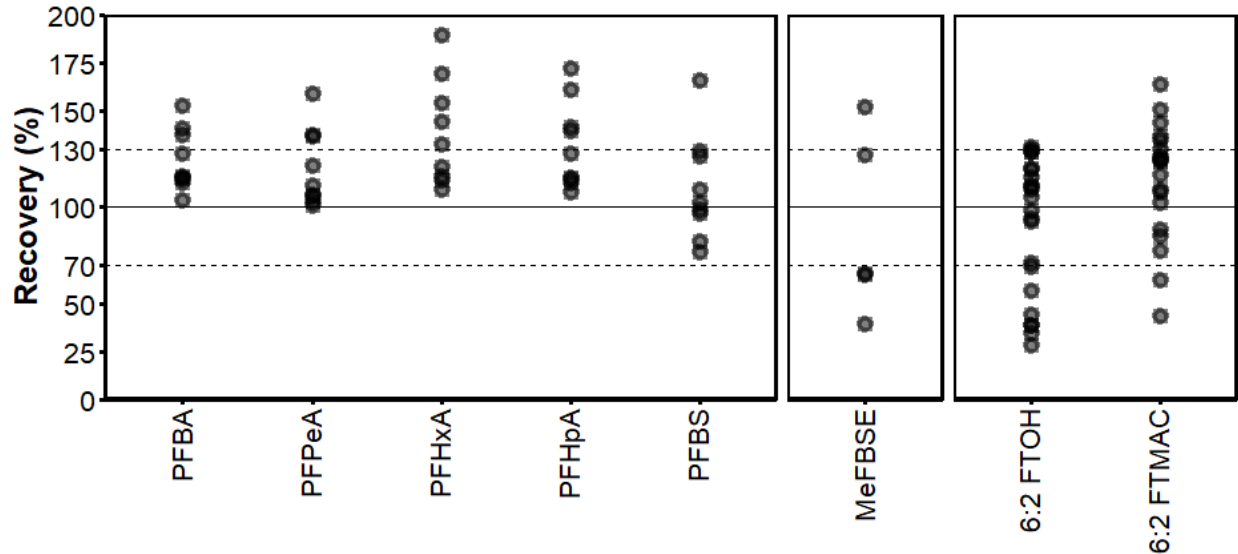


Figure 21. Recovery of PFAS in OS-FRM that had a previously measured concentration over 0.5 $\mu\text{g}/\text{kg}$ across 9 nonvolatile, 11 semivolatile, and 23 volatile PFAS batches. 100 % recovery is indicated by a solid line while 70 % and 130 % recoveries are indicated by dashed lines.

A.3.4. PFAS Concentrations in Stressed Firefighter Gloves, Hoods, and Wildland Coats, Shirts, and Pants

The measured PFAS concentrations determined in unstressed firefighter gear textiles in NIST TN 2248 [22] as well as the same firefighter gear textiles following exposure to each stressing process are shown in **Figures 22 to 30**. Scatter plots comparing total nonvolatile or volatile PFAS concentrations before and after each stressing process are in **Figures 11 to 16**.

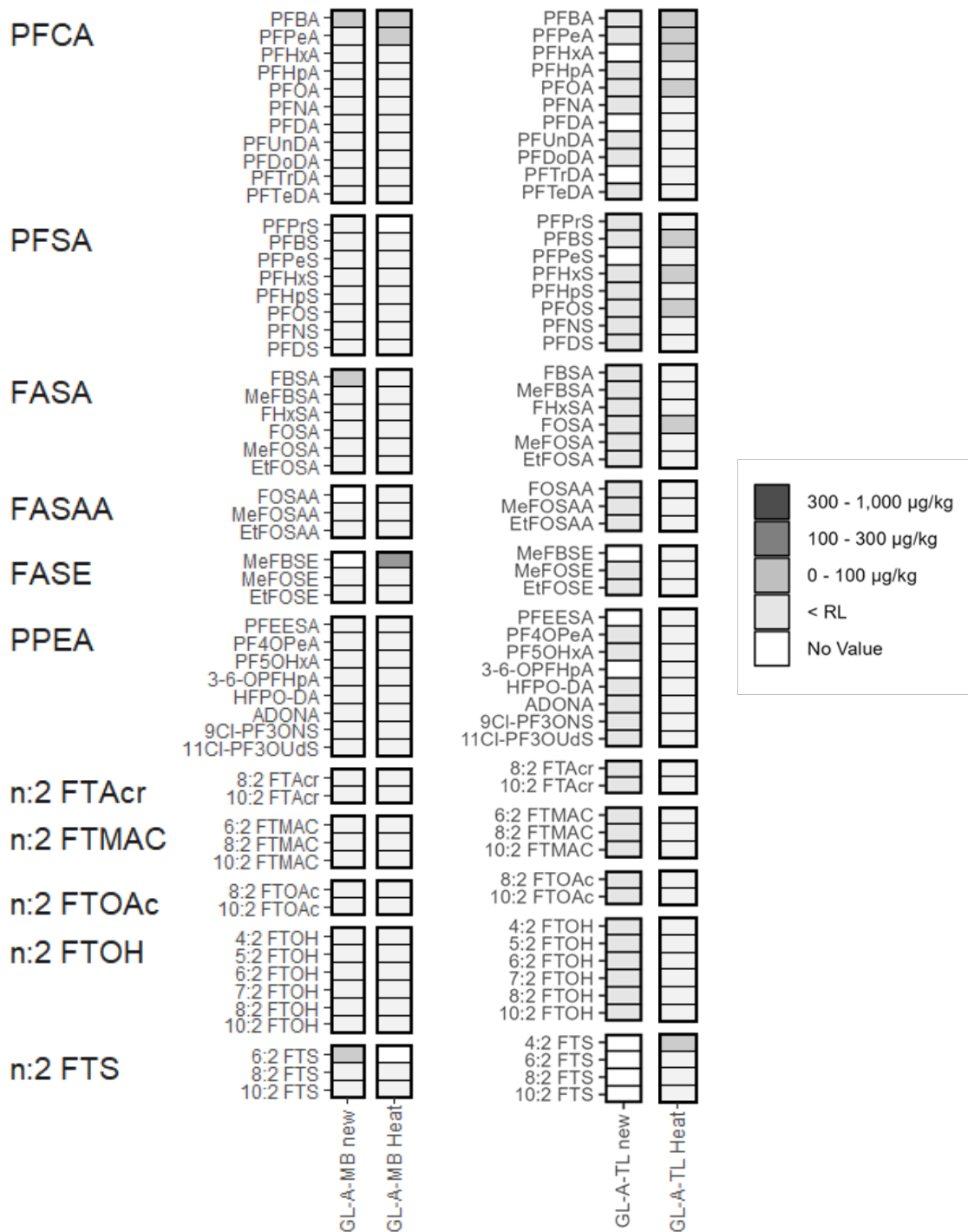


Figure 22. Average PFAS concentrations determined from triplicate analysis of GL-A-MB (left) and GL-A-TL (right) either prior to stressing (new) or following thermal stressing (Heat). Concentrations indicated by shade. Measurements not reported due to unmet QC standards are in white. PFAS concentrations displayed in this figure are also presented in **Table 5** and **Table 6**.

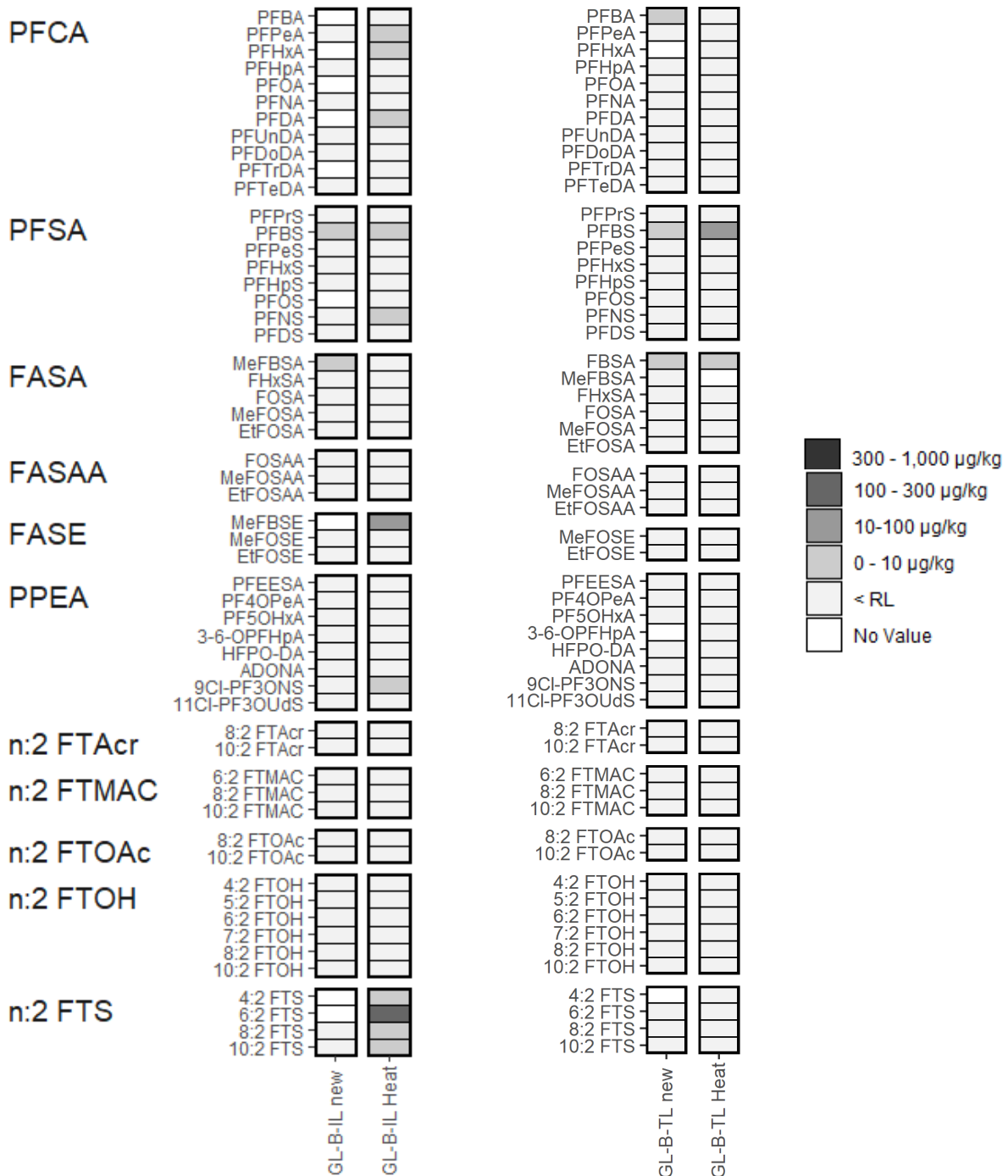


Figure 23. Average PFAS concentrations determined from triplicate analysis of GL-B-IL (left) and GL-B-TL (right) either prior to stressing (new) or following thermal stressing (Heat). Concentrations indicated by shade. Measurements not reported due to unmet QC standards are in white. PFAS concentrations displayed in this figure are also presented in **Table 7** and **Table 8**.

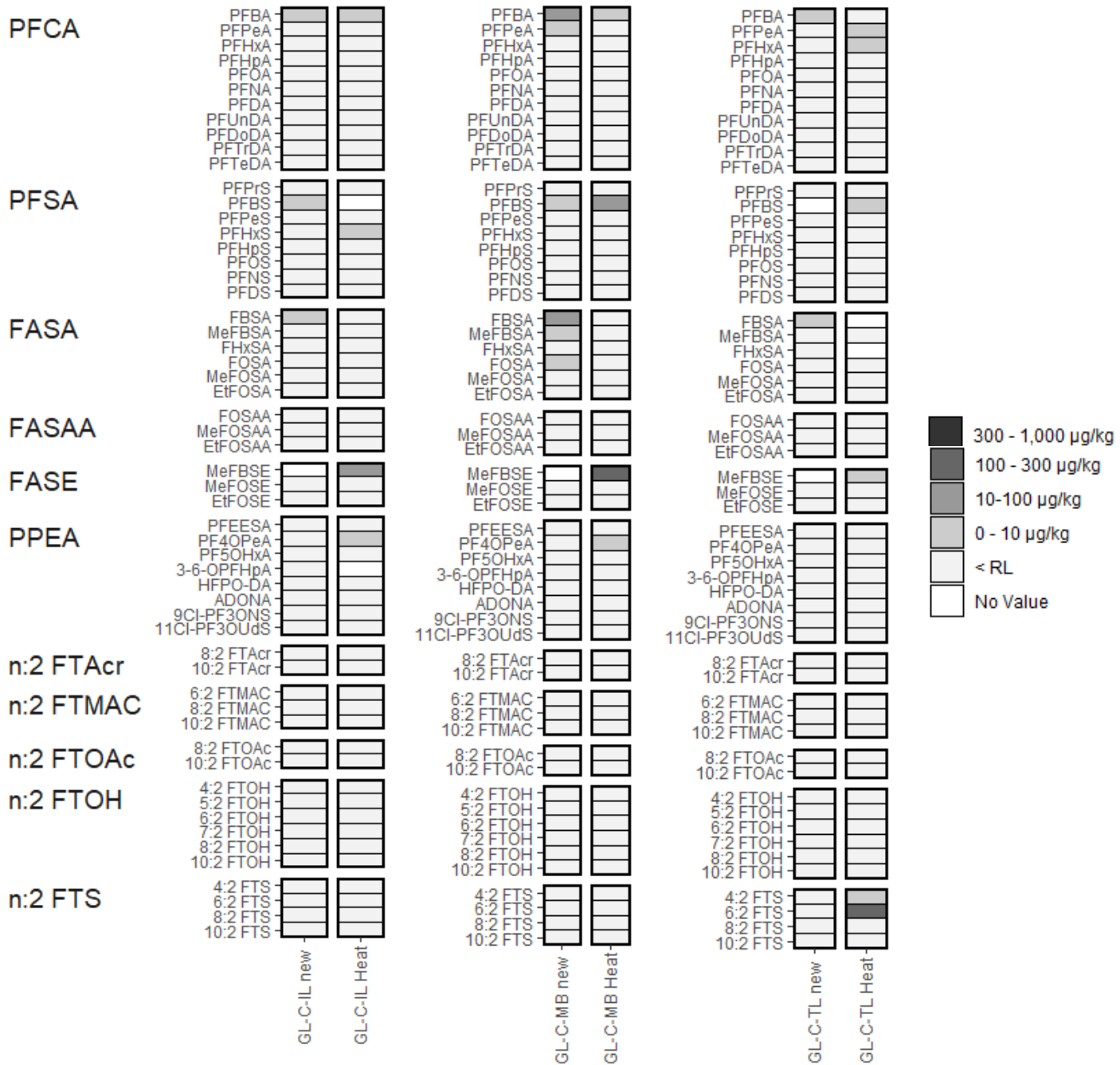


Figure 24. Average PFAS concentrations determined from triplicate analysis of GL-C-IL (left), GL-C-MB (center), and GL-C-TL (right) either prior to stressing (new) or following thermal stressing (Heat). Concentrations indicated by shade. Measurements not reported due to unmet QC standards are in white. PFAS concentrations displayed in this figure are also presented in **Tables 9 to 11**.

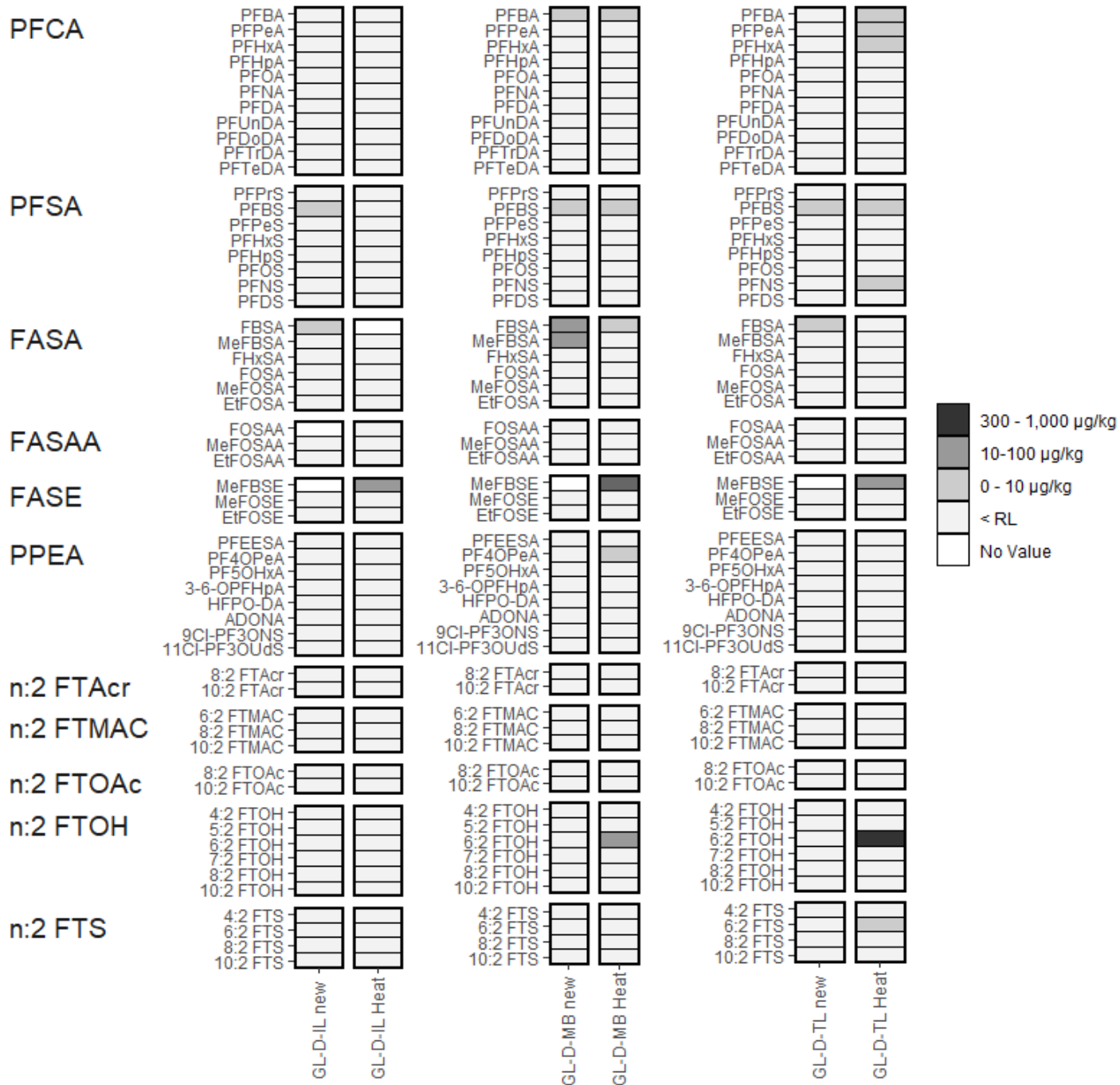


Figure 25. Average PFAS concentrations determined from triplicate analysis of GL-D-IL (left), GL-D-MB (center), and GL-D-TL (right) either prior to stressing (new) or following thermal stressing (Heat). Concentrations indicated by shade. Measurements not reported due to unmet QC standards are in white. PFAS concentrations displayed in this figure are also presented in **Tables 12 to 14**.

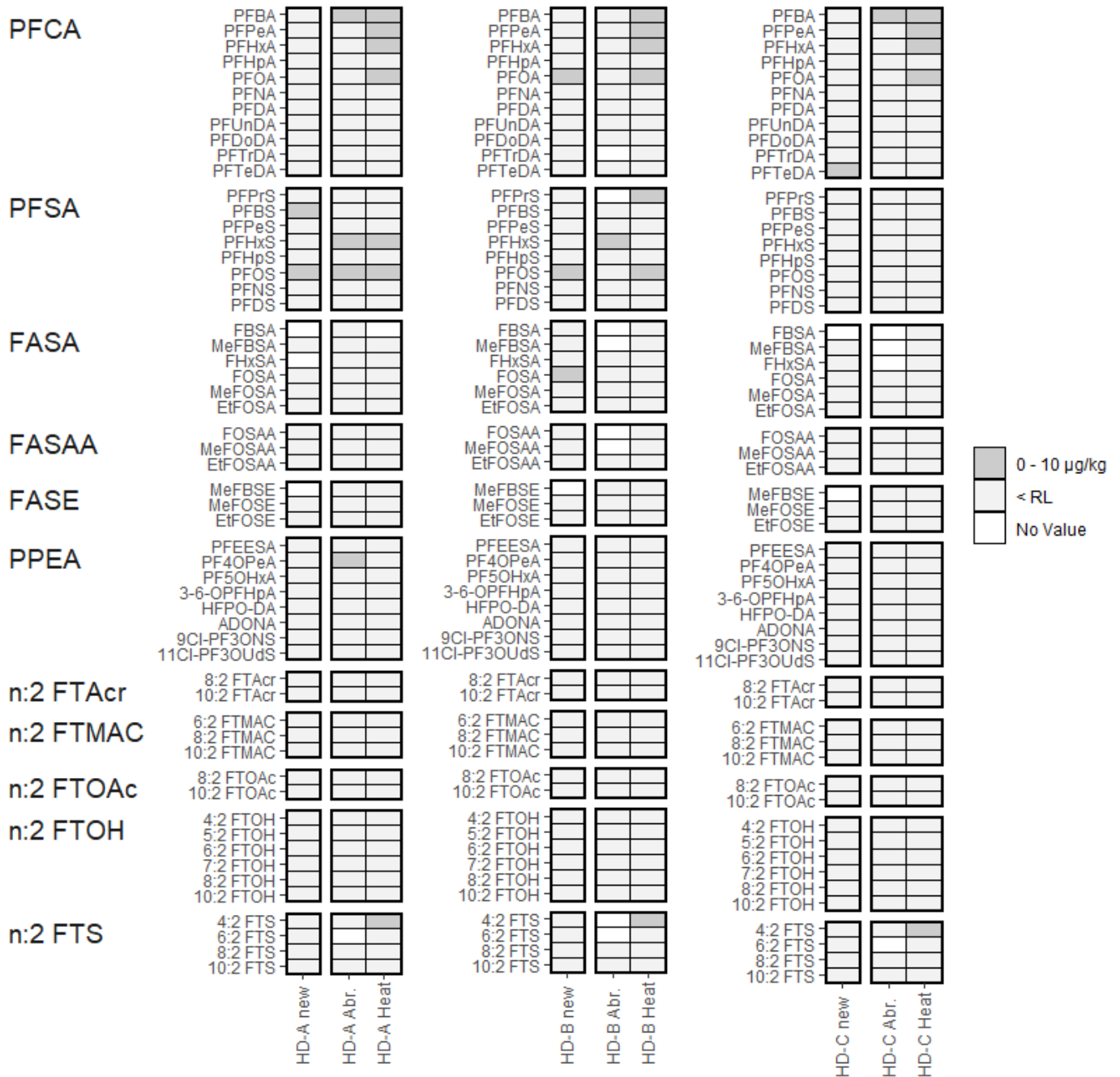


Figure 26. Average PFAS concentrations determined from triplicate analysis of HD-A (left), HD-B (center), and HD-C (right) either prior to stressing (new), following abrasion (Abr.), or following thermal stressing (Heat). Concentrations indicated by shade. Measurements not reported due to unmet QC standards are in white. PFAS concentrations displayed in this figure are also presented in **Tables 15 to 20**.

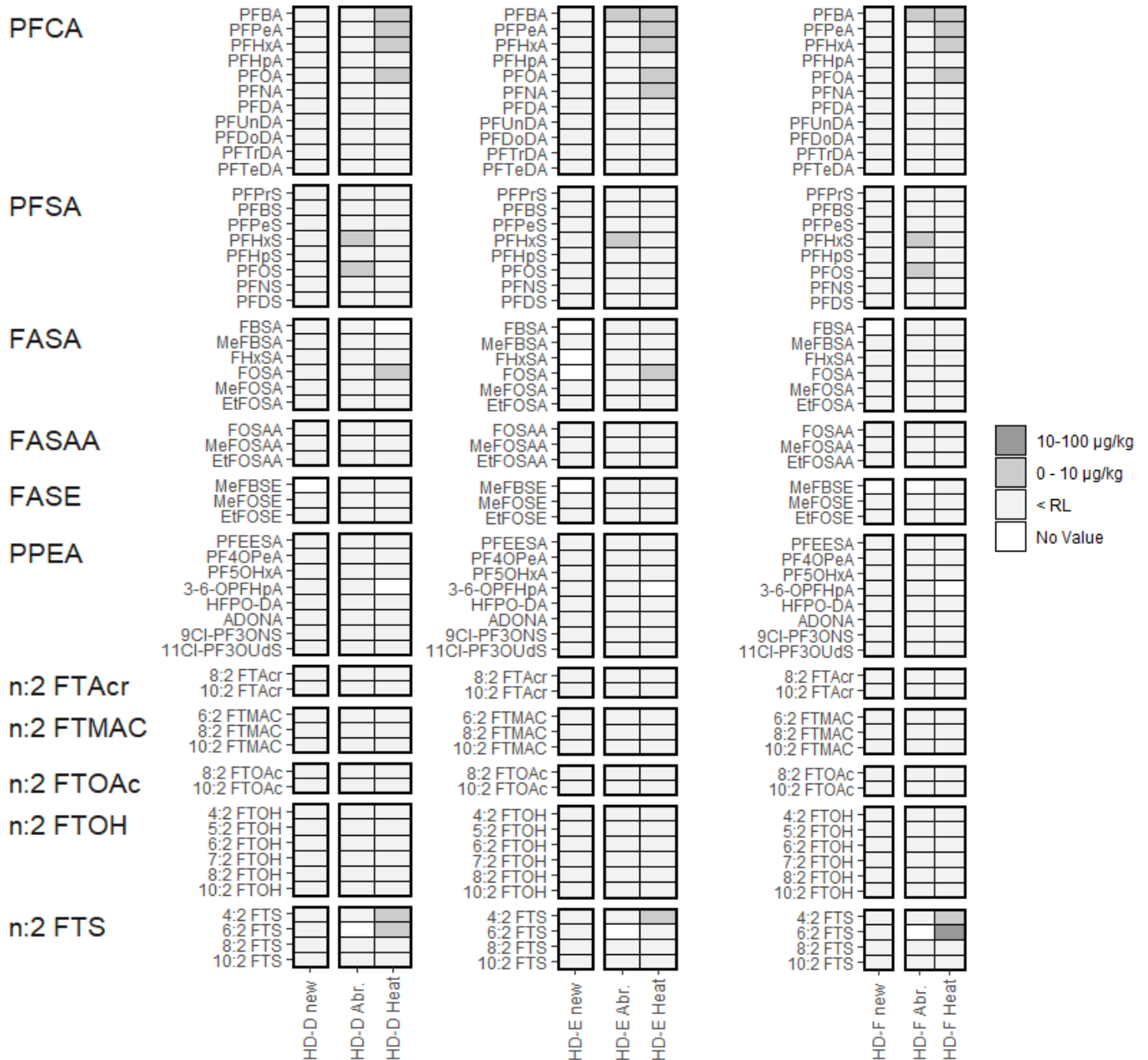


Figure 27. Average PFAS concentrations determined from triplicate analysis of HD-D (left), HD-E (center), and HD-F (right) either prior to stressing (new), or following abrasion (Abr.), or following thermal stressing (Heat). Concentrations indicated by shade. Measurements not reported due to unmet QC standards are in white. PFAS concentrations displayed in this figure are also presented in **Tables 21 to 26**.

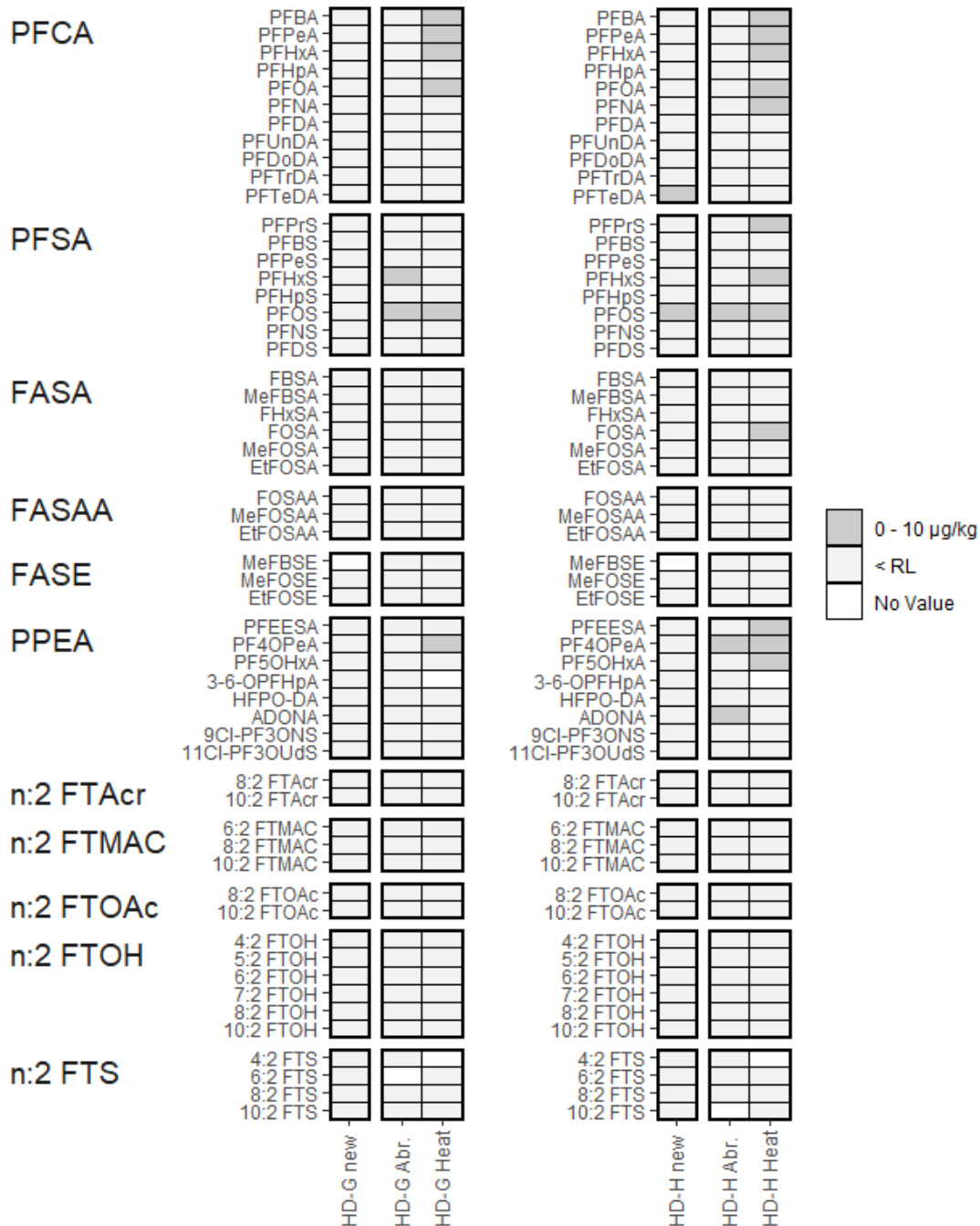


Figure 28. Average PFAS concentrations determined from triplicate analysis of HD-G (left) and HD-H (right) either prior to stressing (new), or following abrasion (Abr.), or following thermal stressing (Heat). Concentrations indicated by shade. Measurements not reported due to unmet QC standards are in white. PFAS concentrations displayed in this figure are also presented in **Tables 27 to 30**.

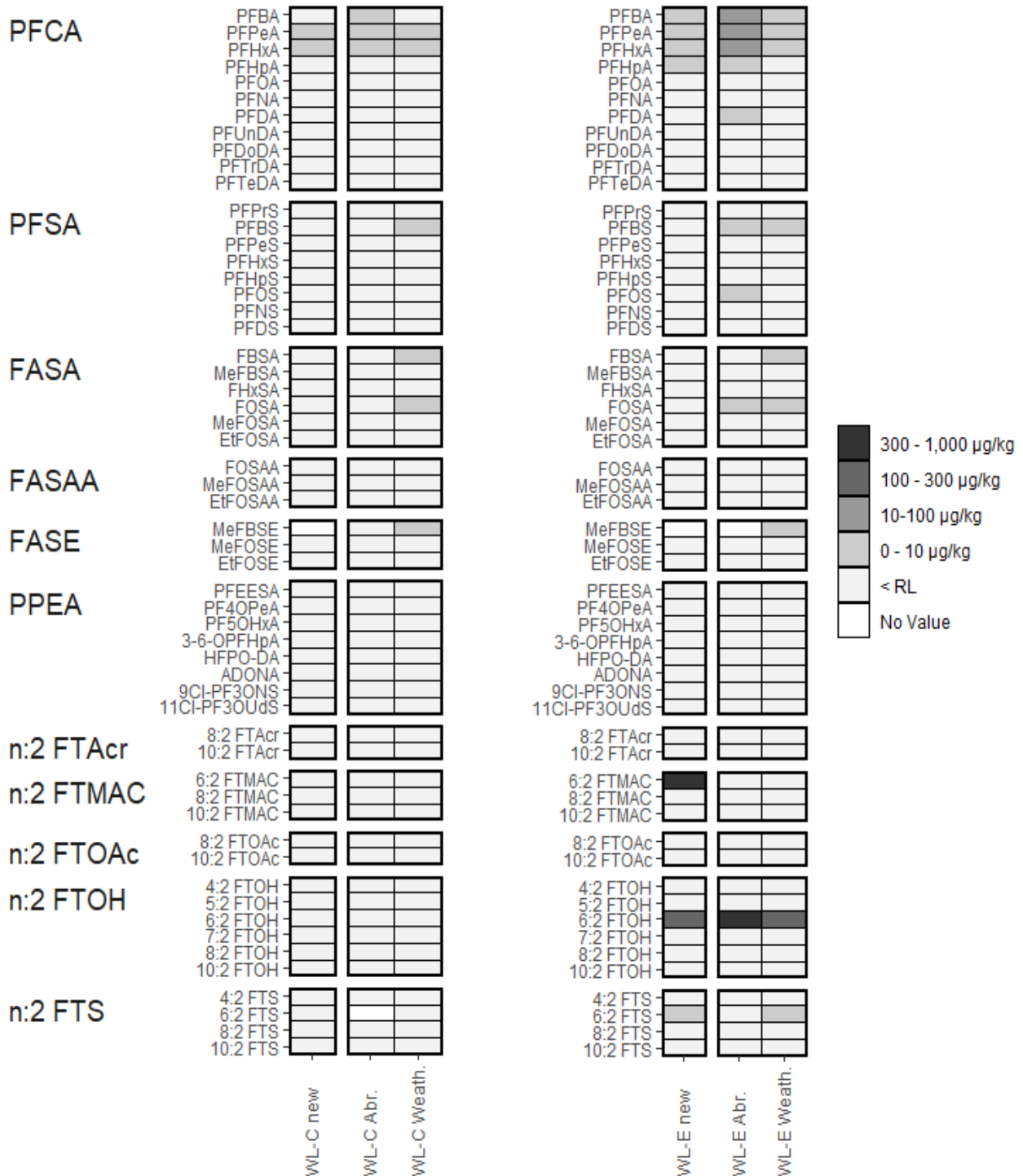


Figure 29. Average PFAS concentrations determined from triplicate analysis of WL-C (left) and WL-E (right) either prior to stressing (new) or following abrasion (Abr) or exposure to UV stressing (weath.). Concentrations indicated by shade. Measurements not reported due to unmet QC standards are in white. PFAS concentrations displayed in this figure are also presented in **Tables 31 to 34.**

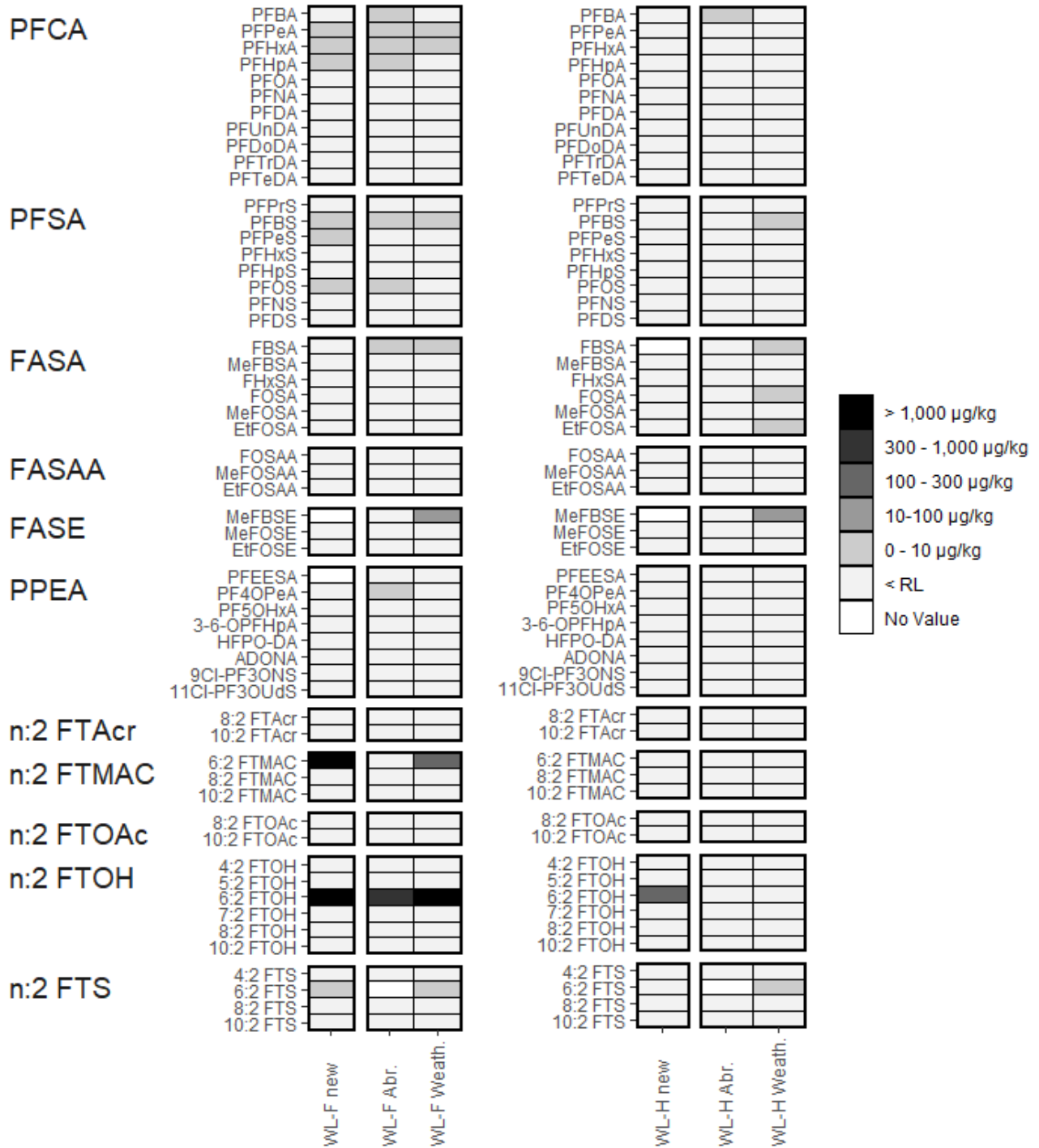


Figure 30. Average PFAS concentrations determined from triplicate analysis of WL-F (left) and WL-H (right) either prior to stressing (new) or following abrasion (Abr) or exposure to UV stressing (weath.). Concentrations indicated by shade. Measurements not reported due to unmet QC standards are in white. PFAS concentrations displayed in this figure are also presented in **Tables 35 to 38**.

Appendix B. List of Abbreviations and Acronyms

10:2 FTAc

10:2 fluorotelomer acrylate

6:2 FTMAC

6:2 fluorotelomer methacrylate

6:2 FTOH

6:2 fluorotelomer alcohol

6:2 FTS

6:2 fluorotelomer sulfonate

8:2 FTAc

8:2 fluorotelomer acrylate

ADONA

4,8-dioxa-3H-perfluorononanoate

CAS RN

Chemical Abstract Service Registry Number

CCB

Continuing calibration blank

CCV

Continuing calibration verification

CSD

Chemical Sciences Division

DWR

Durable water repellent

ePTFE

Expanded polytetrafluoroethylene

FASA

Perfluoroalkane sulfonamide

FASAA

Per- and polyfluoroalkane sulfonamido acetic acid

FASE

Perfluoroalkane sulfonamido ethanol

FBSA

Perfluorobutane sulfonamide

FRD

Fire Research Division

FT

Fluorotelomerization

GC-MS

Gas chromatography-mass spectrometry

GL

Glove

HFPO-DA

Hexafluoropropylene oxide dimer acid

HD

Hood

HPLC

High performance liquid chromatography

IL

Inner Liner

INJ

Injection standard

IS

Internal standard

ISO

International Organization for Standardization

LC

Liquid chromatography

MB

Moisture barrier

MeFBSE

N-Methyl perfluorobutane sulfonamidoethanol

MS

Mass spectrometry

MS/MS

Tandem mass spectrometry

n:2 FTAc

n:2 fluorotelomer acrylate

n:2 FTOAc

n:2 fluorotelomer acetate

n:2 FTOH

n:2 fluorotelomer alcohol

n:2 FTMAC

n:2 fluorotelomer methacrylate

n:2 FTS

n:2 fluorotelomer sulfonate

MeFASE

N-Methylperfluoroalkyl sulfonamidoethanol

NV

Nonvolatile

NFPA

National Fire Protection Association

NIST

National Institute of Standards and Technology

OS

Outer shell

PBI

Polybenzimidazole

PFAS

Per- and polyfluoroalkyl substances

PFBA

Perfluorobutanoic acid

PFBS

Perfluorobutane sulfonic acid

PFCA

Perfluorocarboxylic acid

PFDA

Perfluorodecanoic acid

PFHpA

Perfluoroheptanoic acid

PFHxA

Perfluorohexanoic acid

PFPeA

Perfluoropentanoic acid

PFNA

Perfluorononanoic acid

PFOA

Perfluorooctanoic acid

PFOS

Perfluorooctane sulfonic acid

PFSA

Perfluoroalkane sulfonic acid

PPB

Parts per billion

PPEA

Per- and polyfluoroalkyl ether acid

PTFE

Polytetrafluoroethylene

QC

Quality control

RL

Reporting limit

RM

Reference material

RT

Retention time

SCBA

Self-contained breathing apparatus

SV

Semivolatile

SPE

Solid phase extraction

TL

Thermal liner

TN

Technical Note

UV

Ultraviolet

V

Volatile

WL

Wildland